

DIAGRAM DRIVEN COMPUTER GENERATION OF EQUATION-OF-MOTION
COUPLED CLUSTER EQUATIONS FOR PERTURBED QUANTUM
OSCILLATORS

by

CARSON HUEY-YOU

Bachelor of Science, May 2017
Texas Christian University
Fort Worth, TX

Master of Science, December 2019
Texas Christian University
Fort Worth, TX

Submitted to the Graduate Faculty of the
College of Science and Engineering
Texas Christian University
in partial fulfillment of the requirements
for the degree of

Doctor of Philosophy

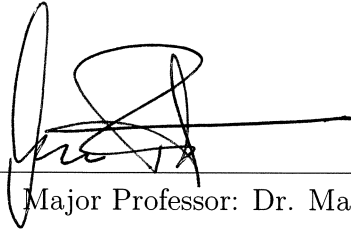
May 2024

DIAGRAM DRIVEN COMPUTER GENERATION OF EQUATION-OF-MOTION
COUPLED CLUSTER EQUATIONS FOR PERTURBED QUANTUM
OSCILLATORS

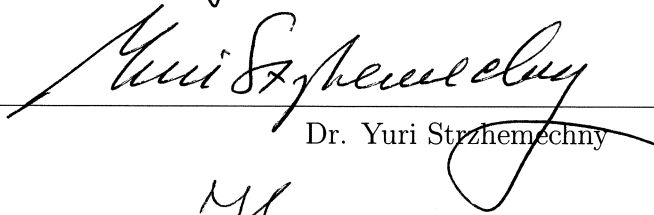
by

Carson Huey-You

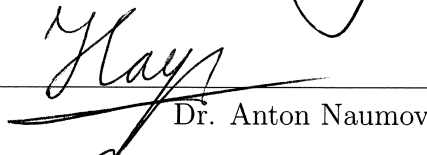
Dissertation Approved:



Major Professor: Dr. Magnus Rittby



Dr. Yuri Stozhemchny



Dr. Anton Naumov



Dr. Ken Richardson



For The College of Science and Engineering

ACKNOWLEDGEMENTS

As I write this, it has been eleven years since I first became affiliated with TCU. This has been an incredible journey, and there are so many people that I have to thank for bringing me along the way.

My mom started homeschooling me when I was a very young age. I was always particularly fascinated by learning how things work, and I have to credit her with making learning fun. To this day, I still recall many trips to the library and watching educational shows like Bill Nye with my brother. We had plenty of less educational hours and downtime too, but this was building the foundation for where I would end up. My mom and my brother have always been there to support me, and that hasn't changed through the entire duration of my work. To them go the first thanks, and I'd like them to know I'll always be there for them the same way they've been there for me.

At the point when I graduated high school, I began the process of looking for colleges. At ten years old, I came across Texas Christian University, not knowing it was the place I would spend another decade growing up. I mentioned in the thesis that Dr. Rittby had an incredibly positive influence in my life, but I believe his effect on this journey should be more pronounced. From such a young age and over the course of the past ten years as I've grown up, he's been patient and encouraging while providing the scientific knowledge and discipline I would need to arrive at this point. I can say with certainty that I've also inherited a few of his traits when it comes to the way we approach problems, both in physics and in life. I'm incredibly thankful to have him as an advisor and mentor, and I appreciate him looking out for me through all these years.

I'd also like to thank all of my undergraduate classmates, fellow graduate students, and all of the faculty here for making these years as amazing as they were. Especially to those in the College of Science & Engineering where I spent the majority of my time, this place has truly become a second home for me, and I'm proud to have shared it with all of you.

Most importantly of all, I feel as if these acknowledgements would be incomplete without mention of God's role in this journey. As a Christian, I honestly have God to thank for all of the blessings and opportunities I've come across thus far, as well as any that I'll come across in the future. Whether putting me in certain situations or placing certain people in my life, I take this section to highlight his involvement every step of the way. Further than that, there are *so, so* many times in my life when I've had to simply rely on faith. It's truly thanks to Him that I am where I am now, and that I've made it through the other side of this process.

Contents

List of Figures	v
List of Tables	vi
1 Introduction	1
1.1 Motivation	1
1.2 Occupation Number Representation	4
1.3 Perturbation Theory	8
2 Methodology	11
2.1 Coupled Cluster Method for the Ground State	11
2.2 Normal Ordering and Wick's Theorem	14
2.3 Equation-of-Motion Coupled Cluster Method for Excited States	18
2.4 Infinite Orders and Truncation	23
3 Diagrammatic Approach	26
3.1 Diagrammatic Representation of Normal Ordered Operators	26
3.2 Amplitude Symmetry Requirements	29
3.3 Solving the Non-Linear Cluster Amplitude Equations	36
3.4 Calculating Energies	41
3.5 Bogoliubov Transformations	43
3.6 Computational Scheme	48
4 Considerations of Parity	52
4.1 Effects on Ladder Operators	52
4.2 Simplifications for Even Parity Perturbations	55
5 The Quadratic Perturbation	59
5.1 Connecting Diagrams	59

5.2	Quadratic Excited States	69
5.3	Quadratic Bogoliubov Transformations	73
5.4	Links to Perturbation Theory	79
6	Higher Order Perturbations	82
6.1	Connecting Diagrams	82
6.2	Further Notes	87
7	Computer Generated Equations	89
7.1	Specifying Inputs	93
7.2	Static Methods	97
7.3	Allowed Connections	101
7.4	Uniqueness	107
8	Generalization for Multiple Oscillators	117
8.1	Normal Ordering of a Three-Mode System	117
8.2	Changes in the Effective Hamiltonian	122
8.3	Future Work	129
8.4	Conclusion	134
	Appendix	137
A	Details of Symmetrization	137
B	Isotopes and Elasticity	141
C	Generated Code	145
	References	156
	Vita	
	Abstract	

List of Figures

1	Flowchart for calculating the ground state and excited state energies. . .	51
2	The number of diagrams generated using a maximum order V_4 and a given T_n , sorted into different categories based on their uniqueness. Values in the legend are shown for T_{20} , before filtering for degeneracy.	111
3	Diagrams marked as degenerate, generated using a maximum order V_4 and a given T_n . One original copy of a degenerate diagram is saved, while any repeated instances are removed. Values in the legend are shown for T_{20} . .	112
4	Flowchart for generating iterative connections of all diagrams.	116

List of Tables

1	Inputs to a diagram object.	90
2	Ensuring a diagram is valid.	91
3	A diagrammatic object from the perturbed Hamiltonian.	94
4	Partitioning a diagram.	96
5	Diagrammatic attributes from (7.13).	100
6	Diagrammatic attributes resulting from the connection between \hat{Q}_0^4 and $t_3 t_4 t_5$	106
7	Coefficients for the single and multiple-oscillator interpretation of diagrams for each case.	107
8	Diagrams resulting from the connection between \hat{Q}_0^4 and $t_3^2 t_5$	108
9	Further examples of degenerate components.	110
10	The number of final diagrams in the generated equations, using maximum orders V_4 and T_n	113

Chapter 1

Introduction

1.1 Motivation

When trying to understand the behavior of a quantum mechanical system, one often has to resort to seeking approximate solutions to the Schrödinger equation due to the complexity of the interactions involved. In atomic and molecular physics, for example, one is faced with describing the many-body system of electrons, for which no exact solution exists. Finding sufficiently accurate approximate solutions is thus necessary in the quest to understand the finer details of the periodic table, molecular reaction dynamics, and so on.

To find the eigenvalues and eigenvectors of a given Hamiltonian, one might try to diagonalize a matrix representation in the associated Hilbert space of functions. However, this space is generally infinite-dimensional, and the convergence toward accurate eigenvalues and eigenvectors may be slow depending on the choice of functions.

Alternatively, there is the idea of defining an approximate Hamiltonian which is close

enough to the original that a more accurate solution to the problem can be found by treating the neglected interactions as a perturbation. Essentially, one tries to ‘turn off’ parts of the interaction which prohibits an exact solution. This leaves a system which can be described by an unperturbed Hamiltonian for which exact solutions are known or can be found, at least within the limits of a finite space of functions spanning the relevant space. Such approximate solutions could now form the basis with which one can pursue more accurate solutions through a variety of methods.

In the case of electronic structure theory, the Hartree-Fock (HF) or self-consistent-field (SCF) model often serves as the starting point for more sophisticated analysis [Szabo & Ostlund (1996)]. In the case of describing the vibrational degrees of freedom of a molecule, the lowest order approximation is typically a simple set of non-interacting harmonic oscillators. In both of these cases, one makes use of the language of second quantization, where occupation number operators are used to create or annihilate single particle states. In the electronic case, these operators obey fermionic anti-commutation relations, whereas harmonic oscillator operators are governed by bosonic commutation relations.

Perhaps the most straightforward way to find improved solutions beyond the unperturbed system is by the use of standard perturbation theory. Here, the wavefunctions and energies of the system are obtained as infinite series where the hope is that reasonably accurate results can be obtained with only a small number of terms, provided of course that the series converges at all. The perturbation approach is conceptually appealing, in that the term-by-term contributions can be visualized as consisting of an ever-increasing number of ways that the particles involved can interact for a given perturbation.

We have previously [[Huey-You \(2020\)](#), [Huey-You & Rittby \(2024\)](#)] presented work where we adopted ideas developed and used in perturbative approaches for the solution of the non-relativistic problem of interacting electrons (fermions), to the problem of finding solutions to a set of perturbed harmonic oscillators (bosons). This involved developing a diagrammatic approach to analyzing the equations of the so called ‘equation-of-motion coupled cluster’ (EoM-CC) method applied to perturbed quantum harmonic oscillators.

Coupled cluster (CC) methods have previously been used to study anharmonic oscillators by a number of authors. Early work [[Hsue & Chern \(1984\)](#), [Kaulfuss & Altenbokum \(1986\)](#), [Bishop & Flynn \(1988\)](#)] focused on the method’s convergence behavior for simple perturbations, whereas more recent studies [[Banik et al. \(2008\)](#), [Christiansen \(2004a\)](#), [Christiansen \(2004b\)](#)] presented the application of CC methods to perturbed oscillators modeling molecular vibrational motion.

In this work, we continue the development of our diagrammatic approach [[Huey-You & Rittby \(2024\)](#)] to CC methods applied to perturbed oscillators in an attempt to generalize the construction of the required equations for the EoM-CC approach to such systems. We also further develop the use of a novel scheme of iterative Bogoliubov transformations [[Huey-You \(2020\)](#)], in order to improve general convergence characteristics of the CC amplitude equations. Finally, in anticipation of growing complexity when applying our methods to a set of coupled harmonic oscillators, we develop Python code which makes use of our diagrammatic approach to generate the necessary code to implement the EoM-CC method for a given perturbation and set of coupled cluster excitation operators.

1.2 Occupation Number Representation

Let us begin by writing the Hamiltonian for a set of quantum harmonic oscillators. Each oscillator is indexed by i , corresponding to some position q_i and momentum p_i .

$$H_0 = \sum_i \left(\frac{1}{2m} p_i^2 + \frac{1}{2} m \omega_i^2 q_i^2 \right) \quad ; \quad p_i = -i\hbar \frac{\partial}{\partial q_i} \quad (1.1)$$

As we are dealing with a set of oscillators, it becomes convenient to frame the problem using the canonical ‘occupation number’ formalism. This entails defining a set of creation operators a_i^\dagger and annihilation operators a_i as follows.

$$a_i^\dagger = \sqrt{\frac{m\omega_i}{2\hbar}} \left(q_i - \frac{i}{\omega_i} p_i \right) \quad ; \quad a_i = \sqrt{\frac{m\omega_i}{2\hbar}} \left(q_i + \frac{i}{\omega_i} p_i \right) \quad (1.2)$$

Together, these are known as ladder operators. These operators are defined such that they satisfy the following bosonic commutation relations.

$$[a_i, a_j^\dagger] = \delta_{ij} \quad ; \quad [a_i, a_j] = 0 \quad ; \quad [a_i^\dagger, a_j^\dagger] = 0 \quad (1.3)$$

There are a few properties to keep in mind when one of these operators acts on the system ket. As a result of their definitions, creation and annihilation operators increase and decrease the number of quanta n_i for a particular i th oscillator respectively.

$$\begin{aligned} a_i^\dagger |n_1, \dots, n_i, \dots, n_N\rangle &= \sqrt{n_i + 1} |n_1, \dots, n_i + 1, \dots, n_N\rangle \\ a_i |n_1, \dots, n_i, \dots, n_N\rangle &= \sqrt{n_i} |n_1, \dots, n_i - 1, \dots, n_N\rangle \end{aligned} \quad (1.4)$$

This has the added effect that an annihilation operator acting on an oscillator in its ground state ($n_i = 0$) would necessarily result in zero. The ground state of the entire system is that for which all oscillators are in their respective ground states.

$$|0\rangle = |0_1, \dots, 0_N\rangle \quad (1.5)$$

We can describe the unperturbed system of harmonic oscillators with individual frequencies ω_i using the above formalism, by inverting the operator definitions in (1.2).

$$q_i = \sqrt{\frac{\hbar}{2m\omega_i}} (a_i^\dagger + a_i) \quad ; \quad p_i = i\sqrt{\frac{m\omega_i\hbar}{2}} (a_i^\dagger - a_i) \quad (1.6)$$

In the new operator representation, the Hamiltonian in (1.1) and the Schrödinger equation are written as follows.

$$H_0 = \sum_{i=1}^N \left(a_i^\dagger a_i + \frac{1}{2} \right) \hbar\omega_i \quad ; \quad H_0 |n_1, \dots, n_N\rangle = E_{n_1, \dots, n_N} |n_1, \dots, n_N\rangle \quad (1.7)$$

What would otherwise be a set of differential equations in q_i and p_i are thus transformed into what is effectively a set of algebraic equations. The energy eigenvalues for this ‘unperturbed’ case are well known, and can be expressed as follows.

$$E_{n_1, \dots, n_N} = \sum_i \left(n_i + \frac{1}{2} \right) \hbar\omega_i \quad (1.8)$$

For the derivations and results in this paper, we will set $\hbar = 1$ for simplicity. This factor can be easily re-introduced at any point.

Allow us now to apply some perturbation V to the system. Any perturbation based upon powers of q_i or p_i can be transformed from the regular coordinate space into ladder operators, using the same relations in (1.6). Let us therefore consider an example perturbation expressed as a power series in q_i , for simplicity.

$$V = c + \sum_i \alpha_i q_i + \sum_{ij} \beta_{ij} q_i q_j + \sum_{ijk} \gamma_{ijk} q_i q_j q_k + \sum_{ijkl} \delta_{ijkl} q_i q_j q_k q_l + \dots \quad (1.9)$$

Note that the restriction to q_i is only illustrative, and any following discussions can be applied to a more general perturbation in powers of q_i and p_i . We choose to apply the commutation relations, such that any terms from the polynomial can be written in the form $(a_i^\dagger a_j^\dagger \dots)(a_r a_s \dots)$. Writing terms with leading creation and trailing annihilation operators as such is a process known as normal-ordering. We can then rearrange V to be of the following form.

$$V = V_0 + V_1 + V_2 + V_3 + V_4 + \dots \quad (1.10)$$

Each term V_m consists of all combinations of m normal-ordered operators, with the

first few terms expressed below as examples.

$$\begin{aligned}
V_0 &= (\text{scalar}) \quad ; \quad V_1 = \sum_i \left(Q_i a_i^\dagger + Q^i a_i \right) \\
V_2 &= \sum_{ij} \left(\frac{1}{2!} Q_{ij} a_i^\dagger a_j^\dagger + Q_i^j a_i^\dagger a_j + \frac{1}{2!} Q^{ij} a_i a_j \right) \\
V_3 &= \sum_{ijk} \left(\frac{1}{3!} Q_{ijk} a_i^\dagger a_j^\dagger a_k^\dagger + \frac{1}{2!} Q_{ij}^k a_i^\dagger a_j^\dagger a_k + \frac{1}{2!} Q_i^{jk} a_i^\dagger a_j a_k + \frac{1}{3!} Q^{ijk} a_i a_j a_k \right) \\
V_4 &= \sum_{ijkl} \left(\frac{1}{4!} Q_{ijkl} a_i^\dagger a_j^\dagger a_k^\dagger a_l^\dagger + \frac{1}{3!} Q_{ijk}^l a_i^\dagger a_j^\dagger a_k^\dagger a_l + \frac{1}{2!} \frac{1}{2!} Q_{ij}^{kl} a_i^\dagger a_j^\dagger a_k a_l + \right. \\
&\quad \left. \frac{1}{3!} Q_i^{jkl} a_i^\dagger a_j a_k a_l + \frac{1}{4!} Q^{ijkl} a_i a_j a_k a_l \right)
\end{aligned} \tag{1.11}$$

In the above perturbation, we use Q to denote the coefficients for specific operator terms. The placement of indices on each coefficient correspond to which type of ladder operator is acting on the indexed oscillator. Specifically we will use subscripts to represent any creation operators and superscripts to represent any annihilation operators, a convention which is repeated throughout the paper.

Given the commutation relations in (1.3), the coefficients Q are invariant with respect to permutations solely within the subscript or superscript indices. Furthermore, if the perturbation is Hermitian, taking the complex conjugate of a coefficient is equivalent to the interchange of all subscripts with superscripts.

$$Q_{ijk}^{lm} = Q_{jik}^{ml} = Q_{kji}^{lm} = \dots \quad ; \quad (Q_{ijk}^{lm})^* = Q_{lm}^{ijk} \tag{1.12}$$

With the form of our perturbation defined above, let us also call the perturbed system ket $|\tilde{\alpha}\rangle$. This allows us to write the Schrödinger equation for a system of coupled

anharmonic oscillators as follows.

$$H|\tilde{\alpha}\rangle = (H_0 + V)|\tilde{\alpha}\rangle = \tilde{E}_\alpha|\tilde{\alpha}\rangle \quad (1.13)$$

1.3 Perturbation Theory

As we plan to approach a very general perturbed system, one may consider the use of perturbation theory. This entails expressing the energy for some perturbed state using order-by-order corrections, with each correction based upon a higher power of the perturbation. Though we will not explicitly use the method in this paper, we include a very brief presentation for reference.

Let us call the corresponding unperturbed state for this calculation some $|\alpha\rangle$. The general form of each correction is then well known, and can be derived using what is referred to as the Bracketing Theorem. This entails first defining the resolvent, R .

$$R = \sum_{\beta \neq \alpha} \frac{|\beta\rangle\langle\beta|}{(E_\alpha - E_\beta)} \quad (1.14)$$

Higher powers of R allow us to express certain parts of the energy corrections directly.

For example, the R^2 term is written as follows.

$$\begin{aligned} R^2 &= \sum_{\beta \neq \alpha} \sum_{\gamma \neq \alpha} \frac{|\beta\rangle\langle\beta|\gamma\rangle\langle\gamma|}{(E_\alpha - E_\beta)(E_\alpha - E_\gamma)} \\ &= \sum_{\beta \neq \alpha} \sum_{\gamma \neq \alpha} \frac{|\beta\rangle\delta_{\beta\gamma}\langle\gamma|}{(E_\alpha - E_\beta)(E_\alpha - E_\gamma)} = \sum_{\beta \neq \alpha} \frac{|\beta\rangle\langle\beta|}{(E_\alpha - E_\beta)^2} \end{aligned} \quad (1.15)$$

Alongside the resolvent, we utilize the bracketing definition $\langle X \rangle = \langle \alpha | X | \alpha \rangle$. This way, the n th order correction can be written with brackets resulting from $V(RV)^{n-1}$.

$$\begin{aligned}
E^{(1)} &= \langle V \rangle \quad ; \quad E^{(2)} = \langle VRV \rangle \\
E^{(3)} &= \langle V(RV)^2 \rangle - \langle V \rangle \langle VR^2V \rangle \\
E^{(4)} &= \langle V(RV)^3 \rangle - \langle V \rangle [\langle VR(RV)^2 \rangle + \langle (VR)^2RV \rangle] + \\
&\quad \langle V \rangle^2 \langle VR^3V \rangle - \langle VRV \rangle \langle VR^2V \rangle
\end{aligned} \tag{1.16}$$

Apart from the leading $\langle V(RV)^{n-1} \rangle$ term, we also have terms where more brackets have been inserted around V , VRV , etc. in all possible ways (apart from those which include the leftmost and rightmost V). A term with n_B brackets also has an associated sign of $(-1)^{n_B}$. Following this pattern and expanding the resolvent powers, an example for the first three energy corrections are shown below.

$$\begin{aligned}
E^{(1)} &= \langle \alpha | V | \alpha \rangle \quad ; \quad E^{(2)} = \sum_{\beta \neq \alpha} \frac{\langle \alpha | V | \beta \rangle \langle \beta | V | \alpha \rangle}{(E_\alpha - E_\beta)} \\
E^{(3)} &= \sum_{\beta \neq \alpha} \sum_{\gamma \neq \alpha} \frac{\langle \alpha | V | \beta \rangle \langle \beta | V | \gamma \rangle \langle \gamma | V | \alpha \rangle}{(E_\alpha - E_\beta)(E_\alpha - E_\gamma)} - \langle \alpha | V | \alpha \rangle \sum_{\beta \neq \alpha} \frac{\langle \alpha | V | \beta \rangle \langle \beta | V | \alpha \rangle}{(E_\alpha - E_\beta)^2}
\end{aligned} \tag{1.17}$$

The perturbed energy is then expressed as the sum of the unperturbed energy $E^{(0)}$ and all of the energy corrections, which must be truncated at some point.

$$\tilde{E} = E^{(0)} + E^{(1)} + E^{(2)} + E^{(3)} + \dots \tag{1.18}$$

Rather than following perturbation theory, we have chosen to employ the coupled

cluster method for a handful of reasons. The main advantage given by coupled cluster theory lies in its differing treatment of corrections to the calculated energies. Perturbation theory does include all possible excitations, but in turn, forces us to truncate the order of energy corrections used (i.e., at some $E^{(n)}$).

Coupled cluster theory is defined in such a way that allows us to include energy corrections to infinite order from each excitation level in the cluster operator. This way, the excitation levels of the cluster operator we use are truncated, rather than the order of the energy corrections. The general derivation for the EoM-CC method is discussed in the following section. Then, the remainder of the paper expands upon this using diagrams and Pythonic code for any arbitrary orders of the perturbation and cluster operator.

Chapter 2

Methodology

2.1 Coupled Cluster Method for the Ground State

Coupled cluster methods have been in wide use since their introduction [Coester (1958), Coester & Kümmel (1960), Čížek (1966), Paldus & Čížek (1975)], in both nuclear and electronic structure calculations [Bishop (1991), Bartlett & Musiał (2007)]. In CC methods, one makes use of an exponential operator involving appropriate excitation operators, which in principle can generate the exact ground state wavefunction and energy. Perturbative approaches become notoriously complex as one includes higher and higher orders of the perturbation, or as in the case of CC theory, higher levels of excitation in the cluster operator. Such methods are typically referred to as CCD, CCSD, CCSDT, and so on reflecting the level of truncation of the excitation operators (doubles only; singles and doubles; singles, doubles, and triples respectively).

We begin the EoM-CC derivation by considering the Schrödinger equation for the

ground state of our perturbed system, denoting the state itself as $|\tilde{0}\rangle$.

$$H|\tilde{0}\rangle = (H_0 + V)|\tilde{0}\rangle = \tilde{E}_0|\tilde{0}\rangle \quad (2.1)$$

The states of the unperturbed system form a complete set, allowing us to express $|\tilde{0}\rangle$ as a linear combination of all possible unperturbed excitations. There are a number of ways to accomplish this, but the CC method entails defining the cluster operator T .

$$T = T_1 + T_2 + T_3 + \dots = \sum_k t_k a_k^\dagger + \frac{1}{2!} \sum_{kl} t_{kl} a_k^\dagger a_l^\dagger + \frac{1}{3!} \sum_{klm} t_{klm} a_k^\dagger a_l^\dagger a_m^\dagger + \dots \quad (2.2)$$

The coefficients t in each operator are referred to as cluster amplitudes. Though these would technically generate the desired states, it becomes far more useful to apply e^T in practice. This way, the inverse of the operator is given by e^{-T} , and the linear combination for the perturbed ground state is as follows.

$$|\tilde{0}\rangle = e^T|0\rangle = \left(1 + T + \frac{1}{2!}T^2 + \frac{1}{3!}T^3 + \dots\right)|0\rangle \quad (2.3)$$

This relation is used to rewrite the perturbed Schrödinger equation in (2.1), directly solving for \tilde{E}_0 .

$$H|\tilde{0}\rangle = He^T|0\rangle = \tilde{E}_0e^T|0\rangle \quad ; \quad e^{-T}He^T|0\rangle = \tilde{E}_0|0\rangle \quad ; \quad \tilde{E}_0 = \langle 0|e^{-T}He^T|0\rangle \quad (2.4)$$

Analysis surrounding the term $e^{-T}He^T$ is therefore key to the remainder of our discussion. We first note that this is a similarity transformation of the more general form

$H \rightarrow P^{-1}HP$, which among other things conserves the spectrum of eigenvalues. Given that we have used the exponential cluster operator in the transformation, the Baker-Campbell-Hausdorff (BCH) expansion provides us with a view of any terms we should consider.

$$e^{-T}He^T = H + [H, T] + \frac{1}{2!}[[H, T], T] + \frac{1}{3!}[[[H, T], T], T] + \dots \quad (2.5)$$

Despite the fact that the exponential operator e^T is an infinite series, it can be shown in practice that the expansion in (2.5) is self-truncating for any finite expansion as in (1.9). Let us therefore select some maximum order perturbation V_M . The cluster operator T in (2.2) is the only other thing that needs to be truncated for the sake of calculations, for which we also select some maximum order T_N .

Inclusion of higher order cluster amplitudes would lead to better approximations of the ground state, but deriving precise equations by hand for each amplitude is an increasingly demanding process. Such equations are obtained by projecting all possible unperturbed excited states onto the Schrödinger equation in (2.4). The process will be explained in further detail later, but is included here for reference.

$$\left. \begin{aligned} \langle 0|a_i e^{-T} H e^T|0\rangle &= 0 \\ \langle 0|a_i a_j e^{-T} H e^T|0\rangle &= 0 \\ \langle 0|a_i a_j a_k \dots e^{-T} H e^T|0\rangle &= 0 \end{aligned} \right\} \rightarrow t_i, t_{ij}, t_{ijk}, \dots \quad (2.6)$$

Calculating the cluster amplitudes entails finding solutions for a number of coupled non-linear equations, given by some increasing number of annihilation operators acting on $e^{-T}He^T$. We seek to address the many combined operator terms in a more algorithmic

manner, which could be applied either by hand or in code.

2.2 Normal Ordering and Wick's Theorem

Wick's theorem will serve as our starting point, a convenient method for expressing an operator term as its normal-ordered part and any terms that follow. The theorem defines two operations, one of which is the simple normal-ordering described earlier. The other is a 'contraction', occurring between some a_i and an a_j^\dagger to its right. These will be denoted by curly brackets and bullet symbols, respectively.

$$\{a_i a_j^\dagger\} = a_j^\dagger a_i \quad ; \quad a_i^\bullet a_j^{\bullet\dagger} = \delta_{ij} \quad (2.7)$$

Given enough operators in an individual term, one could also write multiple contractions so long as they occur between distinct pairs of operators. Wick's theorem then states that a term \hat{A} , comprised of some product of creation and annihilation operators, can be written using a sum of all possible normal-ordered single contractions, normal-ordered double contractions, and so on.

$$\hat{A} = \{\hat{A}\} + \sum_{single} \{\hat{A}^\bullet\} + \sum_{double} \{\hat{A}^{\bullet\bullet}\} + \dots \quad (2.8)$$

As an example, consider the sum of all operators of the form $a_i a_j a_k^\dagger a_l^\dagger$. Rather than normal-ordering an individual product of operators alone, we choose to apply Wick's Theorem to the sum as it becomes far more useful, following the form of terms such as

(1.11) or (2.2). The normal-ordered term with no contractions is shown below.

$$\hat{A} = \sum_{ijkl} a_i a_j a_k^\dagger a_l^\dagger \quad \rightarrow \quad \{\hat{A}\} = \sum_{ijkl} \{a_i a_j a_k^\dagger a_l^\dagger\} = \sum_{ijkl} a_k^\dagger a_l^\dagger a_i a_j \quad (2.9)$$

Note that as we include a sum over oscillator indices i , j , k , and l , the upper limit of the sums will simply be the number of oscillators in the system. Furthermore, we are able to permute indices of the summation so long as the type of ladder operator is retained, allowing us to collect terms of the same form as shown below for the singly and doubly contracted cases.

$$\begin{aligned} \sum_{single} \{\hat{A}^\bullet\} &= \sum_{ijkl} \left(\{a_i^\bullet a_j a_k^\dagger a_l^\dagger\} + \{a_i^\bullet a_j a_k^\dagger a_l^\dagger\} + \{a_i a_j^\bullet a_k^\dagger a_l^\dagger\} + \{a_i a_j^\bullet a_k^\dagger a_l^\dagger\} \right) \\ &= \sum_{ijkl} \left(\{a_j a_l^\dagger \delta_{ik}\} + \{a_j a_k^\dagger \delta_{il}\} + \{a_i a_l^\dagger \delta_{jk}\} + \{a_i a_k^\dagger \delta_{jl}\} \right) \\ &= \sum_{ijkl} \left(a_l^\dagger a_j \delta_{ik} + a_k^\dagger a_j \delta_{il} + a_l^\dagger a_i \delta_{jk} + a_k^\dagger a_i \delta_{jl} \right) \\ &= 4 \sum_{ijkl} a_l^\dagger a_j \delta_{ik} = 4 \sum_{jkl} a_l^\dagger a_j = 4N \sum_{jl} a_l^\dagger a_j \end{aligned} \quad (2.10)$$

$$\begin{aligned} \sum_{double} \{\hat{A}^{\bullet\bullet}\} &= \sum_{ijkl} \left(\{a_i^\bullet a_j^{\bullet\bullet} a_k^\dagger a_l^\dagger\} + \{a_i^\bullet a_j^{\bullet\bullet} a_k^\dagger a_l^\dagger\} \right) \\ &= \sum_{ijkl} (\{\delta_{ik} \delta_{jl}\} + \{\delta_{il} \delta_{jk}\}) = \sum_{ijkl} (\delta_{ik} \delta_{jl} + \delta_{il} \delta_{jk}) = 2 \sum_{ij} 1 = 2N^2 \end{aligned}$$

Multiple bullets are used to differentiate contracted pairs, but hold no further significance. After inclusion of the sums and permuting indices, we note that each order contracted results in an added power of N in the coefficient. As triple and higher order

contractions are impossible for the given term, we can write the following equality.

$$\sum_{ijkl} a_i a_j a_k^\dagger a_l^\dagger = \sum_{ijkl} a_k^\dagger a_l^\dagger a_i a_j + 4N \sum_{jl} a_l^\dagger a_j + 2N^2 \quad (2.11)$$

The theorem is especially useful in relation to the BCH expansion. Consider for example the first commutator, $[H, T] = HT - TH$. Any terms in TH are normal-ordered by definition, as the cluster operator only adds more leading a_i^\dagger operators to the already normal-ordered Hamiltonian. The commutator as a whole can then be expressed as a sum of any possible contractions between the two terms.

$$\begin{aligned} [H, T] &= HT - TH = HT - \{HT\} \\ &= \sum_{single} \{(HT)^\bullet\} + \sum_{double} \{(HT)^{\bullet\bullet}\} + \dots \end{aligned} \quad (2.12)$$

There exists a bit of nuance to highlight in the above equation, as we now have two terms H and T . We require both to actively participate, such that a contraction can only occur between an a_i in H and an a_j^\dagger in T . In other words, neither term can contract with itself. We will refer to the sum of all possible contractions between two terms as expressed in (2.12) as their ‘connection’, denoted using a C subscript.

Let us also define the ‘open’ part of a normal-ordered operator as that which has a nonzero amount of creation or annihilation operators. Then, the ‘closed’ part of that term would contain any remaining scalars. This allows us to separate parts of equations

such as (1.7) for more well defined analysis.

$$H_0 = \sum_{i=1}^N \left(a_i^\dagger a_i + \frac{1}{2} \right) \omega_i \quad ; \quad H_{0,open} = \sum_{i=1}^N a_i^\dagger a_i \omega_i \quad ; \quad H_{0,closed} = \frac{1}{2} \sum_{i=1}^N \omega_i \quad (2.13)$$

As such, any operator can be written straightforwardly as a sum of its open and closed parts. Together with the concept of connections, we can apply the two formalisms to the entire BCH expansion.

$$\begin{aligned} e^{-T} H e^T &= e^{-T} (H_{open} + H_{closed}) e^T = e^{-T} H_{open} e^T + H_{closed} \\ e^{-T} H_{open} e^T &= H_{open} + (HT)_C + \frac{1}{2!} (HT^2)_C + \frac{1}{3!} (HT^3)_C + \dots = (He^T)_C \end{aligned} \quad (2.14)$$

The term $(He^T)_C$ will result in its own series of operators, as well as some scalars which fall out of the connections. Therefore, we can separate them once again and write out the explicit terms needed to calculate $e^{-T} H e^T$.

$$\begin{aligned} e^{-T} H e^T &= e^{-T} H_{open} e^T + H_{closed} \\ &= (He^T)_C + H_{closed} \\ &= (He^T)_{C,open} + (He^T)_{C,closed} + H_{closed} \end{aligned} \quad (2.15)$$

The ability to express these three parts separately is extremely convenient for the EoM-CC method, as the ground state energy can be directly expressed as a sum of the closed parts of our equation.

$$\tilde{E}_0 = (He^T)_{C,closed} + H_{closed} \quad (2.16)$$

The cluster amplitude equations in (2.6) also become much more approachable. The only surviving terms which contribute to any given $t_{ijk\dots}$ are connected and open, and also must be combinations of only a_i^\dagger operators so as not to eliminate the ground state ket.

$$\left. \begin{aligned} \langle 0|a_i(He^T)_{C,open}|0\rangle &= 0 \\ \langle 0|a_i a_j(He^T)_{C,open}|0\rangle &= 0 \\ \langle 0|a_i a_j a_k\dots(He^T)_{C,open}|0\rangle &= 0 \end{aligned} \right\} \rightarrow t_i, t_{ij}, t_{ijk}, \dots \quad (2.17)$$

Although Wick's Theorem does provide us with a way to directly manipulate terms in H and T , expressing their numerous connections in the operator representation can be a lengthy process. That said, we can also use the formalism for connected operators to approach the excited state derivation.

2.3 Equation-of-Motion Coupled Cluster Method for Excited States

The EoM-CC [Sekino & Bartlett (1984), Geertsens et al. (1989)] is a hybrid method where an effective Hamiltonian is constructed from a CC calculation, which then is subsequently diagonalized in the space of unperturbed states leading to information about the excited state spectrum of the problem. In order to derive the excited state energies, we begin by examining the excited states themselves. Let us express some k th excited state of the perturbed system as a linear combination over the unperturbed basis, just

as we did for the ground state. We will reserve e^T for the ground state expansion, and therefore will pick a more general excitation operator Ω_k^\dagger with new coefficients. This operator would still generate all unique singly excited states, doubly excited states, and so on, just as before with e^T .

$$|\phi_k\rangle = \Omega_k^\dagger |0\rangle \quad (2.18)$$

Using the above definition, the Schrödinger equation can be manipulated as follows.

$$\begin{aligned} H|\phi_k\rangle &= \tilde{E}_k|\phi_k\rangle \\ H\Omega_k^\dagger |0\rangle &= \tilde{E}_k\Omega_k^\dagger |0\rangle \\ He^Te^{-T}\Omega_k^\dagger |0\rangle &= \tilde{E}_ke^Te^{-T}\Omega_k^\dagger |0\rangle \\ e^{-T}He^Te^{-T}\Omega_k^\dagger |0\rangle &= \tilde{E}_ke^{-T}\Omega_k^\dagger |0\rangle \end{aligned} \quad (2.19)$$

By inserting the identity $e^Te^{-T} = 1$, we have rewritten the equation in terms of our more familiar transformed Hamiltonian. It then becomes useful to expand all of the open and closed terms in $e^{-T}He^T$, noting that the sum of the closed terms is simply the perturbed ground state given in (2.16). We also group the two common operators on either side as some $\tilde{\Omega}_k^\dagger$ for convenience.

$$\begin{aligned} \tilde{\Omega}_k^\dagger &= e^{-T}\Omega_k^\dagger \quad ; \quad e^{-T}He^T\tilde{\Omega}_k^\dagger |0\rangle = \tilde{E}_k\tilde{\Omega}_k^\dagger |0\rangle \\ \left((He^T)_{C,open} + \tilde{E}_0 \right) \tilde{\Omega}_k^\dagger |0\rangle &= \tilde{E}_k\tilde{\Omega}_k^\dagger |0\rangle \end{aligned} \quad (2.20)$$

The following notation is introduced, such that the above equation can be written

more clearly in terms of some $\bar{\mathbf{H}}$ matrix and its eigenvalues.

$$\bar{\mathbf{H}} = (He^T)_{C,open} \quad ; \quad \Delta\tilde{E}_k = \tilde{E}_k - \tilde{E}_0 \quad ; \quad \bar{\mathbf{H}}\tilde{\Omega}_k^\dagger|0\rangle = \Delta\tilde{E}_k\tilde{\Omega}_k^\dagger|0\rangle \quad (2.21)$$

We will refer to the $\bar{\mathbf{H}}$ matrix as the ‘effective’ Hamiltonian, with eigenvalues representing the gap between the ground state and a given k th excited state energy. The exact form for $\bar{\mathbf{H}}$ is discussed later, though we note that its elements in the multiple oscillator case become block matrices corresponding to the multiple ways to excite the system.

$$\begin{pmatrix} 0 & \langle 0|\bar{\mathbf{H}}|1\rangle & \langle 0|\bar{\mathbf{H}}|2\rangle & \cdots \\ \langle 1|\bar{\mathbf{H}}|0\rangle & \langle 1|\bar{\mathbf{H}}|1\rangle & \langle 1|\bar{\mathbf{H}}|2\rangle & \cdots \\ \langle 2|\bar{\mathbf{H}}|0\rangle & \langle 2|\bar{\mathbf{H}}|1\rangle & \langle 2|\bar{\mathbf{H}}|2\rangle & \cdots \\ \vdots & \vdots & \vdots & \ddots \end{pmatrix} \begin{pmatrix} s_{0k} \\ s_{1k} \\ s_{2k} \\ \vdots \end{pmatrix} = \Delta\tilde{E}_k \begin{pmatrix} s_{0k} \\ s_{1k} \\ s_{2k} \\ \vdots \end{pmatrix} \quad (2.22)$$

The element $\langle 0|\bar{\mathbf{H}}|0\rangle$ will always be zero, as all terms in $\bar{\mathbf{H}}$ are open by definition. The above is an infinite matrix, which must be truncated at some maximum size for any calculations in practice. Given that $\bar{\mathbf{H}}$ is highly dependent on the behavior of T , there are a few nuances to keep in mind when diagonalizing the matrix.

No Cluster Amplitudes: ($T = 0$)

Let us first establish the behavior for a case in which the EoM-CC approach is not taken, effectively selecting $T = 0$. The transformed Hamiltonian $e^{-T}He^T$ simply reduces to the regular Hamiltonian, and the newly introduced operator reduces such that $\tilde{\Omega}_k^\dagger = \Omega_k^\dagger$.

$$\bar{\mathbf{H}} = H_{open} \quad ; \quad \bar{\mathbf{H}}\Omega_k^\dagger|0\rangle = \Delta\tilde{E}_k\Omega_k^\dagger|0\rangle \quad (2.23)$$

As higher order expansion coefficients in the Ω_k^\dagger operator are included, the eigenstate more and more closely resembles the exact k th excited state. This is identical to the equation in the second line of (2.19).

All Cluster Amplitudes: ($T = \text{Infinite Series}$)

We now introduce the series of cluster amplitudes, for which the equations are given by $\langle m|\bar{\mathbf{H}}|0\rangle = 0$ as outlined in (2.17). If infinitely many amplitudes are included and fully converged, then the entire first column of the infinite $\bar{\mathbf{H}}$ matrix is necessarily zero. This has the effect of decoupling the ground state energy from the remaining excited states.

$$\bar{\mathbf{H}} = \begin{pmatrix} 0 & \langle 0|\bar{\mathbf{H}}|1\rangle & \langle 0|\bar{\mathbf{H}}|2\rangle & \cdots \\ 0 & \langle 1|\bar{\mathbf{H}}|1\rangle & \langle 1|\bar{\mathbf{H}}|2\rangle & \cdots \\ 0 & \langle 2|\bar{\mathbf{H}}|1\rangle & \langle 2|\bar{\mathbf{H}}|2\rangle & \cdots \\ \vdots & \vdots & \vdots & \ddots \end{pmatrix} \quad (2.24)$$

Truncated Cluster Amplitudes: ($T = \text{Finite Series}$)

The above case is what happens in theory, but numerical calculations require truncation of both the matrix and the cluster amplitudes. To approximate the ground state up to the Z th excited state, let us truncate the matrix at some particular $Z + 1$ dimensionality. In the case where T_N is of higher order than Z , we still see that the ground state

decouples for the truncated view of the matrix.

$$N \geq Z \quad \rightarrow \quad \bar{\mathbf{H}} = \begin{pmatrix} 0 & \langle 0|\bar{\mathbf{H}}|1\rangle & \langle 0|\bar{\mathbf{H}}|2\rangle & \cdots & \langle 0|\bar{\mathbf{H}}|Z\rangle \\ 0 & \langle 1|\bar{\mathbf{H}}|1\rangle & \langle 1|\bar{\mathbf{H}}|2\rangle & \cdots & \langle 1|\bar{\mathbf{H}}|Z\rangle \\ 0 & \langle 2|\bar{\mathbf{H}}|1\rangle & \langle 2|\bar{\mathbf{H}}|2\rangle & \cdots & \langle 2|\bar{\mathbf{H}}|Z\rangle \\ \vdots & \vdots & \vdots & \ddots & \vdots \\ 0 & \langle Z|\bar{\mathbf{H}}|1\rangle & \langle Z|\bar{\mathbf{H}}|2\rangle & \cdots & \langle Z|\bar{\mathbf{H}}|Z\rangle \end{pmatrix} \quad (2.25)$$

For lower order approximations of T , however, this image of the matrix changes. Excluding higher order amplitudes results in their associated elements $\langle m|\bar{\mathbf{H}}|0\rangle$ no longer being zero. The first eigenvalue $\Delta\tilde{E}_k$ is then nonzero, and we instead find some correction to the ground state energy. As such, all states become coupled again.

$$N < Z \quad \rightarrow \quad \bar{\mathbf{H}} = \begin{pmatrix} 0 & \langle 0|\bar{\mathbf{H}}|1\rangle & \langle 0|\bar{\mathbf{H}}|2\rangle & \cdots & \langle 0|\bar{\mathbf{H}}|Z\rangle \\ 0 & \langle 1|\bar{\mathbf{H}}|1\rangle & \langle 1|\bar{\mathbf{H}}|2\rangle & \cdots & \langle 1|\bar{\mathbf{H}}|Z\rangle \\ 0 & \langle 2|\bar{\mathbf{H}}|1\rangle & \langle 2|\bar{\mathbf{H}}|2\rangle & \cdots & \langle 2|\bar{\mathbf{H}}|Z\rangle \\ \vdots & \vdots & \vdots & \ddots & \vdots \\ \langle Z|\bar{\mathbf{H}}|0\rangle & \langle Z|\bar{\mathbf{H}}|1\rangle & \langle Z|\bar{\mathbf{H}}|2\rangle & \cdots & \langle Z|\bar{\mathbf{H}}|Z\rangle \end{pmatrix} \quad (2.26)$$

This leads to a situation where the ground state energy \tilde{E}_0 obtained from the EoM-CC approach returns a different value from the ground state energy obtained from diagonalizing $\bar{\mathbf{H}}$. Though this is not an especially large computational issue, it remains a crucial distinction to make.

2.4 Infinite Orders and Truncation

With the form of the effective Hamiltonian matrix discussed above, we note the advantageous manner by which coupled cluster theory manipulates infinite order contributions. The cluster operator e^T and its inverse e^{-T} are expressed below.

$$\begin{aligned} e^T &= 1 + T + \frac{1}{2!}T^2 + \frac{1}{3!}T^3 + \dots \\ e^{-T} &= 1 - T + \frac{1}{2!}T^2 - \frac{1}{3!}T^3 + \dots \end{aligned} \tag{2.27}$$

Note that both the exponential cluster operator and its inverse exclusively consist of products of a^\dagger . As there are no annihilation operators included, the matrix representation of e^T must be lower triangular.

$$e^T = \begin{pmatrix} 1 & 0 & 0 & \dots \\ \langle 1|e^T|0\rangle & 1 & 0 & \dots \\ \langle 2|e^T|0\rangle & \langle 2|e^T|1\rangle & 1 & \dots \\ \vdots & \vdots & \vdots & \ddots \end{pmatrix} \tag{2.28}$$

We note that for the multiple oscillator case, the states $|1\rangle$, $|2\rangle$, etc. must again represent the blocks of all possible single, double, etc. excitations. The leading 1 in the Taylor expansion is the only term which has no raising or lowering affect as a scalar, thereby appearing along the diagonal alone. Using the same arguments, the inverse

matrix has a nearly identical form shown below.

$$e^{-T} = \begin{pmatrix} 1 & 0 & 0 & \cdots \\ \langle 1|e^{-T}|0\rangle & 1 & 0 & \cdots \\ \langle 2|e^{-T}|0\rangle & \langle 2|e^{-T}|1\rangle & 1 & \cdots \\ \vdots & \vdots & \vdots & \ddots \end{pmatrix} \quad (2.29)$$

In the excited state derivation, we calculate the precise contributions to $\bar{\mathbf{H}}$ in an element by element manner, where different contributions are given by terms in $(He^T)_{C,open}$. Allow us to express the matrix of open and connected terms as follows, relating it directly to the transformed Hamiltonian $e^{-T}He^T$.

$$\bar{\mathbf{H}} = (He^T)_{C,open} = e^{-T}He^T - \tilde{E}_0 \quad (2.30)$$

Matrix elements of $\bar{\mathbf{H}}$ can then be written in terms of elements of each of the constituent operators, by taking advantage of the unperturbed eigenvector basis being complete.

$$\begin{aligned} \langle m|\bar{\mathbf{H}}|n\rangle &= \langle m|e^{-T}He^T|n\rangle - \delta_{mn}E_0 \\ &= \sum_{ij}^{\infty} \langle m|e^{-T}|i\rangle \langle i|H|j\rangle \langle j|e^T|n\rangle - \delta_{mn}E_0 \end{aligned} \quad (2.31)$$

Recall that in practice, the $\bar{\mathbf{H}}$ matrix must be truncated to some $(Z + 1)$ dimensionality, accounting for the ground state up to the Z th excited state. The coupled cluster formalism allows us to still indirectly consider contributions from the full Hamiltonian

matrix H of an infinite size, regardless of what truncated view we select. Truncations in this sense are instead applied to e^{-T} and e^T , reducing them from infinite square matrices to matrices of size $(Z + 1) \times \infty$ and $\infty \times (Z + 1)$ respectively.

Chapter 3

Diagrammatic Approach

3.1 Diagrammatic Representation of Normal Ordered Operators

Diagrammatic techniques are ways to simplify and streamline the derivation of the necessary equations for fermionic perturbation theory and CC methods. Such techniques have been put to extensive use in the analysis of the perturbed many-body system of electrons [Bartlett & Musial (2007)], while adoptions of diagrammatic techniques for perturbed harmonic oscillators have been much less extensive.

We now have enough groundwork to build a diagrammatic representation of any product of normal-ordered operators needed for the above EoM-CC calculations. To keep things simple, we begin with a horizontal line, representing the associated coefficient of the term and acting as the vertex line of the diagram. Any operators a_i^\dagger or a_i are then represented by vertical lines, leading up or down from the vertex line respectively. A few

choice terms from the perturbed Hamiltonian and cluster operator are shown below as examples.

$$\frac{1}{2!} \sum_{ij} Q^{ij} a_i a_j = \frac{1}{2!} \sum_{ij} Q^{ij} \left[\begin{array}{c} \text{---} \\ | \\ a_i \text{---} \\ | \\ a_j \end{array} \right] ; \quad \frac{1}{2!} \sum_{kl} t_{kl} a_k^\dagger a_l^\dagger = \frac{a_k^\dagger \left[\begin{array}{c} | \\ \text{---} \\ | \\ \frac{1}{2!} \sum_{kl} t_{kl} \end{array} \right] a_l^\dagger}{2!} \quad (3.1)$$

A dotted vertex line will be used to represent terms in the Hamiltonian, while a solid vertex line is used for cluster amplitudes. The length of any given line will have no significance, as we only care for the overall structure of the diagrammatic term. When writing and interpreting these diagrams, most of the explicit labels above become redundant. The type of operator is already defined by the direction of the vertical line, factorial coefficients can be derived later on, and any constants be directly inferred by the numbers of creation and annihilation operators. Therefore, we only truly need to label the associated operator indices for any given term.

$$\frac{1}{2!} \sum_{ij} Q^{ij} a_i a_j = i \left[\begin{array}{c} \text{---} \\ | \\ j \end{array} \right] ; \quad \frac{1}{2!} \sum_{kl} t_{kl} a_k^\dagger a_l^\dagger = k \left[\begin{array}{c} | \\ \text{---} \\ | \\ l \end{array} \right] \quad (3.2)$$

These will be the diagrams used in practice when evaluating products of connected operators from $(He^T)_C$. Let us take the simple example of a Hamiltonian under some

quadratic perturbation. This would result in a handful of V_2 terms, expressed below.

$$\begin{aligned}
H_{open} &= \sum_{ij} \omega_i^j \delta_{ij} a_i^\dagger a_j + \frac{1}{2!} \sum_{ij} Q_{ij} a_i^\dagger a_j^\dagger + \sum_{ij} Q_i^j a_i^\dagger a_j + \frac{1}{2!} \sum_{ij} Q^{ij} a_i a_j \\
&= \begin{array}{c} \text{---} \times \text{---} \\ | \\ i \\ | \\ j \end{array} + i \begin{array}{c} | \\ | \\ \text{---} \\ | \\ j \end{array} + \begin{array}{c} \blacksquare \text{---} \\ | \\ i \\ | \\ j \end{array} + i \begin{array}{c} \text{---} \\ | \\ | \\ | \\ j \end{array} \tag{3.3}
\end{aligned}$$

The cross and square symbols on the vertices are used to differentiate the ω_i^j energy term and the Q_i^j perturbation term, as they have the same diagrammatic structure. We will also represent the cluster operator T in (2.2) using diagrams.

$$\begin{aligned}
T &= T_1 + T_2 + T_3 + \dots = \sum_k t_k a_k^\dagger + \frac{1}{2!} \sum_{kl} t_{kl} a_k^\dagger a_l^\dagger + \frac{1}{3!} \sum_{klm} t_{klm} a_k^\dagger a_l^\dagger a_m^\dagger + \dots \\
&= \begin{array}{c} | \\ \bullet \\ k \end{array} + \begin{array}{c} | \\ | \\ \text{---} \\ | \\ k \quad l \end{array} + \begin{array}{c} | \\ | \\ | \\ \text{---} \\ | \\ k \quad l \quad m \end{array} + \dots \tag{3.4}
\end{aligned}$$

With this formalism, connecting two diagrams becomes an easy task. Given how a contraction is defined, this is best visualized diagrammatically as connecting a down-facing line in H and an up-facing line in T .

$$\left(\hat{Q}^{ij} \cdot T_4 \right)_C = \begin{array}{c} \text{---} \\ | \\ | \\ | \\ | \\ \text{---} \\ l \quad a \quad i \quad j \quad k \end{array} + \begin{array}{c} \text{---} \\ | \\ | \\ | \\ | \\ \text{---} \\ a \quad b \quad i \quad j \end{array} \tag{3.5}$$

Here we have used the shorthand notation \hat{Q}^{ij} to represent the associated term in the Hamiltonian from (3.3). Note that the connected line only requires one index, as the other is removed by the Kronecker delta in (2.7). The connected terms above include a singly connected as well as a doubly connected term, which together are the only

possible structures that can result from a contraction between the two diagrams. That being said, some extra care is required with regard to the indices in the results. This evokes a discussion surrounding symmetry and the interchanging of these indices, which should be thoroughly investigated before any diagrams can be fully interpreted.

3.2 Amplitude Symmetry Requirements

When working in the operator representation, there exist two ways of reordering indices which should be reflected in the diagrammatic scheme. The first method comes as a result of commutation relations in (1.3), allowing us the ability to freely exchange creation operator indices with each other or annihilation operator indices with each other, so long as the two are kept distinct and are in normal order.

$$\left[a_i^\dagger, a_j^\dagger \right] = 0 \quad ; \quad \left[a_i, a_j \right] = 0 \quad \rightarrow \quad \frac{1}{3!} \sum_{ijk} t_{ijk} a_i^\dagger a_j^\dagger a_k^\dagger = \frac{1}{3!} \sum_{ijk} t_{ijk} a_k^\dagger a_i^\dagger a_j^\dagger = \dots \quad (3.6)$$

We note that this manner of exchange only applies to the operators, but leaves the coefficient intact. The other method makes use of the summation itself, as the indices being summed over can be arbitrarily assigned. This affects both the coefficient and any associated operators, as shown below.

$$\sum_{ijk\dots} = \sum_{kji\dots} = \sum_{kij\dots} = \dots \quad \rightarrow \quad \frac{1}{3!} \sum_{ijk} t_{ijk} a_i^\dagger a_j^\dagger a_k^\dagger = \frac{1}{3!} \sum_{kij} t_{kij} a_k^\dagger a_i^\dagger a_j^\dagger = \dots \quad (3.7)$$

Any connected terms should exhibit the same behavior as well. This requires us to take an extra step in symmetrizing the result, when returning from the diagrams back

into operator representation. Let us write the following as an example, including both the diagram and the result from Wick's Theorem for a specific case.

$$\left(\hat{Q}_i^j \cdot T_2\right)_C = \blacksquare \begin{array}{c} \text{---} i \\ | \\ a \end{array} \begin{array}{c} | \\ | \\ j \end{array} = \sum_{ij} \sum_a (Q_i^a t_{aj}) a_i^\dagger a_j^\dagger \quad (3.8)$$

Clearly, the above indices are not symmetric with respect to interchanging the operators. Instead, symmetry can be forced onto the term by splitting it apart and including all possible sets of permuted indices.

$$\sum_{ij} \sum_a (Q_i^a t_{aj}) a_i^\dagger a_j^\dagger = \frac{1}{2} \sum_{ij} \sum_a (Q_i^a t_{aj} + Q_j^a t_{ai}) a_i^\dagger a_j^\dagger \quad (3.9)$$

When interpreting diagrams by hand or implementing them into code, the coefficient will be symmetrized as shown above. Any indices for unconnected upwards-facing vertical lines are required to commute, and therefore we can write the following for the example.

$$\blacksquare \begin{array}{c} \text{---} i \\ | \\ a \end{array} \begin{array}{c} | \\ | \\ j \end{array} = \blacksquare \begin{array}{c} \text{---} j \\ | \\ a \end{array} \begin{array}{c} | \\ | \\ i \end{array} \quad (3.10)$$

Allow us then to define the product of two normal-ordered terms with symmetrized coefficients after n contractions, for use in diagrammatic interpretation. Consider the

two generalized versions of some perturbation term and cluster amplitude.

$$\begin{aligned}\hat{Q}_{rs\dots}^{ij\dots} &= \frac{1}{K!} \frac{1}{L!} \sum_{ij\dots rs\dots} Q_{rs\dots}^{ij\dots} \binom{\text{(L indices)}}{\text{(K indices)}} (a_r^\dagger a_s^\dagger \dots)_{\text{(K operators)}} (a_i a_j \dots)_{\text{(L operators)}} \\ T_M &= \frac{1}{M!} \sum_{uv\dots} t_{uv\dots} \binom{\text{(M indices)}}{\text{(M indices)}} (a_u^\dagger a_v^\dagger \dots)_{\text{(M operators)}}\end{aligned}\tag{3.11}$$

Ideally, we wish to interpret any written connected diagram into the form below, where the associated coefficient is already symmetrized.

$$\hat{\Pi}_{rs\dots}^{ij\dots} = \frac{1}{R!} \frac{1}{S!} \sum_{ij\dots rs\dots} \Pi_{rs\dots}^{ij\dots} \binom{\text{(S indices)}}{\text{(R indices)}} (a_r^\dagger a_s^\dagger \dots)_{\text{(R operators)}} (a_i a_j \dots)_{\text{(S operators)}}\tag{3.12}$$

As R and S consist of any remaining creation and annihilation operators after connections, they can be expressed in terms of K , L , M , and n . The creation operators in the final result come from the K amount in $\hat{Q}_{rs\dots}^{ij\dots}$ and the M amount in T_M , while annihilation operators can only be sourced from the L amount in $\hat{Q}_{rs\dots}^{ij\dots}$. An n th contraction then removes n annihilation operators in $\hat{Q}_{rs\dots}^{ij\dots}$ and n creation operators in T_M , allowing us to write the following equalities.

$$R = K + M - n \quad ; \quad S = L - n\tag{3.13}$$

R and S will be called the ‘signature’ of the diagram, providing information about the connected term’s overall structure. Later on, this will be used to sort diagrams with the same number of creation and annihilation operators when evaluating the cluster amplitude equations in (2.17).

Let us also generalize the process of symmetrizing shown in (3.9). The same diagram and its associated coefficient are provided below, isolated from any sums and operators for better clarity.

$$\begin{array}{c}
 \blacksquare \cdots \cdots \cdots \\
 \begin{array}{|c}
 i \\
 \hline
 a \\
 \hline
 \end{array}
 \begin{array}{|c}
 \hline
 j \\
 \hline
 \end{array}
 \end{array}
 \quad
 Q_i^a t_{aj} \rightarrow \frac{1}{2} (Q_i^a t_{aj} + Q_j^a t_{ai}) \quad (3.14)$$

As the only source for annihilation operators is the perturbed Hamiltonian term $\hat{Q}_{rs\dots}^{ij\dots}$, any interchange of their indices is symmetric by default. The inclusion of any annihilation operators in $\hat{Q}_{rs\dots}^{ij\dots}$ therefore has no effect on the number of terms required for symmetrization. In the example below, the creation operators indexed by i and j must be permuted, while the annihilation operators indexed by k and l are not.

$$\begin{array}{c}
 \begin{array}{|c}
 i \\
 \hline
 \cdots \cdots \cdots \\
 \hline
 k \\
 \hline
 \end{array}
 \begin{array}{|c}
 l \\
 \hline
 \hline
 \end{array}
 \begin{array}{|c}
 a \\
 \hline
 \hline
 \end{array}
 \begin{array}{|c}
 j \\
 \hline
 \hline
 \end{array}
 \end{array}
 \quad
 Q_i^{akl} t_{aj} \rightarrow \frac{1}{2} (Q_i^{akl} t_{aj} + Q_j^{akl} t_{ai}) \quad (3.15)$$

Creation operators on the same vertex line are also symmetric by default. The only permutations which need be accounted for are given by the exchange of indices on different vertices as shown below.

$$\begin{array}{c}
 \begin{array}{|c}
 i \\
 \hline
 \cdots \cdots \cdots \\
 \hline
 a \\
 \hline
 \end{array}
 \begin{array}{|c}
 j \\
 \hline
 b \\
 \hline
 \end{array}
 \begin{array}{|c}
 k \\
 \hline
 \hline
 \end{array}
 \begin{array}{|c}
 l \\
 \hline
 \hline
 \end{array}
 \end{array}
 \quad
 Q_{ij}^{ab} t_{abkl} \rightarrow \frac{1}{6} (Q_{ij}^{ab} t_{abkl} + Q_{kj}^{ab} t_{abli} + Q_{lj}^{ab} t_{abki} + \\
 Q_{ik}^{ab} t_{abjl} + Q_{il}^{ab} t_{abkj} + Q_{kl}^{ab} t_{abij}) \quad (3.16)$$

Here we see that the fully symmetrized expansion does not include an exchange of

i and j alone, nor an exchange of k and l alone. With this in mind, let us denote the expanded symmetrized coefficient of a given diagram as follows.

$$Q_{rs..ij..t_{ab..uv..}} \rightarrow \frac{1}{V_n} (Q_{rs..ij..t_{ab..uv..}})_\sigma \quad (3.17)$$

In the above equation, V_n represents the number of permuted terms a coefficient must be separated into in order to achieve symmetry. The subscript σ then denotes the expanded sum containing each of those permuted terms. For example, the symmetrizing in (3.16) can be analyzed as follows.

$$V_n = 6 \quad ; \quad (Q_{ij}^{ab} t_{abkl})_\sigma = Q_{ij}^{ab} t_{abkl} + Q_{kj}^{ab} t_{abli} + Q_{lj}^{ab} t_{abki} + \\ Q_{ik}^{ab} t_{abjl} + Q_{il}^{ab} t_{abkj} + Q_{kl}^{ab} t_{abij} \quad (3.18)$$

The value of V_n can be explicitly derived using combinatorics. The result is included here, for which further details and examples are shown in Section A of the Appendix.

$$V_n(K, M) = \frac{(K + M - n)!}{K!(M - n)!} \quad (3.19)$$

This value accounts for the symmetry of any unconnected operators, but the connected ones should be dealt with as well. More specifically, we wish to find the number of possible unique n th contractions which could be represented by a given diagram, which we will call some U_n . The value of this U_n is provided here, with its derivation also in-

cluded in Section A of the Appendix.

$$U_n(L, M) = \frac{L!M!}{(L-n)!(M-n)!} \frac{1}{n!} \quad (3.20)$$

By collecting the above coefficients as well as the ones in (3.11), we find that the full coefficient simplifies greatly for the n th connection between two diagrams.

$$Y_n(K, L, M) = \frac{1}{K!} \frac{1}{L!} \frac{1}{M!} \frac{U_n(L, M)}{V_n(K, M)} = \frac{1}{(K+M-n)!(L-n)!} \frac{1}{n!} = \frac{1}{R!} \frac{1}{S!} \frac{1}{n!} \quad (3.21)$$

We wish to keep the R and S factorials separate in order to write the result to mirror (3.12). The coefficient $\Pi_{rs\dots}^{ab\dots}$ can then be written as follows, again using σ to denote the symmetrized expansion.

$$\Pi_{rs\dots}^{ab\dots} = \frac{1}{n!} (Q_{rs\dots}^{ab\dots} t_{uv\dots})_\sigma \quad (3.22)$$

This constitutes a general method for expressing a connection between any two operators in H and e^T . Continuing from (3.5), we can interpret the connected diagrams to find terms in the BCH expansion.

$$\begin{aligned} (\hat{Q}^{ij} \cdot T_4)_C &= \left[\begin{array}{c} \text{---} \\ | \\ l \quad a \quad i \quad j \quad k \end{array} \right] + \left[\begin{array}{c} \text{---} \\ | \\ a \quad b \quad i \quad j \end{array} \right] \\ &= \frac{1}{3!} \frac{1}{1!} \sum_{ijk,l} \sum_a \frac{1}{1!} (Q^{al} t_{aijk})_\sigma a_i^\dagger a_j^\dagger a_k^\dagger a_l + \frac{1}{2!} \frac{1}{0!} \sum_{ij} \sum_{ab} \frac{1}{2!} (Q^{ab} t_{abij})_\sigma a_i^\dagger a_j^\dagger \end{aligned} \quad (3.23)$$

In the special case of the single oscillator, there exists only one index to sum over,

and the operators in (3.11) simplify substantially.

$$\hat{Q}_K^L = \frac{1}{K!} \frac{1}{L!} Q_K^L (a^\dagger)^K (a)^L \quad ; \quad T_M = \frac{1}{M!} t_M (a^\dagger)^M \quad (3.24)$$

The permuted terms denoted by the σ subscript pose an important caveat in the single oscillator case. We still find that the same number of permutations V_n are required to properly symmetrize a coefficient. With only one oscillator in the system, however, the indices all refer to the same oscillator (i.e., $a = b = i = j = k = l = \dots = 1$), and therefore the sum collapses.

$$\begin{aligned} (Q_{ij}^{ab} t_{abkl})_\sigma &= Q_{ij}^{ab} t_{abkl} + Q_{kj}^{ab} t_{abli} + Q_{lj}^{ab} t_{abki} + Q_{ik}^{ab} t_{abjl} + Q_{il}^{ab} t_{abkj} + Q_{kl}^{ab} t_{abij} \\ (Q_2^2 t_4)_\sigma &= Q_2^2 t_4 + Q_2^2 t_4 + Q_2^2 t_4 + Q_2^2 t_4 + Q_2^2 t_4 + Q_2^2 t_4 = 6Q_2^2 t_4 \end{aligned} \quad (3.25)$$

Effectively, this operation reintroduces a factor of V_n in the single oscillator case. To better convert from the single oscillator case into the multiple oscillator case and back, we will write the symmetrizing factor to mirror (3.19).

$$(Q_K^L t_M)_\sigma = V_n Q_K^L t_M = \frac{(K+M-n)!}{K!(M-n)!} Q_K^L t_M \quad (3.26)$$

As symmetry over one index is a trivial matter, the connected product of the two terms now simplifies substantially.

$$\hat{\Pi}_R^S = \frac{1}{R!} \frac{1}{S!} \Pi_R^S (a^\dagger)^R (a)^S \quad ; \quad \Pi_R^S = \frac{1}{n!} \frac{(K+M-n)!}{K!(M-n)!} Q_K^L t_M \quad (3.27)$$

The factorial coefficients derived above include ones relating to the operator signature, connections, and symmetry of the diagram. A fourth factorial coefficient is also included, not from the interpretation of diagrammatic structure, but instead directly from the expansion of the exponential e^T in (2.5). We will use a diamond \diamond symbol above such factorials when interpreting diagrammatic terms, to differentiate them from the other structural factorials.

We present the methodology surrounding the remaining energy calculations in the single oscillator representation, noting that the theoretical concepts and examples can be generalized back to the multiple oscillator case. For diagrammatic interpretation, this is simply accomplished by inserting the appropriate sums and indices, then replacing the symmetrized coefficient by the actual permuted terms in $(Q_{rs..}^{ij..} t_{uv..})_\sigma$.

$$\begin{aligned}
 \begin{array}{|c|c|} \hline | \\ \hline \end{array} &= \frac{1}{4!} \frac{1}{1!} \frac{1}{2!} \frac{1}{2!} \overset{\diamond}{1} \left(Q_1^4 \frac{4!}{1!2!1!} t_3 t_3 \right) a^\dagger a^\dagger a^\dagger a^\dagger a \\
 \\
 \begin{array}{|c|c|c|} \hline i \\ \hline \end{array} &= \frac{1}{4!} \frac{1}{1!} \frac{1}{2!} \frac{1}{2!} \overset{\diamond}{1} \sum_{ijkl,m} \sum_{abc} (Q_i^{abcm} t_{ajk} t_{bcl})_\sigma a_i^\dagger a_j^\dagger a_k^\dagger a_l^\dagger a_m \\
 \begin{array}{|c|c|c|} \hline j & k & a \\ \hline \end{array} & \begin{array}{|c|c|c|} \hline m & b & c & l \\ \hline \end{array}
 \end{aligned} \tag{3.28}$$

3.3 Solving the Non-Linear Cluster Amplitude

Equations

This diagrammatic scheme will be used to express the terms in $(He^T)_{C,open}$. After the diagrams are all accounted for, they can be sorted into a total ‘collection’ of diagrams

with the same overall structure. We will refer to such a collection as \hat{W}_R^S , denoted by a diagram with a double solid line for its vertex. This represents the sum of all diagrams with a certain operator signature R and S , an example of which is provided below for the collection \hat{W}_3^0 .

$$\begin{aligned}
\hat{W}_3^0 &= \text{Diagram with double solid line vertex} \\
&= \text{Diagram 1} + \text{Diagram 2} + \text{Diagram 3} + \text{Diagram 4} + \text{Diagram 5} + \text{Diagram 6} + \text{Diagram 7} + \text{Diagram 8} + \text{Diagram 9} + \text{Diagram 10} + \text{Diagram 11} + \text{Diagram 12} + \text{Diagram 13} + \text{Diagram 14} + \text{Diagram 15} + \dots
\end{aligned} \tag{3.29}$$

For reference, these diagrams are interpreted in their original operator representation below. We have removed the associated $a^\dagger a^\dagger a^\dagger$ from each term for simplicity.

$$\begin{aligned}
\frac{1}{3!} W_3^0 &= \frac{1}{3!} Q_3^0 + \frac{1}{3!} \omega \frac{3!}{1!2!} t_3 + \frac{1}{3!} Q_1^1 \frac{3!}{1!2!} t_3 + \frac{1}{3!} Q_0^1 t_4 + \\
&\frac{1}{3!} \frac{1}{2!} Q_2^2 \frac{3!}{2!1!} t_3 + \left(\frac{1}{3!} Q_0^2 \frac{3!}{1!2!} t_2 t_3 + \frac{1}{3!} \frac{1}{2!} Q_0^2 t_5 + \frac{1}{3!} Q_0^2 t_1 t_4 \right) + \\
&\frac{1}{3!} Q_2^1 \frac{3!}{2!1!} t_2 + \left(\frac{1}{3!} Q_1^2 \frac{3!}{1!2!} t_1 t_3 + \frac{1}{3!} \overset{\diamond}{\frac{1}{2!}} Q_1^2 \frac{3!}{1!1!1!} t_2 t_2 + \frac{1}{3!} \frac{1}{2!} Q_1^2 \frac{3!}{1!2!} t_4 \right) + \dots
\end{aligned} \tag{3.30}$$

At this point we return to the EoM-CC discussion, applying the diagrams and collections to derive any relevant cluster amplitudes t_n . These will be calculated using the coupled non-linear equations generated from (2.17), which can be written as follows for

the single oscillator case.

$$\left. \begin{aligned} \langle 0|a(He^T)_{C,open}|0\rangle &= 0 \\ \langle 0|aa(He^T)_{C,open}|0\rangle &= 0 \\ \langle 0|aaa\dots(He^T)_{C,open}|0\rangle &= 0 \end{aligned} \right\} \rightarrow t_1, t_2, t_3, \dots \quad (3.31)$$

The only diagrams which would contribute to a specific t_n equation are therefore those with exclusively creation operators. Any such diagrams would constitute a collection of the form \hat{W}_n^0 .

$$\begin{aligned} \langle 0|(a)^n(He^T)_{C,open}|0\rangle &= 0 \\ \langle 0|(a)^n\hat{W}_n^0|0\rangle &= 0 \\ \frac{1}{n!}W_n^0\langle 0|(a)^n(a^\dagger)^n|0\rangle &= 0 \rightarrow W_n^0 = 0 \end{aligned} \quad (3.32)$$

Therefore, the set of amplitudes t_n are simply solutions to the system of coupled non-linear equations $W_n^0 = 0$. These solutions can be found iteratively, by selecting some term in W_n^0 which directly connects to t_n alone. For consistency, we choose this to be the energy term $(\hat{\omega} \cdot T_n)_C$, denoted by the cross symbol in (3.29). This term comes from the unperturbed Hamiltonian, and will exist regardless of the perturbation or amplitude chosen. The equation can be manipulated to ‘solve’ for this diagram, as shown below for the t_3 case.

$$\begin{array}{c} \text{---} \\ | \\ | \\ \text{---} \end{array} = 0 \quad \rightarrow \quad \times \text{---} \begin{array}{c} | \\ | \\ | \\ \text{---} \end{array} = - \begin{array}{c} \text{---} \\ | \\ | \\ \text{---} \end{array} + \times \text{---} \begin{array}{c} | \\ | \\ | \\ \text{---} \end{array} \quad (3.33)$$

We will interpret the diagram on the left hand side as it appears in (3.30), simplifying the factorials down.

$$\frac{1}{2!}\omega t_3 = - \text{diagram} + \text{diagram} \quad (3.34)$$

This can be turned into an iterative scheme, where the associated diagrams are recalculated at each step using the full set of amplitudes until $t_3^{(i)}$ converges.

$$t_3^{(i+1)} = \frac{- \text{diagram}^{(i)} + \text{diagram}^{(i)}}{\frac{1}{2!}\omega} = \frac{-\frac{1}{3!}W_3^{0(i)} + \frac{1}{2!}\omega t_3^{(i)}}{\frac{1}{2!}\omega} \quad (3.35)$$

The coefficient W_3^0 is a function of all amplitudes, which couples the iterative scheme over all t_n equations. It should also be noted that there are a number of ways to affect the associated rate of convergence for the overall set of equations. First of all, the energy term $(\hat{\omega} \cdot T_3)_C$ is not the only diagram which connects to t_3 in the first order. Two other diagrams are shown in (3.29) which fulfill such a criterion.

$$\text{diagram} = \frac{1}{2!}\omega t_3 \quad ; \quad \text{diagram} = \frac{1}{2!}Q_1^1 t_3 \quad ; \quad \text{diagram} = \frac{1}{2!}\frac{1}{2!}Q_2^2 t_3 \quad (3.36)$$

Diagrams of this form can be picked out of the collection, to be incorporated in the iterative scheme as well. This can be used to improve convergence rates.

$$t_3^{(i+1)} = \frac{- \text{diagram}^{(i)} + \text{diagram}^{(i)} + \text{diagram}^{(i)} + \text{diagram}^{(i)} + \dots}{\frac{1}{2!}\omega + \frac{1}{2!}Q_1^1 + \frac{1}{2!}\frac{1}{2!}Q_2^2 + \dots} \quad (3.37)$$

Allow us now to generalize this equation for any cluster amplitude. The precise form of diagrams that can be moved into the iterative scheme are the fully connected results of some $(\hat{Q}_k^k \cdot T_n)_C$. The resulting diagram of interest would necessarily have an $n, 0$ operator signature, one k th order connection, and two groups of a^\dagger operators to symmetrize.

$$\sum_k^{n \geq k} \left(\frac{1}{n!} \frac{1}{0!} \cdot \frac{1}{k!} \cdot \frac{n!}{k!(n-k)!} Q_k^k t_n \right) = \sum_k^{n \geq k} \left(\frac{1}{k!} \frac{1}{k!(n-k)!} Q_k^k t_n \right) \quad (3.38)$$

Given the general interpretation of some energy term $(\hat{\omega} \cdot T_n)_C$, the iterative equation for t_n can be written as follows.

$$t_n^{(i+1)} = \frac{-\frac{1}{n!} W_n^{0(i)} + \frac{1}{(n-1)!} \omega t_n^{(i)} + \sum_k^{n \geq k} \left(\frac{1}{k!} \frac{1}{k!(n-k)!} Q_k^k t_n^{(i)} \right)}{\frac{1}{(n-1)!} \omega + \sum_k^{n \geq k} \left(\frac{1}{k!} \frac{1}{k!(n-k)!} Q_k^k \right)} \quad (3.39)$$

Again, it is not actually required to include any $(\hat{Q}_k^k \cdot T_n)_C$ diagrams in the above equation. They have no effect on the final converged value of the cluster amplitudes, only the convergence rate.

The values of $t_n^{(i)}$ from this scheme tend to be oscillatory, hopping between two solutions which converge as we continue to iterate. Instead of iterating directly from one value to the next, we can anticipate the oscillatory behavior and ‘guess’ a value which is the average of the two solutions. This entails running calculations using the midpoint of the two previous iterations, effectively shown below.

$$f(t_n^{(i)}) \rightarrow f\left(\frac{t_n^{(i)} + t_n^{(i-1)}}{2}\right) \quad (3.40)$$

3.4 Calculating Energies

Using the diagrammatic formalism, the perturbed ground state calculation becomes relatively straightforward. Recall the definition of (2.16), which states that the ground state energy consists only of closed terms in the Hamiltonian and any closed connected diagrams. Let us first express the closed terms in the Hamiltonian.

$$H_{closed} = \frac{1}{2}\omega + V_0 \tag{3.41}$$

In the above equation, V_0 represents the total scalar after all polynomial terms in the perturbation from (1.9) have been normal ordered. These scalars only come from even terms which can be fully contracted, for example the aa^\dagger in q^2 , the $(aa^\dagger aa^\dagger + aaaa^\dagger a^\dagger)$ in q^4 , and so on. We can therefore write the explicit form of V_0 as follows for the single oscillator.

$$V_0 = c + \frac{1}{2}\beta + \frac{3}{4}\delta + \dots \tag{3.42}$$

The other part of the ground state equation contains any closed terms from $(He^T)_C$. This is represented by the collection of diagrams \hat{W}_0^0 generated earlier.

$$\begin{aligned} (He^T)_{C,closed} &= \hat{W}_0^0 \\ &= \begin{array}{c} \text{---} \\ | \\ \bullet \end{array} + \left(\begin{array}{|c|} \hline \\ \hline \end{array} + \begin{array}{c} \text{---} \\ | \\ \bullet \end{array} \begin{array}{c} \text{---} \\ | \\ \bullet \end{array} \right) + \left(\begin{array}{|c|} \hline \\ \hline \end{array} \begin{array}{|c|} \hline \\ \hline \end{array} + \begin{array}{c} \text{---} \\ | \\ \bullet \end{array} \begin{array}{|c|} \hline \\ \hline \end{array} \right) + \\ &\quad \left(\begin{array}{c} \text{---} \\ | \\ \bullet \end{array} \begin{array}{c} \text{---} \\ | \\ \bullet \end{array} \begin{array}{c} \text{---} \\ | \\ \bullet \end{array} \right) + \left(\begin{array}{|c|} \hline \\ \hline \end{array} \begin{array}{|c|} \hline \\ \hline \end{array} \begin{array}{|c|} \hline \\ \hline \end{array} + \begin{array}{c} \text{---} \\ | \\ \bullet \end{array} \begin{array}{|c|} \hline \\ \hline \end{array} \begin{array}{|c|} \hline \\ \hline \end{array} \right) + \\ &\quad \left(\begin{array}{c} \text{---} \\ | \\ \bullet \end{array} \begin{array}{c} \text{---} \\ | \\ \bullet \end{array} \begin{array}{|c|} \hline \\ \hline \end{array} + \begin{array}{c} \text{---} \\ | \\ \bullet \end{array} \begin{array}{c} \text{---} \\ | \\ \bullet \end{array} \begin{array}{c} \text{---} \\ | \\ \bullet \end{array} \begin{array}{c} \text{---} \\ | \\ \bullet \end{array} + \begin{array}{|c|} \hline \\ \hline \end{array} \begin{array}{|c|} \hline \\ \hline \end{array} \right) + \dots \end{array} \tag{3.43}$$

Note that the only perturbation coefficients to appear in the ground state energy are of the form \hat{Q}_0^n . Hamiltonian terms with any associated a^\dagger operators cannot be reduced by connections, and therefore will only appear later in the amplitude convergence or excited state calculations.

Furthermore, the maximum perturbation order M limits which cluster amplitudes contribute directly. As V_M can form a closed diagram with the same order T_M at maximum, higher order amplitudes do not explicitly appear in the ground state equation. They instead provide corrections to lower order amplitudes when the EoM-CC convergence process takes place, resulting in more precise calculation of the ground state energy indirectly.

$$\begin{aligned}
\tilde{E}_0 &= H_{closed} + (He^T)_{C,closed} \\
&= \frac{1}{2}\omega + V_0 + W_0^0 \\
&= \frac{1}{2}\omega + V_0 + (Q_0^1 t_1) + \left(\frac{1}{2!} Q_0^2 t_2 + \frac{\hat{\diamond}}{2!} Q_0^2 t_1 t_1 \right) + \\
&\quad \left(\frac{1}{3!} Q_0^3 t_3 + \frac{1}{2!} Q_0^3 t_1 t_2 + \frac{\hat{\diamond}}{3!} Q_0^3 t_1 t_1 t_1 \right) + \\
&\quad \left(\frac{1}{4!} Q_0^4 t_4 + \frac{1}{3!} Q_0^4 t_1 t_3 + \frac{1}{2!} \frac{\hat{\diamond}}{2!} Q_0^4 t_1 t_1 t_2 + \frac{\hat{\diamond}}{4!} Q_0^4 t_1 t_1 t_1 t_1 + \frac{1}{2!} \frac{1}{2!} \frac{\hat{\diamond}}{2!} Q_0^4 t_2 t_2 \right) + \dots
\end{aligned} \tag{3.44}$$

This is the explicit form of the ground state energy, which can be easily calculated given the converged amplitudes from the previous section.

Let us also explore the excited state energies, derived from the effective Hamiltonian matrix $\bar{\mathbf{H}}$. The general form of this matrix was discussed in Section 2.3, though now we have a method by which to express the terms in $(He^T)_{C,open}$. The collections of

diagrams \hat{W}_m^n will directly contribute to the matrix elements, depending on the number of operators each one is associated with.

It should be noted that an element $\langle m|\bar{\mathbf{H}}|n\rangle$ does not only consist of W_m^n diagrams, but instead consists of all diagrams with a difference of operators $m - n$. For example, contributions to the matrix element $\langle 3|\bar{\mathbf{H}}|4\rangle$ should include all of \hat{W}_0^1 , \hat{W}_1^2 , \hat{W}_2^3 , and so on. The general form for any such contribution to the overall matrix element can be written as follows.

$$\langle m|\hat{W}_k^l|n\rangle = \frac{1}{k!} \frac{1}{l!} W_k^l \langle m|(a^\dagger)^k (a)^l|n\rangle = W_k^l \frac{\sqrt{m!n!}}{(n-l)!k!!} \quad \text{iff } m - k = n - l \quad (3.45)$$

Other diagrams provide no contribution to $\langle m|\bar{\mathbf{H}}|n\rangle$. Furthermore, a given collection of diagrams would only appear along one particular diagonal of the effective Hamiltonian. In other words, diagrams which appear in $\langle m|\bar{\mathbf{H}}|n\rangle$ would also necessarily appear in $\langle m+1|\bar{\mathbf{H}}|n+1\rangle$, $\langle m+2|\bar{\mathbf{H}}|n+2\rangle$, and so on, but nowhere else in the matrix.

3.5 Bogoliubov Transformations

To increase accuracy in calculated energies, the strategies of the EoM-CC method are to include higher levels of excitations in the cluster operator (2.2), or increase the space in which the effective Hamiltonian is diagonalized. The form of the Hamiltonian itself has an added effect on the precision of ground state calculations. This is highlighted by transforming the basis, from ladder operators a and a^\dagger to a more optimum set of ladder operators b and b^\dagger . This process is known as performing a Bogoliubov transformation

[Bogoljubov (1958), Hsue et al. (1985)]. Let us define the new ladder operators as follows.

$$b^\dagger = Fa^\dagger + Ga + D \quad ; \quad b = F^*a + G^*a^\dagger + D^* \quad (3.46)$$

We seek a transformation for which the b and b^\dagger operators still satisfy the bosonic commutation relation in (1.3), and therefore exhibit any other expected ladder operator behavior in their own $|n\rangle_b$ basis.

$$[b, b^\dagger] = 1 \quad ; \quad b^\dagger |n\rangle_b = \sqrt{n+1} |n+1\rangle_b \quad ; \quad b |n\rangle_b = \sqrt{n} |n-1\rangle_b \quad (3.47)$$

For simplicity, let us also assume the set of coefficients F , G , and D are real. Given that the commutation relation holds true for the transformed operators, we can then expand them to find a relation equating the two coefficients F and G .

$$\begin{aligned} [b, b^\dagger] &= bb^\dagger - b^\dagger b \\ &= (Fa^\dagger + Ga + D)(Fa + Ga^\dagger + D) - (Fa + Ga^\dagger + D)(Fa^\dagger + Ga + D) \quad (3.48) \\ &= F^2 - G^2 = 1 \end{aligned}$$

The transformed operator b must also annihilate the ground state in its basis, $|0\rangle_b$. Let S represent a general cluster operator akin to the T we've been using, such that we can express the transformed ground state as a linear combination over the complete set of states from a and a^\dagger .

$$|0\rangle_b = e^S |0\rangle \quad \rightarrow \quad b |0\rangle_b = be^S |0\rangle = 0 \quad (3.49)$$

Applying e^{-S} to either side, we can derive a set of relations using the BCH expansion. The Ga^\dagger term would commute with any term in e^S , and D is merely a constant, both of which allow us to write the following equation.

$$e^{-S}be^S |0\rangle = e^{-S}(Fa + Ga^\dagger + D)e^S |0\rangle = ((Fa, e^S)_C + Ga^\dagger + D) |0\rangle = 0 \quad (3.50)$$

Matching coefficients on either side and employing the use of (3.48), we arrive at the explicit relation between the cluster amplitudes and the Bogoliubov coefficients.

$$F = (1 - s_2^2)^{-1/2} \quad ; \quad G = -Fs_2 \quad ; \quad D = -Fs_1 \quad (3.51)$$

Given any cluster amplitudes s_1 and s_2 , we have the ability to construct a new set of transformed operators which satisfy all of the expected behavior using the above F , G , and D . For our case, we choose the converged cluster amplitudes $s_1 = t_1$ and $s_2 = t_2$ when we apply the above transformation to the problem. These transformations can then be applied iteratively, forming new Hamiltonians that can be solved diagrammatically for further accuracy. A generalized version of the unperturbed Hamiltonian can be written for such a scheme as follows.

$$H_0 = \frac{1}{2}\omega + \Delta a^\dagger a + \Lambda a^\dagger a^\dagger + \Lambda a a + \Gamma \quad ; \quad \Delta^{(0)} = \omega, \quad \Lambda^{(0)} = 0, \quad \Gamma^{(0)} = 0 \quad (3.52)$$

Though the original unperturbed Hamiltonian would have no Λ and Γ , the generalized form should account for any cross-terms that fall out of future iterative transformations. For an example of how this looks in practice, consider the above Hamiltonian with a

quartic polynomial perturbation. Note here that the q 's (and generally, p 's) in the perturbation inherently contain some combination of a^\dagger and a operators as shown in (1.6), and therefore must be transformed to the new basis too.

$$H = \frac{1}{2}\omega + \Delta a^\dagger a + \Lambda a^\dagger a^\dagger + \Lambda a a + \Gamma + (\alpha q + \beta q^2 + \gamma q^3 + \delta q^4) \quad (3.53)$$

By directly inverting and substituting in the operator definitions of (3.46) and collecting terms, one can prove that the above Hamiltonian can be rearranged into an identical form after being transformed.

$$H_b = \frac{1}{2}\omega + \Delta_b b^\dagger b + \Lambda_b b^\dagger b^\dagger + \Lambda_b b b + \Gamma_b + (\alpha_b q_b + \beta_b q_b^2 + \gamma_b q_b^3 + \delta_b q_b^4) \quad (3.54)$$

The new coefficients of the transformed Hamiltonian after one iteration are therefore defined as follows.

$$\begin{aligned} \Delta_b &= (F^2 + G^2)\Delta - 4FG\Lambda \\ \Lambda_b &= (F^2 + G^2)\Lambda - FG\Delta \\ \Gamma_b &= \Gamma + G^2\Delta - 2FG\Lambda + \left(\alpha\xi + (2\beta + \Delta + 2\Lambda)\frac{1}{2}\xi^2 + \gamma\xi^3 + \delta\xi^4 \right) \\ \alpha_b &= \mu (\alpha + (2\beta + \Delta + 2\Lambda)\xi + 3\gamma\xi^2 + 4\delta\xi^3) \\ \beta_b &= \mu^2 (\beta + 3\gamma\xi + 6\delta\xi^2) \quad ; \quad \gamma_b = \mu^3 (\gamma + 4\delta\xi) \quad ; \quad \delta_b = \mu^4\delta \end{aligned} \quad (3.55)$$

For simplicity, we have also introduced the following constants.

$$\mu = F - G \quad ; \quad \xi = \sqrt{2D}(G - F) \quad (3.56)$$

The above equations hold true for any future iterations as well, allowing us to apply the transformation a number of times to a point of convergence. The first major advantage of Bogoliubov transformations to highlight is that, according to (3.55), the coefficients of the transformed perturbation would converge to smaller values as they are slowly incorporated into the simple constant Γ . Though the perturbation coefficients generally do not converge to zero, the ability to decrease them by transferring some amount into the unperturbed Hamiltonian is still invaluable.

For every new effective Hamiltonian, we would run the EoM-CC equations to converge our cluster amplitudes in the transformed basis, resulting in a new t_1 and t_2 to create the next set of operators. The ground state equations can be recalculated after any of these iterations, using the closed parts of the new Hamiltonian and its associated connected terms. Firstly, the new scalar Γ should be included in H_{closed} , shown below.

$$H_{closed} = \frac{1}{2}\omega + \Gamma + V_0 \quad (3.57)$$

We also wish to include new diagrams from the generalized Hamiltonian, which is a relatively straightforward process. The Λ terms have an identical structure to the \hat{Q}_0^2 and \hat{Q}_2^0 diagrams, so therefore the two pairs can be collected into the same coefficients. Along with the diagram for $\omega a^\dagger a$ which has been generalized to some $\Delta a^\dagger a$, we can use

these new coefficients when interpreting diagrams in H and $(He^T)_C$.

$$\begin{aligned}
\begin{array}{|c} \times \cdots \\ \hline \end{array} & : \quad \omega a^\dagger a \quad \rightarrow \quad \Delta a^\dagger a \\
\begin{array}{|c} \hline \cdots \\ \hline \end{array} & : \quad \frac{1}{2!} Q_2^0 a^\dagger a^\dagger \quad \rightarrow \quad \frac{1}{2!} (Q_2^0 + 2!\Lambda) a^\dagger a^\dagger \\
\begin{array}{|c} \hline \hline \end{array} & : \quad \frac{1}{2!} Q_0^2 aa \quad \rightarrow \quad \frac{1}{2!} (Q_0^2 + 2!\Lambda) aa
\end{aligned} \tag{3.58}$$

This substitution applies to the two closed \hat{Q}_0^2 diagrams in the ground state calculation, as well as any others contributing to excited states. These would then represent the only steps needed to generalize the diagrammatic method. The second major advantage we find comes from (3.46), where we expect the coefficients to approach values of $F \rightarrow 1$, $G \rightarrow 0$, and $D \rightarrow 0$ as the iterative transformations converge. Given their explicit expressions in (3.51), running these iterations to convergence will necessarily result in a basis where our cluster amplitudes t_1 and t_2 both converge to zero.

3.6 Computational Scheme

As we have completed the discussion for deriving ground state and excited state energies, we can construct a code which runs through all the necessary numerical calculations. An explicit flowchart of the steps taken in this section are provided in [Figure 1](#).

(a.) Generate Diagrams

Based on the input truncation for V_M and T_N , we most crucially require a method to generate all possible diagrams. This should result in any nonzero collections \hat{W}_R^S , which would be referenced throughout later equations. It should be noted

that saving the resulting collections in some file would be ideal, as the generating process would then only need be run once for a given M and N . This is a deeply involved process, which acts as the core of the project to be addressed in detail later.

(b.) **Converge Amplitudes**

The iterative scheme to converge amplitudes is the next step. A number of parameters could be changed here by the user to affect convergence. These include which diagrams are included in the denominator, oscillatory dampening, and the tolerance with which to consider t_n converged. Rather than converging one amplitude order and then the next, the iterative scheme must run simultaneously over all t_n amplitudes, as their equations are coupled together by definition.

(c.) **Matrix Elements**

After calculating the ground state energy, we move on to the excited states. The construction of the matrix is represented as a loop of sorts, as all elements $\langle m|\bar{\mathbf{H}}|n\rangle$ must be calculated individually. For this reason, we note that constructing the matrix in practice takes up some nontrivial amount of time. This depends on the number of diagrams contributing to each given element, which in turn depends on the chosen perturbation and amplitude truncations V_M and T_N . Increasing matrix size to calculate higher excited states or increasing M and N to include more diagrams would therefore both lengthen the process.

(d.) **Bogoliubov Transformations**

We first note that Bogoliubov transformations can in principle be calculated im-

mediately after converging the cluster amplitudes, as the new Hamiltonian only depends on t_1 and t_2 . That being said, it is also possible to use any new Hamiltonians to generate their own ground state and excited state energies. In doing so, we can more easily track the effect of each iterative transformation on the overall system.

(e.) **Energy Output**

After the spectrum of eigenvalues is calculated from the diagonalized matrix $\overline{\mathbf{H}}$, some energy correction may appear depending on the matrix size and included amplitude orders. This does not occur in the physically accurate infinite case, nor for matrices of a truncated size $Z \leq N$, but is still shown for cases where it may be relevant.

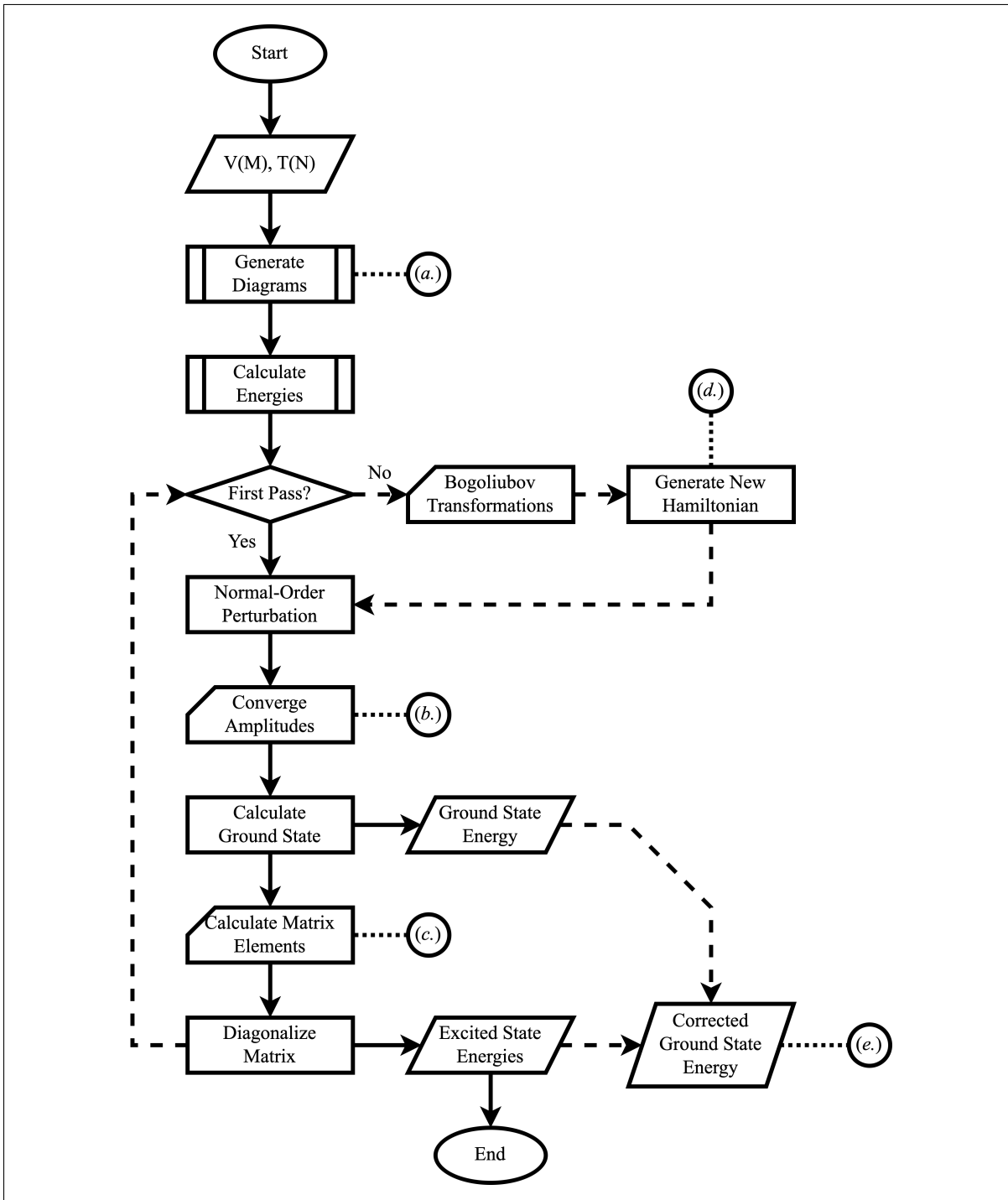


Figure 1: Flowchart for calculating the ground state and excited state energies.

Chapter 4

Considerations of Parity

4.1 Effects on Ladder Operators

As is common with many problems in physics, considering parity in certain systems of perturbed oscillators can greatly simplify our calculations. Proving that parity exists in the unperturbed case is trivial, and can be achieved by testing the transformation ($q \rightarrow -q$ and $p \rightarrow -p$) on (1.1). To derive the same result in the operator representation, allow us to define the parity operator P as follows.

$$P = e^{i\pi a^\dagger a} \tag{4.1}$$

The operator is defined such that eigenstates of the unperturbed Hamiltonian all have definite parity. Specifically, the parity operator will have eigenvalues of ± 1 depending on

whether the state is even or odd.

$$P |n\rangle = e^{i\pi a^\dagger a} |n\rangle = e^{i\pi n} |n\rangle = (-1)^n |n\rangle \quad (4.2)$$

Given this expression, we can make a handful of conclusions regarding symmetry in the perturbed case as well. This can be achieved by deriving some relation between P and any term in the perturbed Hamiltonian H . We begin by writing the result of some normal ordered product of ladder operators acting on an unperturbed state $|n\rangle$.

$$(a^\dagger)^k (a)^l |n\rangle = \frac{\sqrt{n!(n+k-l)!}}{(n-l)!} |n+k-l\rangle \quad (4.3)$$

The excitation level of the state is thus changed by $(k-l)$. If the parity operator is applied to the above equation, the coefficient is simply multiplied by a power of -1 .

$$P(a^\dagger)^k (a)^l |n\rangle = (-1)^{n+k-l} \frac{\sqrt{n!(n+k-l)!}}{(n-l)!} |n+k-l\rangle \quad (4.4)$$

Alternatively, we could apply the parity operator before any ladder operators. In this case, P acts directly on $|n\rangle$, and the power of -1 is not changed by k and l .

$$(a^\dagger)^k (a)^l P |n\rangle = (-1)^n \frac{\sqrt{n!(n+k-l)!}}{(n-l)!} |n+k-l\rangle \quad (4.5)$$

Together, these two equations form very general commutation relations between P and any operators which might be found in H . If the disparity in powers of -1 is even, we find that both results are identical and the terms commute. If the disparity in powers is

odd, the terms will anti-commute. The anti-commutator is denoted by the ‘+’ subscript below, such that $[A, B]_+ = AB + BA$.

$$\begin{aligned} [P, (a^\dagger)^k (a)^l] &= 0 \quad \text{iff} \quad (k - l) \text{ is even.} \\ [P, (a^\dagger)^k (a)^l]_+ &= 0 \quad \text{iff} \quad (k - l) \text{ is odd.} \end{aligned} \tag{4.6}$$

Consider for example, the unperturbed Hamiltonian as shown in (1.7). As it only contains two ladder operators, we know immediately that it commutes with the parity operator. Therefore, H and P share a common basis of eigenstates.

$$[P, H_0] = 0 \tag{4.7}$$

Any perturbation with an even number of ladder operators must also necessarily commute with P . Grouping terms in the perturbation by orders V_m allows us to write the following.

$$[P, V_2] = [P, V_4] = [P, V_6] = \dots = [P, V_{2a}] = 0 \tag{4.8}$$

As a result, the eigenstates of a Hamiltonian under any purely even perturbation (e.g., quadratic, quartic, sextic, octic, etc.) will have well defined parity identical to the associated eigenstate of the unperturbed Hamiltonian.

$$H_{\text{even}} = H_0 + V_0 + V_2 + V_4 + \dots \quad \rightarrow \quad [P, H_{\text{even}}] = 0 \tag{4.9}$$

Multiple simplifications in our formalism become applicable in the case of an even perturbation, but do not apply if parity is disrupted by the inclusion of any odd or-

ders. Even the lowest order inclusion of some V_1 term returns the problem to being asymmetrical, and the resulting perturbed eigenstates have no parity.

$$H = H_0 + V_0 + V_1 + V_2 + V_4 + \dots \quad \rightarrow \quad [P, H] = [P, V_1] \neq 0 \quad (4.10)$$

A similarly destructive phenomenon occurs in the case of an exclusively odd perturbation (e.g., linear, cubic, quintic, septic, etc.). Even if all perturbation orders are odd, the number of ladder operators in the unperturbed Hamiltonian is always two. Symmetry remains mixed in such a case, and the resulting perturbed eigenstates still have no parity.

$$H = H_0 + V_1 + V_3 + V_5 + \dots \quad \rightarrow \quad [P, H] \neq 0 \quad (4.11)$$

We will therefore limit discussion in the coming section to the simplifications exclusively found for H_{even} , before providing an example of a low-order even perturbation later in the document.

4.2 Simplifications for Even Parity Perturbations

Due to the fact that much of the coupled cluster formalism surrounds calculation of the perturbed ground state $|\tilde{0}\rangle$, we now focus our attention there. The unperturbed ground state $|0\rangle$ is known to be of even parity, and therefore $|\tilde{0}\rangle$ will be even as well. This means that rather than including all cluster operators as in (2.2), the new perturbed

ground state of H_{even} can be expressed as a linear combination of only even states.

$$T = T_2 + T_4 + T_6 + \dots \quad ; \quad t_1 = t_3 = t_5 = \dots = 0 \quad (4.12)$$

All of the V_M and T_N diagrammatic calculations would then continue as usual in the Python code. Diagram collections are still generated, sorted, and used to calculate the ground state energy, although any diagrams which include odd cluster amplitudes are calculated as having a value of zero. These odd cluster amplitudes would next come into use for Bogoliubov transformations, noting their form as given in (3.51). The resulting coefficients, such as those in (3.55) for the quartic case, are greatly simplified with $t_1 = D = \xi = 0$. The only remaining terms in the transformation are thus shown below.

$$\begin{aligned} \Delta_b &= (F^2 + G^2)\Delta - 4FG\Lambda \\ \Lambda_b &= (F^2 + G^2)\Lambda - FG\Delta \\ \Gamma_b &= \Gamma + G^2\Delta - 2FG\Lambda \\ \beta_b &= \mu^2\beta \quad ; \quad \delta_b = \mu^4\delta \quad ; \quad \mu = F - G \end{aligned} \quad (4.13)$$

This is the main reduction for calculations of the ground state, but the excited state derivation is notably simplified as well. Given that the odd cluster amplitudes become zero, nonzero diagrams will only be the result of connections between the even terms in the Hamiltonian with some combination of even cluster operators. Therefore, any collections of diagrams \hat{W}_k^l at this stage have an operator signature such that $(k - l)$ is even as well. Contributions to any matrix elements evaluated between states with an

odd difference as calculated in (3.45) will be zero, leading to the effective Hamiltonian matrix $\bar{\mathbf{H}}$ taking on a checkerboard pattern.

$$\bar{\mathbf{H}} = \begin{pmatrix} 0 & 0 & \langle 0|\bar{\mathbf{H}}|2\rangle & 0 & \cdots \\ 0 & \langle 1|\bar{\mathbf{H}}|1\rangle & 0 & \langle 1|\bar{\mathbf{H}}|3\rangle & \cdots \\ \langle 2|\bar{\mathbf{H}}|0\rangle & 0 & \langle 2|\bar{\mathbf{H}}|2\rangle & 0 & \cdots \\ 0 & \langle 3|\bar{\mathbf{H}}|1\rangle & 0 & \langle 3|\bar{\mathbf{H}}|3\rangle & \cdots \\ \vdots & \vdots & \vdots & \vdots & \ddots \end{pmatrix} \quad (4.14)$$

In this way, the elements of the matrix are completely decoupled by parity. Rearranging $\bar{\mathbf{H}}$ allows for the use of two separate block matrices, with one containing all even states and the other containing all odd states.

$$\begin{pmatrix} 0 & \langle 0|\bar{\mathbf{H}}|2\rangle & \langle 0|\bar{\mathbf{H}}|4\rangle & \cdots \\ \langle 2|\bar{\mathbf{H}}|0\rangle & \langle 2|\bar{\mathbf{H}}|2\rangle & \langle 2|\bar{\mathbf{H}}|4\rangle & \cdots \\ \langle 4|\bar{\mathbf{H}}|0\rangle & \langle 4|\bar{\mathbf{H}}|2\rangle & \langle 4|\bar{\mathbf{H}}|4\rangle & \cdots \\ \vdots & \vdots & \vdots & \ddots \end{pmatrix} \begin{pmatrix} s_{0k} \\ s_{2k} \\ s_{4k} \\ \vdots \end{pmatrix} = \Delta \tilde{E}_k \begin{pmatrix} s_{0k} \\ s_{2k} \\ s_{4k} \\ \vdots \end{pmatrix} \quad (4.15)$$

$$\begin{pmatrix} \langle 1|\bar{\mathbf{H}}|1\rangle & \langle 1|\bar{\mathbf{H}}|3\rangle & \langle 1|\bar{\mathbf{H}}|5\rangle & \cdots \\ \langle 3|\bar{\mathbf{H}}|1\rangle & \langle 3|\bar{\mathbf{H}}|3\rangle & \langle 3|\bar{\mathbf{H}}|5\rangle & \cdots \\ \langle 5|\bar{\mathbf{H}}|1\rangle & \langle 5|\bar{\mathbf{H}}|3\rangle & \langle 5|\bar{\mathbf{H}}|5\rangle & \cdots \\ \vdots & \vdots & \vdots & \ddots \end{pmatrix} \begin{pmatrix} s_{1k} \\ s_{3k} \\ s_{5k} \\ \vdots \end{pmatrix} = \Delta \tilde{E}_k \begin{pmatrix} s_{1k} \\ s_{3k} \\ s_{5k} \\ \vdots \end{pmatrix} \quad (4.16)$$

Although this reduced form of the matrix is not explicitly utilized in the more general code outlined in Figure 1 to keep things general, it still becomes useful to note the

decoupling of states when analyzing results. Allow us now to present a simple example where these results are applicable.

Chapter 5

The Quadratic Perturbation

5.1 Connecting Diagrams

In order to highlight the effects of parity, we look to the purely quadratic case. For a single oscillator in the q coordinate representation, such a perturbation may take the form of $V = \beta q^2$. Converting this to our normal-ordered operator representation results in the following expansion.

$$\beta q^2 = \frac{\beta}{2} (a^\dagger a^\dagger + 2a^\dagger a + aa + 1) \tag{5.1}$$

Each operator term in the perturbation would contain a product of two ladder operators. Let us briefly generalize to a multiple oscillator perturbation in order to discuss the full scope of the quadratic case, using the form shown in (1.11). This is the lowest-order

even perturbation, only including operators from the term V_2 alongside the scalar V_0 .

$$\begin{aligned}
V &= V_2 + V_0 \\
&= \frac{1}{2!} \sum_{ij} Q_{ij} a_i^\dagger a_j^\dagger + \sum_{ij} Q_i^j a_i^\dagger a_j + \frac{1}{2!} \sum_{ij} Q^{ij} a_i a_j + V_0
\end{aligned} \tag{5.2}$$

This quadratic perturbation will be added on to the unperturbed Hamiltonian, H_0 , to form the Hamiltonian of the system. Let us therefore separate the open and closed parts of the new Hamiltonian, expressing its open part using the diagrammatic scheme as follows.

$$\begin{aligned}
H_{open} &= \sum_{ij} \omega_i^j \delta_{ij} a_i^\dagger a_j + \frac{1}{2!} \sum_{ij} Q_{ij} a_i^\dagger a_j^\dagger + \sum_{ij} Q_i^j a_i^\dagger a_j + \frac{1}{2!} \sum_{ij} Q^{ij} a_i a_j \\
&= \begin{array}{c} \mathbf{x} \cdots \cdots \\ \left| \begin{array}{c} i \\ \hline j \end{array} \right. \\ \hline \end{array} + i \left[\begin{array}{c} \left| \begin{array}{c} \hline \\ \hline \end{array} \right. \\ \hline \end{array} \right] j + \begin{array}{c} \mathbf{\blacksquare} \cdots \cdots \\ \left| \begin{array}{c} i \\ \hline j \end{array} \right. \\ \hline \end{array} + i \left[\begin{array}{c} \left| \begin{array}{c} \hline \\ \hline \end{array} \right. \\ \hline \end{array} \right] j
\end{array} \tag{5.3}
\end{aligned}$$

$$H_{closed} = V_0 + \frac{1}{2} \sum_i \omega_i$$

The above diagrams in the open part were introduced as an example in (3.3). The form of the quadratic Hamiltonian allows us to make a handful of simplifications, starting with the cluster operators required for our calculation. As all included terms are of even parity, the cluster operator T takes on the form shown in (4.12).

$$T = T_2 + T_4 + T_6 + \dots \tag{5.4}$$

Any odd amplitudes are immediately taken to be zero. Additionally, note that the

term in H_{open} with the greatest number of annihilation operators is \hat{Q}^{ij} . With a maximum of two annihilation operators, the maximum number of amplitudes that can possibly connect is also two, leading to the self-truncation of the BCH expansion in (2.5). As a result, the only terms in the exponential cluster operator e^T which can connect are those below and including T^2 .

$$e^T \rightarrow 1 + T + \frac{1}{2!}T^2 \quad (5.5)$$

Note that this is not a truncation of e^T itself, but rather a simplification in practice as connections with higher-order terms cannot be created. There is one further simplification that can be made uniquely in the quadratic case. Let us begin by looking for terms in the perturbed Hamiltonian which directly contribute to the cluster equations (i.e., the collections of diagrams \hat{W}_n^0). The only such term is \hat{Q}_{ij} , which would be used in the calculation for T_2 . It can also be proven that using T_2 alone, generating diagrams which contribute to higher order cluster amplitudes is impossible with the given Hamiltonian. To illustrate this, we first truncate the cluster operator T at T_2 .

$$\begin{aligned} e^T &= e^{T_2} \rightarrow 1 + T_2 + \frac{1}{2!}T_2^2 \\ &= 1 + k \left[\begin{array}{|c|} \hline \\ \hline \end{array} \right] l + \frac{1}{2!} k \left[\begin{array}{|c|} \hline \\ \hline \end{array} \right] l m \left[\begin{array}{|c|} \hline \\ \hline \end{array} \right] n \end{aligned} \quad (5.6)$$

The connections between the Hamiltonian and e^{T_2} are then represented in diagram-

matic form as follows.

$$\begin{aligned}
(He^{T_2})_C = H_{open} &+ \begin{array}{c} i \\ \vdots \\ \times \text{---} \\ a \end{array} \begin{array}{c} | \\ | \\ | \\ \text{---} \\ | \\ j \end{array} + a \begin{array}{c} \text{---} \\ \square \\ \text{---} \end{array} b + j \begin{array}{c} \text{---} \\ \square \\ \text{---} \end{array} i + \\
& \begin{array}{c} i \\ \vdots \\ \blacksquare \text{---} \\ a \end{array} \begin{array}{c} | \\ | \\ | \\ \text{---} \\ | \\ j \end{array} + i \begin{array}{c} \text{---} \\ \square \\ \text{---} \end{array} \begin{array}{c} \text{---} \\ \square \\ \text{---} \end{array} b \begin{array}{c} | \\ | \\ | \\ \text{---} \\ | \\ j \end{array}
\end{aligned} \tag{5.7}$$

Note the inclusion of the original terms H_{open} shown in (5.3), the result of $(H \cdot 1)_C$. Using the diagrammatic rules, each term is interpreted in the operator representation below.

$$\begin{aligned}
(He^{T_2})_C = H_{open} &+ \frac{1}{2!} \sum_{ij} \sum_a (\omega_i^a \delta_{ai} t_{aj})_\sigma a_i^\dagger a_j^\dagger + \frac{1}{2!} \sum_{ab} Q^{ab} t_{ab} + \\
& \sum_{i,j} \sum_a Q^{aj} t_{ai} a_i^\dagger a_j + \frac{1}{2!} \sum_{ij} \sum_a (Q_i^a t_{aj})_\sigma a_i^\dagger a_j^\dagger + \\
& \frac{1}{2!} \frac{1}{2!} \sum_{ij} \sum_{ab} (Q^{ab} t_{ai} t_{bj})_\sigma a_i^\dagger a_j^\dagger
\end{aligned} \tag{5.8}$$

Given the relatively small number of terms required for symmetrization in this case, let us also write out the permuted σ coefficients explicitly.

$$\begin{aligned}
(He^{T_2})_C = H_{open} &+ \frac{1}{2!} \sum_{ij} \sum_a (\omega_i^a \delta_{ai} t_{aj} + \omega_j^a \delta_{aj} t_{ai}) a_i^\dagger a_j^\dagger + \frac{1}{2!} \sum_{ab} Q^{ab} t_{ab} + \\
& \sum_{i,j} \sum_a Q^{aj} t_{ai} a_i^\dagger a_j + \frac{1}{2!} \sum_{ij} \sum_a (Q_i^a t_{aj} + Q_j^a t_{ai}) a_i^\dagger a_j^\dagger + \\
& \frac{1}{2!} \frac{1}{2!} \sum_{ij} \sum_{ab} (2Q^{ab} t_{ai} t_{bj}) a_i^\dagger a_j^\dagger
\end{aligned} \tag{5.9}$$

This is the full form of the connected Hamiltonian using e^{T_2} . Just as before, we wish

to group terms with the same number of operators together. Gathering all available terms, the only groups formed are \hat{W}_{ij} , \hat{W}_i^j , \hat{W}^{ij} , and the leftover scalar \hat{W}_0^0 from the closed part of the connection.

$$\begin{aligned} (He^{T_2})_{C,open} &= \frac{1}{2!} \sum_{ij} W_{ij} a_i^\dagger a_j^\dagger + \sum_{ij} W_i^j a_i^\dagger a_j + \frac{1}{2!} \sum_{ij} W^{ij} a_i a_j \\ (He^{T_2})_{C,closed} &= W_0^0 \end{aligned} \quad (5.10)$$

The same conclusion can be reached straightforwardly with diagrams, by directly grouping terms in (5.7) into collections based on their signature.

$$(He^{T_2})_{C,open} = i \left[\begin{array}{c} | \\ | \\ \hline | \\ | \end{array} \right]_j + \left[\begin{array}{c} | \\ \hline | \\ | \end{array} \right]_i + i \left[\begin{array}{c} \hline | \\ | \\ | \end{array} \right]_j \quad (5.11)$$

The cluster amplitudes are generally given by the coupled set of equations $W_{ij\dots} = 0$, shown in (3.32) for the single oscillator case. However, no diagrams in $(He^{T_2})_{C,open}$ exist which contribute to T_4 or any higher order cluster amplitudes. Coupled with the crucial fact that none of the unconnected diagrams H_{open} contribute to these higher order amplitudes either, exclusively using T_2 for our calculations is sufficient. Even if T_4 , T_6 , and so on were forcibly included, their values would remain zero during the iterative scheme in the code.

For now, let us express the collections in both their diagrammatic and operator rep-

representations, beginning with \hat{W}_{ij} .

$$\begin{aligned}
\hat{W}_{ij} &= i \left[\begin{array}{c} \text{---} \\ \text{---} \\ | \\ | \\ \text{---} \end{array} \right] j \\
&= i \left[\begin{array}{c} | \\ | \\ \text{---} \\ | \\ | \\ \text{---} \end{array} \right] j + \times \left[\begin{array}{c} i \\ | \\ \text{---} \\ a \\ | \\ | \\ \text{---} \end{array} \right] j + \blacksquare \left[\begin{array}{c} i \\ | \\ \text{---} \\ a \\ | \\ | \\ \text{---} \end{array} \right] j + i \left[\begin{array}{c} \text{---} \\ a \\ \text{---} \\ | \\ | \\ \text{---} \\ b \\ \text{---} \\ | \\ | \\ \text{---} \end{array} \right] j
\end{aligned} \tag{5.12}$$

These diagrams have already been interpreted, but are shown again below without their associated summations and operators in order to focus on the coefficients themselves.

$$\begin{aligned}
\frac{1}{2!} W_{ij} &= \frac{1}{2!} Q_{ij} + \frac{1}{2!} \sum_a (\omega_i^a \delta_{ai} t_{aj} + \omega_j^a \delta_{aj} t_{ai}) + \\
&\frac{1}{2!} \sum_a (Q_i^a t_{aj} + Q_j^a t_{ai}) + \frac{1}{2!} \frac{1}{2!} \sum_{ab} (2Q^{ab} t_{ai} t_{bj})
\end{aligned} \tag{5.13}$$

Similarly, the collection \hat{W}_i^j consists of the following diagrams.

$$\begin{aligned}
\hat{W}_i^j &= \left[\begin{array}{c} \text{---} \\ | \\ | \\ \text{---} \end{array} \right] i = \times \left[\begin{array}{c} i \\ | \\ \text{---} \\ j \\ | \\ | \\ \text{---} \end{array} \right] i + \blacksquare \left[\begin{array}{c} i \\ | \\ \text{---} \\ j \\ | \\ | \\ \text{---} \end{array} \right] i + j \left[\begin{array}{c} \text{---} \\ | \\ a \\ \text{---} \\ | \\ | \\ \text{---} \\ i \end{array} \right] i \\
W_i^j &= \omega_i^j \delta_{ij} + Q_i^j + \sum_a Q^{aj} t_{ai}
\end{aligned} \tag{5.14}$$

The final collection of open diagrams, \hat{W}^{ij} , only contains a singular diagram which comes directly from the perturbed Hamiltonian.

$$\begin{aligned}
\hat{W}^{ij} &= i \left[\begin{array}{c} \text{---} \\ \text{---} \\ | \\ | \\ \text{---} \end{array} \right] j = i \left[\begin{array}{c} | \\ | \\ \text{---} \\ | \\ | \\ \text{---} \end{array} \right] j \\
\frac{1}{2!} W^{ij} &= \frac{1}{2!} Q^{ij}
\end{aligned} \tag{5.15}$$

We should also take care to collect any closed terms from the connection process, into the \hat{W}_0^0 group. These are terms without any remaining operators, and in this case, only one such diagram exists.

$$\begin{aligned}\hat{W}_0^0 &= a \boxed{} b \\ W_0^0 &= \frac{1}{2!} \sum_{ab} Q^{ab} t_{ab}\end{aligned}\tag{5.16}$$

As we have only used T_2 and V_2 in this problem, note that all coefficients $(Q_{ij}, Q_i^j, Q^{ij}, t_{kl})$ have two indices. It is therefore uniquely possible in the quadratic case to write each term using two-dimensional matrices. To accomplish this, let us define three new matrices with elements corresponding to different coefficients.

$$\mathbf{B}_{ij} = Q^{ij} \quad ; \quad \mathbf{J}_{ij} = Q_i^j \quad ; \quad (\mathbf{T}_2)_{ij} = t_{ij}\tag{5.17}$$

A handful of identities involving these matrices can be stated. Firstly, consider the complex conjugate of the \mathbf{B} matrix. This would be the equivalent of taking the complex conjugate of each element Q^{ij} , flipping the superscripts to subscripts. There is no need for a separate Q_{ij} matrix, as both coefficients are implicitly taken care of by \mathbf{B} .

Furthermore, consider the transpose of the \mathbf{B} and \mathbf{T}_2 matrices. As the associated elements are symmetric (i.e., $Q^{ij} = Q^{ji}$, $t_{ij} = t_{ji}$), the two matrices must be as well.

$$(\mathbf{B}_{ij})^* = Q_{ij} \quad ; \quad \mathbf{B}^T = \mathbf{B} \quad ; \quad (\mathbf{T}_2)^T = \mathbf{T}_2\tag{5.18}$$

Using these matrix definitions, let us rewrite (5.13), (5.14), and (5.15).

$$\begin{aligned}
W_{ij} &= (\mathbf{B}_{ij})^* + (\omega_i t_{ij} + \omega_j t_{ij}) + (\mathbf{J}\mathbf{T}_2)_{ij} + (\mathbf{T}_2\mathbf{J})_{ij} + (\mathbf{T}_2\mathbf{B}\mathbf{T}_2)_{ij} \\
W_i^j &= \omega_i \delta_{ij} + \mathbf{J}_{ij} + (\mathbf{T}_2\mathbf{B})_{ij} \\
W^{ij} &= \mathbf{B}_{ij}
\end{aligned} \tag{5.19}$$

Note above that the unconnected ω_i term only contributes to W_i^j for terms pertaining to the same oscillator ($i = j$). The closed W_0^0 collection in (5.16) can also be rewritten, using Tr to denote the trace of a matrix.

$$W_0^0 = \frac{1}{2!} \text{Tr}(\mathbf{B}\mathbf{T}_2) \tag{5.20}$$

As mentioned earlier, the cluster amplitudes are solutions to the coupled set of equations $W_{ij\dots} = 0$. With only one order of amplitudes T_2 , however, we only require one general equation.

$$W_{ij} = (\mathbf{B}_{ij})^* + (\omega_i t_{ij} + \omega_j t_{ij}) + (\mathbf{J}\mathbf{T}_2)_{ij} + (\mathbf{T}_2\mathbf{J})_{ij} + (\mathbf{T}_2\mathbf{B}\mathbf{T}_2)_{ij} = 0 \tag{5.21}$$

Forming an iterative scheme is quickly accomplished by solving for the t_{ij} amplitudes.

$$t_{ij}^{(n+1)} = - \frac{\left[\mathbf{B}^* + \mathbf{J}\mathbf{T}_2^{(n)} + \mathbf{T}_2^{(n)}\mathbf{J} + \mathbf{T}_2^{(n)}\mathbf{B}\mathbf{T}_2^{(n)} \right]_{ij}}{(\omega_i + \omega_j)} \tag{5.22}$$

With such a scheme, we would customarily begin by setting an initial value of $\mathbf{T}_2^{(0)} = 0$. Then, the next matrix iteration $\mathbf{T}_2^{(1)}$ is filled in element by element $t_{ij}^{(1)}$ using the above

equation. This process is repeated until all elements in the \mathbf{T}_2 matrix converge. Once this is achieved, the ground state is calculated from the closed parts of the connected and unconnected Hamiltonian.

$$\begin{aligned}\tilde{E}_0 &= H_{closed} + (He^T)_{C,closed} \\ &= \frac{1}{2} \sum_i \omega_i + V_0 + W_0^0 = E_0 + V_0 + \frac{1}{2!} \text{Tr}(\mathbf{B}\mathbf{T}_2)\end{aligned}\tag{5.23}$$

Let us now show the single oscillator equations explicitly, in order to compare the results. The diagrammatic structures shown in (5.7) are still applicable, only this time they must be interpreted for one oscillator. After the diagrams are sorted into collections, we find the following results.

$$\begin{aligned}\frac{1}{2!}W_2^0 &= \frac{1}{2!}Q_2^0 + \frac{1}{2!}\omega\frac{2!}{1!1!}t_2 + \frac{1}{2!}Q_1^1\frac{2!}{1!1!}t_2 + \frac{1}{2!}\overset{\diamond}{\frac{1}{2!}}Q_0^2\frac{2!}{1!1!}t_2t_2 \\ W_1^1 &= \omega + Q_1^1 + Q_0^2t_2 \\ \frac{1}{2!}W_0^2 &= \frac{1}{2!}Q_0^2 \\ W_0^0 &= \frac{1}{2!}Q_0^2t_2\end{aligned}\tag{5.24}$$

It becomes straightforward to generalize the collections above into the multiple oscillator collections (5.13), (5.14), (5.15), and (5.16). We will therefore continue to list out diagrammatic terms with their single oscillator form like this for longer equations in the next section, knowing that the multiple oscillator form can be easily achieved after applying the appropriate summations and symmetries as outlined by (3.28).

In order to compute the only cluster amplitude t_2 , we again seek the solution for

which $\hat{W}_2^0 = 0$. The term resulting from $(\hat{\omega} \cdot T_2)_C$ is highlighted below.

$$\frac{1}{2!}W_2^0 = \frac{1}{2!}Q_2^0 + \overbrace{\frac{1}{2!}\omega \frac{2!}{1!1!}t_2}^{(\hat{\omega} \cdot T_2)_C} + \frac{1}{2!}Q_1^1 \frac{2!}{1!1!}t_2 + \frac{1}{2!} \overset{\diamond}{\frac{1}{2!}} Q_0^2 \frac{2!}{1!1!} t_2 t_2 = 0 \quad (5.25)$$

Note that in the unique case of the single quadratic perturbation, the ‘coupled set of equations’ used to determine the amplitudes are instead a singular equation $W_2^0 = 0$ in the quadratic case. In this case alone, we have the opportunity to solve for t_2 directly.

$$t_2 = \frac{1}{Q_0^2} \left[-(\omega + Q_1^1) + \left((\omega + Q_1^1)^2 - |Q_0^2|^2 \right)^{1/2} \right] \quad (5.26)$$

This is not the usual case, and therefore we will continue by writing the iterative scheme to converge $t_2^{(n)}$. By solving for the $(\hat{\omega} \cdot T_2)_C$ term as described earlier, we can write an iterative scheme as follows.

$$t_2^{(n+1)} = - \frac{\frac{1}{2!}Q_2^0 + \frac{1}{2!}Q_1^1 \frac{2!}{1!1!}t_2^{(n)} + \frac{1}{2!} \overset{\diamond}{\frac{1}{2!}} Q_0^2 \frac{2!}{1!1!} t_2^{(n)} t_2^{(n)}}{\frac{1}{2!}\omega \frac{2!}{1!1!}} \quad (5.27)$$

In order to make this scheme mirror the matrix form in (5.22), we may cancel the $\frac{1}{2!}$ factorials in the numerator and denominator and simplify any leftover symmetrizing factors.

$$t_2^{(n+1)} = - \frac{Q_2^0 + 2! \cdot Q_1^1 t_2^{(n)} + Q_0^2 t_2^{(n)} t_2^{(n)}}{2! \cdot \omega} \quad (5.28)$$

While this explicit form is a direct visual match to the matrix equations, it becomes

more convenient in code to run a convergence scheme expressed in terms of the associated collection W_n^0 .

$$t_2^{(n+1)} = \frac{-\frac{1}{2!}W_2^{0(n)} + \frac{1}{2!}\omega\frac{2!}{1!1!}t_2^{(n)}}{\frac{1}{2!}\omega\frac{2!}{1!1!}} = \frac{-\frac{1}{2!}W_2^{0(n)} + \omega t_2^{(n)}}{\omega} \quad (5.29)$$

This form now matches the generalized iterative scheme devised in (3.39). As before, we can also choose to separate other diagrams of a particular form (e.g., $(\hat{Q}_1^1 \cdot T_2)_C$ in this case) to change the rate of convergence.

$$t_2^{(n+1)} = \frac{-\frac{1}{2!}W_2^{0(n)} + (\omega + Q_1^1)t_2^{(n)}}{\omega + Q_1^1} \quad (5.30)$$

This is the general scheme that would be used in the code, as if we were expecting an arbitrary V_M and T_N being used. Any of the schemes listed above would necessarily result in the same converged value of t_2 , which is then used to calculate the ground state energy.

$$\begin{aligned} \tilde{E}_0 &= H_{closed} + (He^T)_{C,closed} = \frac{1}{2}\omega + V_0 + \frac{1}{2!}Q_0^2 t_2 \\ &= E_0 + V_0 + \frac{1}{2!}Q_0^2 t_2 \end{aligned} \quad (5.31)$$

5.2 Quadratic Excited States

With the explicit form of the ground state revealed, we now look to calculate the excited state energies from the effective Hamiltonian matrix $\bar{\mathbf{H}}$. The purely quadratic perturbation leaves us with an even Hamiltonian, which we have already shown takes on

the decoupled form in (4.15) and (4.16).

$$\begin{pmatrix} 0 & \langle 0|\bar{\mathbf{H}}|2\rangle & \langle 0|\bar{\mathbf{H}}|4\rangle & \langle 0|\bar{\mathbf{H}}|6\rangle & \cdots \\ \langle 2|\bar{\mathbf{H}}|0\rangle & \langle 2|\bar{\mathbf{H}}|2\rangle & \langle 2|\bar{\mathbf{H}}|4\rangle & \langle 2|\bar{\mathbf{H}}|6\rangle & \cdots \\ \langle 4|\bar{\mathbf{H}}|0\rangle & \langle 4|\bar{\mathbf{H}}|2\rangle & \langle 4|\bar{\mathbf{H}}|4\rangle & \langle 4|\bar{\mathbf{H}}|6\rangle & \cdots \\ \langle 6|\bar{\mathbf{H}}|0\rangle & \langle 6|\bar{\mathbf{H}}|2\rangle & \langle 6|\bar{\mathbf{H}}|4\rangle & \langle 6|\bar{\mathbf{H}}|6\rangle & \cdots \\ \vdots & \vdots & \vdots & \vdots & \ddots \end{pmatrix} \begin{pmatrix} s_{0k} \\ s_{2k} \\ s_{4k} \\ s_{6k} \\ \vdots \end{pmatrix} = \Delta \tilde{E}_k \begin{pmatrix} s_{0k} \\ s_{2k} \\ s_{4k} \\ s_{6k} \\ \vdots \end{pmatrix} \quad (5.32)$$

$$\begin{pmatrix} \langle 1|\bar{\mathbf{H}}|1\rangle & \langle 1|\bar{\mathbf{H}}|3\rangle & \langle 1|\bar{\mathbf{H}}|5\rangle & \langle 1|\bar{\mathbf{H}}|7\rangle & \cdots \\ \langle 3|\bar{\mathbf{H}}|1\rangle & \langle 3|\bar{\mathbf{H}}|3\rangle & \langle 3|\bar{\mathbf{H}}|5\rangle & \langle 3|\bar{\mathbf{H}}|7\rangle & \cdots \\ \langle 5|\bar{\mathbf{H}}|1\rangle & \langle 5|\bar{\mathbf{H}}|3\rangle & \langle 5|\bar{\mathbf{H}}|5\rangle & \langle 5|\bar{\mathbf{H}}|7\rangle & \cdots \\ \langle 7|\bar{\mathbf{H}}|1\rangle & \langle 7|\bar{\mathbf{H}}|3\rangle & \langle 7|\bar{\mathbf{H}}|5\rangle & \langle 7|\bar{\mathbf{H}}|7\rangle & \cdots \\ \vdots & \vdots & \vdots & \vdots & \ddots \end{pmatrix} \begin{pmatrix} s_{1k} \\ s_{3k} \\ s_{5k} \\ s_{7k} \\ \vdots \end{pmatrix} = \Delta \tilde{E}_k \begin{pmatrix} s_{1k} \\ s_{3k} \\ s_{5k} \\ s_{7k} \\ \vdots \end{pmatrix} \quad (5.33)$$

Noting the collections in (5.11), we see that the only number of operators in any open term is two. Therefore, the only nonzero matrix elements are those evaluated between states with a difference of two or less. For example, the element $\langle 7|\bar{\mathbf{H}}|3\rangle$ must necessarily

be zero, as there are no terms associated with $a^\dagger a^\dagger a^\dagger a^\dagger$, $a^\dagger a^\dagger a^\dagger a^\dagger a^\dagger a$, and so on.

$$\begin{pmatrix} 0 & \langle 0|\bar{\mathbf{H}}|2\rangle & 0 & 0 & \cdots \\ \langle 2|\bar{\mathbf{H}}|0\rangle & \langle 2|\bar{\mathbf{H}}|2\rangle & \langle 2|\bar{\mathbf{H}}|4\rangle & 0 & \cdots \\ 0 & \langle 4|\bar{\mathbf{H}}|2\rangle & \langle 4|\bar{\mathbf{H}}|4\rangle & \langle 4|\bar{\mathbf{H}}|6\rangle & \cdots \\ 0 & 0 & \langle 6|\bar{\mathbf{H}}|4\rangle & \langle 6|\bar{\mathbf{H}}|6\rangle & \cdots \\ \vdots & \vdots & \vdots & \vdots & \ddots \end{pmatrix} \begin{pmatrix} s_{0k} \\ s_{2k} \\ s_{4k} \\ s_{6k} \\ \vdots \end{pmatrix} = \Delta \tilde{E}_k \begin{pmatrix} s_{0k} \\ s_{2k} \\ s_{4k} \\ s_{6k} \\ \vdots \end{pmatrix} \quad (5.34)$$

$$\begin{pmatrix} \langle 1|\bar{\mathbf{H}}|1\rangle & \langle 1|\bar{\mathbf{H}}|3\rangle & 0 & 0 & \cdots \\ \langle 3|\bar{\mathbf{H}}|1\rangle & \langle 3|\bar{\mathbf{H}}|3\rangle & \langle 3|\bar{\mathbf{H}}|5\rangle & 0 & \cdots \\ 0 & \langle 5|\bar{\mathbf{H}}|3\rangle & \langle 5|\bar{\mathbf{H}}|5\rangle & \langle 5|\bar{\mathbf{H}}|7\rangle & \cdots \\ 0 & 0 & \langle 7|\bar{\mathbf{H}}|5\rangle & \langle 7|\bar{\mathbf{H}}|7\rangle & \cdots \\ \vdots & \vdots & \vdots & \vdots & \ddots \end{pmatrix} \begin{pmatrix} s_{1k} \\ s_{3k} \\ s_{5k} \\ s_{7k} \\ \vdots \end{pmatrix} = \Delta \tilde{E}_k \begin{pmatrix} s_{1k} \\ s_{3k} \\ s_{5k} \\ s_{7k} \\ \vdots \end{pmatrix} \quad (5.35)$$

This is the general form of the effective Hamiltonian with a quadratic perturbation.

We can simplify things even further if the t_2 amplitude is converged, as the equation used

to find its convergence is simply $\frac{1}{2!}W_2^0 a^\dagger a^\dagger = 0$. In other words, calculating the $\bar{\mathbf{H}}$ matrix with converged values of t_2 means that the $a^\dagger a^\dagger$ collection is zero, causing the elements

$\langle m + 2 | \bar{\mathbf{H}} | m \rangle$ to all become zero in turn.

$$\begin{pmatrix} 0 & \langle 0 | \bar{\mathbf{H}} | 2 \rangle & 0 & 0 & \cdots \\ 0 & \langle 2 | \bar{\mathbf{H}} | 2 \rangle & \langle 2 | \bar{\mathbf{H}} | 4 \rangle & 0 & \cdots \\ 0 & 0 & \langle 4 | \bar{\mathbf{H}} | 4 \rangle & \langle 4 | \bar{\mathbf{H}} | 6 \rangle & \cdots \\ 0 & 0 & 0 & \langle 6 | \bar{\mathbf{H}} | 6 \rangle & \cdots \\ \vdots & \vdots & \vdots & \vdots & \ddots \end{pmatrix} \begin{pmatrix} s_{0k} \\ s_{2k} \\ s_{4k} \\ s_{6k} \\ \vdots \end{pmatrix} = \Delta \tilde{E}_k \begin{pmatrix} s_{0k} \\ s_{2k} \\ s_{4k} \\ s_{6k} \\ \vdots \end{pmatrix} \quad (5.36)$$

$$\begin{pmatrix} \langle 1 | \bar{\mathbf{H}} | 1 \rangle & \langle 1 | \bar{\mathbf{H}} | 3 \rangle & 0 & 0 & \cdots \\ 0 & \langle 3 | \bar{\mathbf{H}} | 3 \rangle & \langle 3 | \bar{\mathbf{H}} | 5 \rangle & 0 & \cdots \\ 0 & 0 & \langle 5 | \bar{\mathbf{H}} | 5 \rangle & \langle 5 | \bar{\mathbf{H}} | 7 \rangle & \cdots \\ 0 & 0 & 0 & \langle 7 | \bar{\mathbf{H}} | 7 \rangle & \cdots \\ \vdots & \vdots & \vdots & \vdots & \ddots \end{pmatrix} \begin{pmatrix} s_{1k} \\ s_{3k} \\ s_{5k} \\ s_{7k} \\ \vdots \end{pmatrix} = \Delta \tilde{E}_k \begin{pmatrix} s_{1k} \\ s_{3k} \\ s_{5k} \\ s_{7k} \\ \vdots \end{pmatrix} \quad (5.37)$$

With the converged t_2 , both matrices become upper diagonal. As such, the eigenvalues are straightforwardly given by the diagonal elements $\langle m | \bar{\mathbf{H}} | m \rangle$ and there is no longer any need for diagonalization.

$$\begin{aligned} \Delta \tilde{E}_m &= \langle m | \bar{\mathbf{H}} | m \rangle = \langle m | \hat{W}_1^1 | m \rangle = m W_1^1 \\ &= m (\omega + Q_1^1 + Q_0^2 t_2) \end{aligned} \quad (5.38)$$

To better explain this result, let us call the value in parentheses some new $\tilde{\omega}$. The

excited states can then be written explicitly as follows.

$$\begin{aligned} \tilde{\omega} = \omega + Q_1^1 + Q_0^2 t_2 \quad \rightarrow \quad \Delta \tilde{E}_m = \tilde{E}_m - \tilde{E}_0 = m\tilde{\omega} \\ \tilde{E}_m = m\tilde{\omega} + \tilde{E}_0 \end{aligned} \tag{5.39}$$

One can also express the ground state energy in terms of this $\tilde{\omega}$.

$$\begin{aligned} \tilde{E}_0 &= \frac{1}{2}\omega + V_0 + \frac{1}{2!}Q_0^2 t_2 \\ &= \frac{1}{2}(\omega + Q_1^1 + Q_0^2 t_2) + \left(V_0 - \frac{1}{2}Q_1^1\right) = \frac{1}{2}\tilde{\omega} + \left(V_0 - \frac{1}{2}Q_1^1\right) \end{aligned} \tag{5.40}$$

The full list of excited state energies is then given by the following equation.

$$\tilde{E}_m = \left(m + \frac{1}{2}\right)\tilde{\omega} + \left(V_0 - \frac{1}{2}Q_1^1\right) \tag{5.41}$$

We have therefore shown that a harmonic oscillator under a purely quadratic perturbation can simply be expressed as a new harmonic oscillator. The ground state energy of the new oscillator has been shifted up by $\left(V_0 - \frac{1}{2}Q_1^1\right)$, and the transition energy of the new oscillator is given by $\tilde{\omega} = \omega + Q_1^1 + Q_0^2 t_2$.

5.3 Quadratic Bogoliubov Transformations

As noted in Section 4.2, the formalism for Bogoliubov transformations simplifies significantly for even perturbations. Let us begin by generalizing the form of the perturbed

Hamiltonian itself, using the coefficients Δ , Λ , and Γ .

$$\begin{aligned}
H &= \frac{\omega}{2} + \Delta^{(0)} a^\dagger a + \Lambda^{(0)} a^\dagger a^\dagger + \Lambda^{(0)} a a + \Gamma^{(0)} + \beta^{(0)} q^2 \\
&= \frac{\omega}{2} + \Delta^{(0)} a^\dagger a + \Lambda^{(0)} a^\dagger a^\dagger + \Lambda^{(0)} a a + \Gamma^{(0)} + \beta^{(0)} \left[\frac{1}{\sqrt{2}} (a^\dagger + a) \right]^2
\end{aligned} \tag{5.42}$$

As is customary, the coefficients keep their initial values of $\Delta^{(0)} = \omega$, $\Lambda^{(0)} = 0$, and $\Gamma^{(0)} = 0$ shown in (3.52). Let us directly apply one Bogoliubov transformation, writing the generalized Hamiltonian in terms of the new operators b^\dagger and b .

$$\begin{aligned}
b &= F a + G a^\dagger & ; & & a &= F b - G b^\dagger \\
b^\dagger &= G a + F a^\dagger & ; & & a^\dagger &= -G b + F b^\dagger
\end{aligned} \tag{5.43}$$

The Δ and Λ terms are expanded and normal-ordered as shown below.

$$\begin{aligned}
\Delta^{(0)} a^\dagger a &= \Delta^{(0)} ((F^2 + G^2) b^\dagger b - F G b^\dagger b^\dagger - F G b b + G^2) \\
\Lambda^{(0)} (a^\dagger a^\dagger + a a) &= \Lambda^{(0)} ((F^2 + G^2) (b^\dagger b^\dagger + b b) - 4 F G b^\dagger b - 2 F G)
\end{aligned} \tag{5.44}$$

The quadratic perturbation must also be transformed, though we note that it takes on a unique form as well.

$$\begin{aligned}
\beta^{(0)} \left[\frac{1}{\sqrt{2}} (a^\dagger + a) \right]^2 &= (F - G)^2 \beta^{(0)} \left[\frac{1}{\sqrt{2}} (b^\dagger + b) \right]^2 \\
&= (F - G)^2 \frac{\beta^{(0)}}{2} (b^\dagger b^\dagger + 2 b^\dagger b + b b + 1)
\end{aligned} \tag{5.45}$$

As the transformed quadratic perturbation will always result in pairs of two operators (and a constant), the perturbed terms could easily be expanded and grouped in with

$\Delta^{(1)}$, $\Lambda^{(1)}$, and $\Gamma^{(1)}$. This suggests that a new ‘unperturbed’ Hamiltonian in the b^\dagger and b representation can be created in a single transformation, similar to what was shown in (5.41) by the excited states.

This can be explicitly achieved using the matrix representation of a Bogoliubov transformation. Let us write the operator definitions in (5.43) as follows.

$$\begin{pmatrix} b \\ b^\dagger \end{pmatrix} = \begin{pmatrix} F & G \\ G & F \end{pmatrix} \begin{pmatrix} a \\ a^\dagger \end{pmatrix} \quad (5.46)$$

The square matrix of coefficients above can be quickly inverted, leading to the two inverse relationships in (5.43).

$$\begin{pmatrix} a \\ a^\dagger \end{pmatrix} = \begin{pmatrix} F & -G \\ -G & F \end{pmatrix} \begin{pmatrix} b \\ b^\dagger \end{pmatrix} \quad (5.47)$$

Let us apply these new matrix transformations to the normal-ordered quadratic Hamiltonian with coefficients Q .

$$H = \omega a^\dagger a + \frac{1}{2!} Q_2^0 a^\dagger a^\dagger + Q_1^1 a^\dagger a + \frac{1}{2!} Q_0^2 a a + V_0 + \frac{1}{2} \omega \quad (5.48)$$

In order to perform matrix transformations here, we must first write the Hamiltonian itself using matrices. This can be done by introducing a new square matrix \mathbf{h}_a .

$$H = \begin{pmatrix} a^\dagger & a \end{pmatrix} \mathbf{h}_a \begin{pmatrix} a \\ a^\dagger \end{pmatrix} + V_0 + \frac{1}{2} \omega \quad (5.49)$$

When expanded out, the matrix multiplication above generates all combinations of a^\dagger and a . These can then be compared to the existing coefficients Q .

$$\begin{pmatrix} a^\dagger & a \end{pmatrix} \begin{pmatrix} \mathbf{h}_{00} & \mathbf{h}_{01} \\ \mathbf{h}_{10} & \mathbf{h}_{11} \end{pmatrix} \begin{pmatrix} a \\ a^\dagger \end{pmatrix} = \mathbf{h}_{00}a^\dagger a + \mathbf{h}_{01}a^\dagger a^\dagger + \mathbf{h}_{10}aa + \mathbf{h}_{11}aa^\dagger \quad (5.50)$$

As the Hamiltonian is assumed to be normal-ordered, we must always have that $\mathbf{h}_{11} = 0$. The other elements of \mathbf{h}_a are written as follows.

$$\mathbf{h}_a = \begin{pmatrix} \omega + Q_1^1 & \frac{1}{2!}Q_2^0 \\ \frac{1}{2!}Q_0^2 & 0 \end{pmatrix} \quad (5.51)$$

A Bogoliubov transformation now entails writing the multiplied matrices above in terms of the new Bogoliubov operators b^\dagger and b . This would change the square matrix \mathbf{h}_a into some new matrix \mathbf{h}_b , with the two related as follows.

$$\begin{pmatrix} a^\dagger & a \end{pmatrix} \mathbf{h}_a \begin{pmatrix} a \\ a^\dagger \end{pmatrix} = \begin{pmatrix} b^\dagger & b \end{pmatrix} \mathbf{h}_b \begin{pmatrix} b \\ b^\dagger \end{pmatrix} \quad (5.52)$$

Using the inverse relationships, it can be shown that \mathbf{h}_b is simply the result of the

following matrix multiplication.

$$\begin{aligned}
\mathbf{h}_b &= \begin{pmatrix} F & -G \\ -G & F \end{pmatrix} \mathbf{h}_a \begin{pmatrix} F & -G \\ -G & F \end{pmatrix} \\
&= \begin{pmatrix} F & -G \\ -G & F \end{pmatrix} \begin{pmatrix} \mathbf{h}_{00} & \mathbf{h}_{01} \\ \mathbf{h}_{10} & \mathbf{h}_{11} \end{pmatrix} \begin{pmatrix} F & -G \\ -G & F \end{pmatrix}
\end{aligned} \tag{5.53}$$

Expanding the product of all three matrices allows us to express \mathbf{h}_b in terms of the known elements of \mathbf{h}_a .

$$\mathbf{h}_b = \begin{pmatrix} \mathbf{h}_{00}F^2 - \mathbf{h}_{01}FG - \mathbf{h}_{10}FG + \mathbf{h}_{11}G^2 & -\mathbf{h}_{00}FG + \mathbf{h}_{01}F^2 + \mathbf{h}_{10}G^2 - \mathbf{h}_{11}FG \\ -\mathbf{h}_{00}FG + \mathbf{h}_{01}G^2 + \mathbf{h}_{10}F^2 - \mathbf{h}_{11}FG & \mathbf{h}_{00}G^2 - \mathbf{h}_{01}FG - \mathbf{h}_{10}FG + \mathbf{h}_{11}F^2 \end{pmatrix} \tag{5.54}$$

The matrix can be greatly simplified using the form of the Hamiltonian. As mentioned before, the operators are normal-ordered such that $\mathbf{h}_{11} = 0$. As the Hamiltonian is Hermitian (i.e., $Q_2^0 = Q_0^2$), we must also have $\mathbf{h}_{10} = \mathbf{h}_{01}$. This allows us to combine terms as follows.

$$\mathbf{h}_b = \begin{pmatrix} \mathbf{h}_{00}F^2 - 2\mathbf{h}_{01}FG & -\mathbf{h}_{00}FG + \mathbf{h}_{01}(F^2 + G^2) \\ -\mathbf{h}_{00}FG + \mathbf{h}_{01}(F^2 + G^2) & \mathbf{h}_{00}G^2 - 2\mathbf{h}_{01}FG \end{pmatrix} \tag{5.55}$$

We lastly use the relationship between F and G defined in (3.51), such that each

element contains some factor of F^2 .

$$\mathbf{h}_b = \begin{pmatrix} \mathbf{h}_{00}F^2 + 2\mathbf{h}_{01}F^2s_2 & \mathbf{h}_{00}F^2s_2 + \mathbf{h}_{01}F^2(1 + s_2^2) \\ \mathbf{h}_{00}F^2s_2 + \mathbf{h}_{01}F^2(1 + s_2^2) & \mathbf{h}_{00}F^2s_2^2 + 2\mathbf{h}_{01}F^2s_2 \end{pmatrix} \quad (5.56)$$

For any value of s_2 chosen, we can make a new transformed matrix of the form \mathbf{h}_b . Let us therefore solve for the value of s_2 needed to diagonalize the matrix (i.e., to make the off-diagonal elements zero).

$$\begin{aligned} \mathbf{h}_{00}F^2s_2 + \mathbf{h}_{01}F^2(1 + s_2^2) &= 0 \\ F^2(\mathbf{h}_{01} + \mathbf{h}_{00}s_2 + \mathbf{h}_{01}s_2^2) &= 0 \\ \mathbf{h}_{01} + \mathbf{h}_{00}s_2 + \mathbf{h}_{01}s_2^2 &= 0 \\ \frac{1}{2!}Q_2^0 + (\omega + Q_1^1)s_2 + \frac{1}{2!}Q_2^0s_2^2 &= 0 \end{aligned} \quad (5.57)$$

Comparing this equation to (5.25), we find that this is equivalent to the convergence criterion for t_2 . In other words, the new Hamiltonian \mathbf{h}_b is proven to become diagonalized after a transformation using the converged amplitude $s_2 = t_2$.

$$\mathbf{h}_b = \begin{pmatrix} \mathbf{h}_{00}F^2 + 2\mathbf{h}_{01}F^2t_2 & 0 \\ 0 & \mathbf{h}_{00}F^2t_2^2 + 2\mathbf{h}_{01}F^2t_2 \end{pmatrix} \quad (5.58)$$

Let us call these two elements $\mathbf{h}_{b,11}$ and $\mathbf{h}_{b,22}$. Factoring out an F^2 , both terms can

be expressed only in terms of t_2 using (3.51).

$$\begin{aligned}\mathbf{h}_{b,11} &= (1 - t_2^2)^{-1} (\mathbf{h}_{00} + 2\mathbf{h}_{01}t_2) \\ \mathbf{h}_{b,22} &= (1 - t_2^2)^{-1} (\mathbf{h}_{00}t_2^2 + 2\mathbf{h}_{01}t_2)\end{aligned}\tag{5.59}$$

With the newly diagonalized \mathbf{h}_b , the matrix multiplication in the Hamiltonian reduces to the following in terms of b^\dagger and b .

$$\begin{aligned}\begin{pmatrix} b^\dagger & b \end{pmatrix} \mathbf{h}_b \begin{pmatrix} b \\ b^\dagger \end{pmatrix} &= \mathbf{h}_{b,11} b^\dagger b + \mathbf{h}_{b,22} b b^\dagger \\ &= (\mathbf{h}_{b,11} + \mathbf{h}_{b,22}) b^\dagger b + \mathbf{h}_{b,22}\end{aligned}\tag{5.60}$$

As expected, the Hamiltonian can be represented by a new harmonic oscillator in b^\dagger and b after only one Bogoliubov transformation.

$$H = (\mathbf{h}_{b,11} + \mathbf{h}_{b,22}) b^\dagger b + \mathbf{h}_{b,22} + V_0 + \frac{1}{2}\omega\tag{5.61}$$

5.4 Links to Perturbation Theory

Let us also provide some context linking the illustrated behavior of the quadratic case to perturbation theory. Recall that by taking the effective Hamiltonian matrix $\overline{\mathbf{H}}$ at $T = 0$, the only remaining terms constitute the open part of the original perturbed Hamiltonian H as shown in (2.23). The coupled cluster results using no amplitudes can therefore be roughly compared with those from perturbation theory.

To start, consider the Hamiltonian matrix truncated at the second excited state for simplicity. The matrix elements themselves include the unperturbed energies along the diagonal, in addition to the other $\langle m|V|n\rangle$ perturbation terms filling out the matrix. We will temporarily employ the shorthand V_{mn} for these elements, such that the Hamiltonian is written as follows.

$$\mathbf{H} = \begin{pmatrix} E_0 + \langle 0|V|0\rangle & \langle 0|V|2\rangle \\ \langle 2|V|0\rangle & E_2 + \langle 2|V|2\rangle \end{pmatrix} = \begin{pmatrix} E_0 + V_{00} & V_{02} \\ V_{20} & E_2 + V_{22} \end{pmatrix} \quad (5.62)$$

Solving for the eigenvalues of the matrix can be accomplished using the characteristic equation. We will call the two solutions λ_0 and λ_2 .

$$\lambda_{0,2} = \frac{1}{2} \left[E_0 + E_2 + V_{00} + V_{22} \pm \left((E_0 - E_2 + V_{00} - V_{22})^2 + 4|V_{20}|^2 \right)^{1/2} \right] \quad (5.63)$$

The eigenvalues above can be written to mirror the form achieved by perturbation theory. This is accomplished using two separate Taylor expansions, the results of which are shown below.

$$\begin{aligned} \lambda_0 &= E_0 + \langle 0|V|0\rangle + \frac{|\langle 2|V|0\rangle|^2}{(E_0 - E_2)} - (\langle 0|V|0\rangle - \langle 2|V|2\rangle) \frac{|\langle 2|V|0\rangle|^2}{(E_0 - E_2)^2} + \dots \\ \lambda_2 &= E_2 + \langle 2|V|2\rangle - \frac{|\langle 2|V|0\rangle|^2}{(E_0 - E_2)} + (\langle 0|V|0\rangle - \langle 2|V|2\rangle) \frac{|\langle 2|V|0\rangle|^2}{(E_0 - E_2)^2} + \dots \end{aligned} \quad (5.64)$$

For this limited case, the sum of energy corrections is identical to (1.17). Each of the

elements of V are known, given by terms from V_0 and V_2 .

$$\begin{aligned} V_{00} &= \langle 0|V_0|0\rangle & ; & & V_{02} &= \langle 0|\hat{Q}_0^2|2\rangle \\ V_{20} &= \langle 2|\hat{Q}_2^0|0\rangle & ; & & V_{22} &= \langle 2|(V_0 + \hat{Q}_1^1)|2\rangle \end{aligned} \tag{5.65}$$

We note that the eigenvalues in (5.64) are represented by an infinite series, which may or may not converge depending on the size of the perturbation. The convergence criterion is dependent upon the values of the Q coefficients, which would change depending on the problem at hand. Similar behavior is to be expected in our methodology, where sufficiently large perturbations may cause divergence when iterating through cluster amplitudes or in other areas of the process.

This concludes our study of the quadratic perturbation, the simplest case of the normal-ordered form in (1.11). The quadratic case has a handful of important physical applications despite its low order, especially noting that a diatomic molecule is the physical analog for a single oscillator. In fact, it can be shown that a perturbation in the molecule's mass or elasticity can be written in the quadratic order [Huey-You & Rittby (2024)]. This derivation, alongside explicit parameters for such a perturbation, is provided in Section B of the Appendix.

Chapter 6

Higher Order Perturbations

6.1 Connecting Diagrams

Let us now consider the case of the quartic perturbation. This entails using all normal-ordered perturbations from V_0 to V_4 , destroying the parity-specific simplifications we previously used by including the odd orders V_1 and V_3 . However, this case is far more representative of the general problem. Following the steps in this case is therefore more akin to what steps the code performs explicitly. The terms used for the full quartic perturbation are all given in (1.11), written here for the single oscillator case.

$$\begin{aligned} V &= V_0 + V_1 + V_2 + V_3 + V_4 \\ &= V_0 + (Q_1^0 a^\dagger + Q_0^1 a) + \left(\frac{1}{2!} Q_2^0 a^\dagger a^\dagger + Q_1^1 a^\dagger a + \frac{1}{2!} Q_0^2 a a \right) + \\ &\quad \left(\frac{1}{3!} Q_3^0 a^\dagger a^\dagger a^\dagger + \frac{1}{2!} Q_2^1 a^\dagger a^\dagger a + \frac{1}{2!} Q_1^2 a^\dagger a a + \frac{1}{3!} Q_0^3 a a a \right) + \\ &\quad \left(\frac{1}{4!} Q_4^0 a^\dagger a^\dagger a^\dagger a^\dagger + \frac{1}{3!} Q_3^1 a^\dagger a^\dagger a^\dagger a + \frac{1}{2!} \frac{1}{2!} Q_2^2 a^\dagger a^\dagger a a + \frac{1}{3!} Q_1^3 a^\dagger a a a + \frac{1}{4!} Q_0^4 a a a a \right) \end{aligned} \tag{6.1}$$

The diagrammatic representation of the Hamiltonian then includes all above terms in addition to the $\hat{\omega}$ diagram.

$$\begin{aligned}
 H_{open} = & \begin{array}{c} \times \text{---} | \\ | \\ \text{---} | \\ | \\ \text{---} | \\ | \\ \text{---} | \\ | \\ \blacksquare \text{---} | \\ | \\ \text{---} | \\ | \\ \text{---} | \end{array} + \begin{array}{c} | \\ | \\ \text{---} | \\ | \\ \text{---} | \\ | \\ \text{---} | \\ | \\ \text{---} | \end{array} + \begin{array}{c} \text{---} | \\ | \\ \text{---} | \\ | \\ \text{---} | \\ | \\ \text{---} | \\ | \\ \text{---} | \end{array} + \begin{array}{c} | \\ | \\ \text{---} | \\ | \\ \text{---} | \\ | \\ \text{---} | \\ | \\ \text{---} | \end{array} + \begin{array}{c} \blacksquare \text{---} | \\ | \\ \text{---} | \\ | \\ \text{---} | \\ | \\ \text{---} | \\ | \\ \text{---} | \end{array} + \begin{array}{c} \text{---} | \\ | \\ \text{---} | \\ | \\ \text{---} | \\ | \\ \text{---} | \\ | \\ \text{---} | \end{array} + \\
 & \begin{array}{c} | \\ | \\ \text{---} | \\ | \\ \text{---} | \\ | \\ \text{---} | \\ | \\ \text{---} | \end{array} + \begin{array}{c} | \\ | \\ \text{---} | \\ | \\ \text{---} | \\ | \\ \text{---} | \\ | \\ \text{---} | \end{array} + \begin{array}{c} | \\ | \\ \text{---} | \\ | \\ \text{---} | \\ | \\ \text{---} | \\ | \\ \text{---} | \end{array} + \begin{array}{c} \text{---} | \\ | \\ \text{---} | \\ | \\ \text{---} | \\ | \\ \text{---} | \\ | \\ \text{---} | \end{array} + \begin{array}{c} | \\ | \\ \text{---} | \\ | \\ \text{---} | \\ | \\ \text{---} | \\ | \\ \text{---} | \end{array} + \\
 & \begin{array}{c} | \\ | \\ \text{---} | \\ | \\ \text{---} | \\ | \\ \text{---} | \\ | \\ \text{---} | \end{array} + \begin{array}{c} | \\ | \\ \text{---} | \\ | \\ \text{---} | \\ | \\ \text{---} | \\ | \\ \text{---} | \end{array} + \begin{array}{c} | \\ | \\ \text{---} | \\ | \\ \text{---} | \\ | \\ \text{---} | \\ | \\ \text{---} | \end{array} + \begin{array}{c} \text{---} | \\ | \\ \text{---} | \\ | \\ \text{---} | \\ | \\ \text{---} | \\ | \\ \text{---} | \end{array}
 \end{aligned} \tag{6.2}$$

As V has now been truncated at the quartic term, we have that the highest allowed connection order is four (with \hat{Q}_0^4). Therefore, the BCH expansion self-truncates after T^4 . In this case, however, we must deal with the full series of even and odd cluster amplitudes.

$$T = T_1 + T_2 + T_3 + T_4 + \dots \quad ; \quad e^T \rightarrow 1 + T + \frac{1}{2!}T^2 + \frac{1}{3!}T^3 + \frac{1}{4!}T^4 \tag{6.3}$$

To calculate the amplitudes, we must also select some order to truncate the cluster operator. This is an arbitrary choice, so let us pick T_4 for this example. This leaves us with four different cluster amplitudes (t_1, t_2, t_3, t_4) to converge in the iterative scheme.

The convergence equation for each amplitude is governed by a different \hat{W}_n^0 collection.

$$\begin{aligned}
\hat{W}_1^0 &= \begin{array}{|c|} \hline \\ \hline \\ \hline \\ \hline \end{array} & ; & \hat{W}_2^0 &= \begin{array}{|c|} \hline \\ \hline \\ \hline \\ \hline \\ \hline \end{array} \\
\hat{W}_3^0 &= \begin{array}{|c|c|} \hline & \\ \hline & \\ \hline & \\ \hline & \\ \hline & \\ \hline \end{array} & ; & \hat{W}_4^0 &= \begin{array}{|c|c|c|} \hline & & \\ \hline & & \\ \hline & & \\ \hline & & \\ \hline & & \\ \hline & & \\ \hline \end{array}
\end{aligned} \tag{6.4}$$

Given the perturbation order V_4 and T_4 , we must write all possible diagrams, sort them into collections, and interpret each each one. This process results in the explicit form of collections \hat{W}_n^0 associated with the amplitude equations, as well as any others which may result from $(He^T)_C$. The other collections are later used to build the effective Hamiltonian matrix $\bar{\mathbf{H}}$ for the excited state calculation.

Once all diagrams are written and interpreted, we find 21 terms in \hat{W}_1^0 , 31 terms in \hat{W}_2^0 , 35 terms in \hat{W}_3^0 , and 35 terms in \hat{W}_4^0 . Due to the number of terms, we will not show all of the diagrammatic expansions explicitly. That said, an example for reference was provided for \hat{W}_3^0 in (3.29). Once all of the diagrams in the four relevant \hat{W}_n^0 collections are written, the single oscillator interpretations are as follows.

$$\begin{aligned}
W_1^0 &= \omega t_1 + Q_1^0 + Q_0^1 t_2 + Q_1^1 t_1 + Q_0^2 \left(\frac{1}{2!} t_3 + t_1 t_2 \right) + Q_1^2 \left(\frac{1}{2!} t_2 + \frac{1}{2!} t_1 t_1 \right) + \\
&Q_0^3 \left(\frac{1}{3!} t_4 + \frac{1}{2!} \frac{1}{2!} t_2 t_2 + \frac{1}{2!} t_1 t_3 + \frac{1}{2!} t_1 t_1 t_2 \right) + Q_1^3 \left(\frac{1}{3!} t_3 + \frac{1}{2!} t_1 t_2 + \frac{1}{3!} t_1 t_1 t_1 \right) + \\
&Q_0^4 \left(\frac{1}{3!} t_1 t_4 + \frac{1}{2!} \frac{1}{2!} t_2 t_3 + \frac{1}{3!} t_2 t_3 + \frac{1}{2!} \frac{1}{2!} t_1 t_2 t_2 + \frac{1}{2!} \frac{1}{2!} t_1 t_1 t_3 + \frac{1}{3!} t_1 t_1 t_1 t_2 \right)
\end{aligned} \tag{6.5}$$

$$\begin{aligned}
\frac{1}{2!}W_2^0 &= \frac{1}{2!}2\omega t_2 + \frac{1}{2!}Q_0^1 t_3 + \frac{1}{2!}Q_2^0 + \frac{1}{2!}2Q_1^1 t_2 + \frac{1}{2!}Q_0^2 \left(\frac{1}{2!}2t_2 t_2 + \frac{1}{2!}t_4 + t_1 t_3 \right) + \\
&\frac{1}{2!}Q_2^1 t_1 + \frac{1}{2!}Q_1^2 \left(\frac{1}{2!}2t_3 + 2t_1 t_2 \right) + \frac{1}{2!}Q_0^3 \left(\frac{1}{2!}t_1 t_4 + \frac{1}{2!}2t_2 t_3 + \right. \\
&\left. \frac{1}{2!}t_2 t_3 + \frac{1}{2!}t_1 t_1 t_3 + \frac{1}{2!}2t_1 t_2 t_2 \right) + \frac{1}{2!}Q_2^2 \left(\frac{1}{2!}t_2 + \frac{1}{2!}t_1 t_1 \right) + \\
&\frac{1}{2!}Q_1^3 \left(\frac{1}{2!} \frac{1}{2!} 2t_2 t_2 + \frac{1}{3!} 2t_4 + \frac{1}{2!} 2t_1 t_3 + \frac{1}{2!} 2t_1 t_1 t_2 \right) + \\
&\frac{1}{2!}Q_0^4 \left(\frac{1}{2!} \frac{1}{3!} 2t_2 t_2 t_2 + \frac{1}{2!} \frac{1}{2!} t_2 t_4 + \frac{1}{3!} 2t_2 t_4 + \frac{1}{2!} \frac{1}{2!} \frac{1}{2!} 2t_3 t_3 + \frac{1}{3!} \frac{1}{2!} t_3 t_3 + \right. \\
&\left. \frac{1}{2!} 2t_1 t_2 t_3 + \frac{1}{2!} t_1 t_2 t_3 + \frac{1}{2!} \frac{1}{2!} t_1 t_1 t_4 + \frac{1}{2!} \frac{1}{2!} 2t_1 t_1 t_2 t_2 + \frac{1}{3!} t_1 t_1 t_1 t_3 \right)
\end{aligned} \tag{6.6}$$

$$\begin{aligned}
\frac{1}{3!}W_3^0 &= \frac{1}{3!}3\omega t_3 + \frac{1}{3!}Q_0^1 t_4 + \frac{1}{3!}3Q_1^1 t_3 + \frac{1}{3!}Q_0^2 (t_1 t_4 + 3t_2 t_3) + \frac{1}{3!}Q_3^0 + \frac{1}{3!}3Q_2^1 t_2 + \\
&\frac{1}{3!}Q_1^2 \left(\frac{1}{2!} 3t_4 + 3t_1 t_3 + \frac{1}{2!} 6t_2 t_2 \right) + \frac{1}{3!}Q_0^3 \left(\frac{1}{2!} t_2 t_4 + \frac{1}{2!} 3t_2 t_4 + \right. \\
&\left. \frac{1}{2!} \frac{1}{2!} 3t_3 t_3 + 3t_1 t_2 t_3 + \frac{1}{2!} t_1 t_1 t_4 + \frac{1}{3!} 6t_2 t_2 t_2 \right) + \frac{1}{3!}Q_3^1 t_1 + \\
&\frac{1}{3!}Q_2^2 \left(\frac{1}{2!} 3t_3 + 3t_1 t_2 \right) + \frac{1}{3!}Q_1^3 \left(\frac{1}{2!} 3t_1 t_4 + \frac{1}{2!} 6t_2 t_3 + \frac{1}{2!} 3t_2 t_3 + \right. \\
&\left. \frac{1}{2!} 6t_1 t_2 t_2 + \frac{1}{2!} 3t_1 t_1 t_3 \right) + \frac{1}{3!}Q_0^4 \left(\frac{1}{3!} t_3 t_4 + \frac{1}{2!} \frac{1}{2!} 3t_3 t_4 + \frac{1}{3!} 3t_3 t_4 + \right. \\
&\left. \frac{1}{2!} t_1 t_2 t_4 + \frac{1}{2!} 3t_1 t_2 t_4 + \frac{1}{2!} \frac{1}{2!} 3t_1 t_3 t_3 + \frac{1}{2!} \frac{1}{2!} 6t_2 t_2 t_3 + \frac{1}{2!} \frac{1}{2!} 3t_2 t_2 t_3 + \right. \\
&\left. \frac{1}{3!} 6t_1 t_2 t_2 t_2 + \frac{1}{2!} 3t_1 t_1 t_2 t_3 + \frac{1}{3!} t_1 t_1 t_1 t_4 \right)
\end{aligned} \tag{6.7}$$

$$\begin{aligned}
\frac{1}{4!}W_4^0 &= \frac{1}{4!}4\omega t_4 + \frac{1}{4!}4Q_1^1 t_4 + \frac{1}{4!}Q_0^2 \left(4t_2 t_4 + \frac{1}{2!}6t_3 t_3 \right) + \frac{1}{4!}6Q_2^1 t_3 + \\
&\frac{1}{4!}Q_1^2 (4t_1 t_4 + 12t_2 t_3) + \frac{1}{4!}Q_0^3 \left(\frac{1}{2!}6t_3 t_4 + \frac{1}{2!}4t_3 t_4 + 4t_1 t_2 t_4 + \frac{1}{2!}6t_1 t_3 t_3 + \right. \\
&\left. \frac{1}{2!}12t_2 t_2 t_3 \right) + \frac{1}{4!}Q_4^0 + \frac{1}{4!}4Q_3^1 t_2 + \frac{1}{4!}Q_2^2 \left(\frac{1}{2!}6t_4 + \frac{1}{2!}12t_2 t_2 + 6t_1 t_3 \right) + \\
&\frac{1}{4!}Q_1^3 \left(\frac{1}{2!}12t_2 t_4 + \frac{1}{2!}4t_2 t_4 + \frac{1}{2!}\frac{1}{2!}12t_3 t_3 + 12t_1 t_2 t_3 + \frac{1}{2!}4t_1 t_1 t_4 + \right. \\
&\left. \frac{1}{3!}24t_2 t_2 t_2 \right) + \frac{1}{4!}Q_0^4 \left(\frac{1}{3!}\frac{1}{2!}4t_4 t_4 + \frac{1}{2!}\frac{1}{2!}\frac{1}{2!}6t_4 t_4 + \frac{1}{2!}4t_1 t_3 t_4 + \frac{1}{2!}6t_1 t_3 t_4 + \right. \\
&\frac{1}{2!}\frac{1}{2!}12t_2 t_3 t_3 + \frac{1}{2!}\frac{1}{2!}6t_2 t_3 t_3 + \frac{1}{2!}\frac{1}{2!}12t_2 t_2 t_4 + \frac{1}{2!}\frac{1}{2!}4t_2 t_2 t_4 + \\
&\left. \frac{1}{2!}12t_1 t_2 t_2 t_3 + \frac{1}{2!}4t_1 t_1 t_2 t_4 + \frac{1}{2!}\frac{1}{2!}6t_1 t_1 t_3 t_3 + \frac{1}{4!}24t_2 t_2 t_2 t_2 \right)
\end{aligned} \tag{6.8}$$

By setting these collections to zero and solving for the $(\hat{\omega} \cdot T_n)_C$ term in each expression, we derive the convergence criterion for each amplitude. Let us write these convergence criteria mirroring the general form in (3.39).

$$t_n^{(i+1)} = \frac{-\frac{1}{n!}W_n^{0(i)} + \frac{1}{(n-1)!}\omega t_n^{(i)}}{\frac{1}{(n-1)!}\omega} \quad ; \quad W_n^{0(i)} = W_n^0(t_1^{(i)}, t_2^{(i)}, t_3^{(i)}, t_4^{(i)}) \tag{6.9}$$

The collections themselves are functions of all the amplitudes, and are thus responsible for ‘coupling’ the convergence equations together in the above representation. We also note that, as shown in (3.39), other diagrams can be pulled out of the collection apart from $(\hat{\omega} \cdot T_n)_C$ to affect the rate of convergence. Once the amplitudes are calculated, we can solve for the ground state energy using the closed collection W_0^0 . These terms were

included in (3.44), given again here for the maximum cluster amplitude T_4 .

$$\begin{aligned}
\tilde{E}_0 &= \frac{1}{2}\omega + V_0 + W_0^0 \\
&= \frac{1}{2}\omega + V_0 + Q_0^1 t_1 + Q_0^2 \left(\frac{1}{2!} t_2 + \frac{\hat{\diamond}}{2!} t_1 t_1 \right) + Q_0^3 \left(\frac{1}{3!} t_3 + \frac{1}{2!} t_1 t_2 + \frac{\hat{\diamond}}{3!} t_1 t_1 t_1 \right) + \\
&\quad Q_0^4 \left(\frac{1}{4!} t_4 + \frac{1}{3!} t_1 t_3 + \frac{1}{2!} \frac{\hat{\diamond}}{2!} t_1 t_1 t_2 + \frac{\hat{\diamond}}{4!} t_1 t_1 t_1 t_1 + \frac{1}{2!} \frac{1}{2!} \frac{\hat{\diamond}}{2!} t_2 t_2 \right)
\end{aligned} \tag{6.10}$$

6.2 Further Notes

Thus far, we have defined a diagrammatic method through which to obtain energy eigenvalues of a system of anharmonic oscillators. This is a general method which can be adapted to any perturbed system, both in the single and multiple oscillator cases. We note that while the collections and equations above were presented in the single oscillator form, they can quickly be generalized to multiple oscillators following the process outlined in (3.28). The main problem we seek to resolve in this paper is the quickly increasing number of terms in the cluster equations for higher order amplitudes, exemplified by the collections in (6.5) through (6.8).

While simple cases such as the quadratic perturbation can have their cluster equations derived manually using diagrams, the sheer number of terms becomes unreasonable to interpret by hand even for relatively low orders of V and T . There exist roughly 130 diagrams explicitly interpreted above for the amplitudes and ground state (in \hat{W}_0^0 , \hat{W}_1^0 , \hat{W}_2^0 , \hat{W}_3^0 , and \hat{W}_4^0), but this does not include the larger number of diagrams which contribute to the effective Hamiltonian and excited states. It can be shown that the total number of diagrams for the V_4 and T_4 case is just over 300, a number which very

quickly increases as higher order amplitudes or perturbations are included.

For this reason, we resort to Python to handle the generation, interpretation, and implementation of diagrams in the coupled cluster process. As we have already outlined the use of Python for the peripheral steps in [Figure 1](#), we write the code in such a way that allows the generated collections to be reliably referenced later on. For example, the iterative scheme in [\(3.39\)](#) requires that the collections \hat{W}_n^0 must be efficiently evaluated at each iteration for any set of amplitudes. Furthermore, the effective Hamiltonian matrix elements must all be calculated individually, based on contributions from \hat{W}_n^0 . By saving a generated file of equations for each collection, we can quickly perform these calculations for any given input.

Chapter 7

Computer Generated Equations

Diagrams cannot quite be put to use in Python visually, but their structural information can be stored and used for calculations with object-oriented code. While we have introduced a general diagrammatic method here and have provided single oscillator equations up to V_4 and T_4 by hand, we will now present a practical manner of generating equations up to any arbitrary order V_M and T_N . We will also limit the discussion in this section to a single oscillator, with possible generalizations for multiple oscillators discussed in the following section.

Often in Python, so-called ‘classes’ are employed as a template to create a number of similar objects, adding a level of functionality and structure to the stored data. Here we wish to define a class, for which each object is a separate diagram. We will later be able to freely manipulate these objects, but first let us discuss their definitions in code. Diagrams will require a few basic pieces of information which are to be input when a new one is initialized. The three structural components of the diagram are all required at this stage - the vertex line representing a term in the perturbed Hamiltonian, any involved

amplitudes, and the connection orders.

Input	Equation Representation	Code Representation
Vertex Line	$Q_K^L a^{\dagger K} a^L$	$K, L, 'Q'$
Amplitudes	$t_i(p), t_j(q), t_k(r), \dots$	$\tau = (i, j, k, \dots)$
Connections		$\chi = (p, q, r, \dots)$

Table 1: Inputs to a diagram object.

Note for this discussion that the indices i, j, k , and so on in the single oscillator context will represent the *number* of associated ladder operators, rather than the index of the oscillator being operated on. For example, some t_3 will denote the third order cluster amplitude which has $a^\dagger a^\dagger a^\dagger$, following (3.24).

For ease of reference, we introduce the list of involved amplitudes τ and associated list of connections χ . These are ordered tuples, such that every τ_n th-order amplitude has an associated χ_n th-order connection. As defined in Section 3.1, these three attributes give enough information to construct one diagram. The inputs must pass a number of different checks during the object's initialization, to ensure that the diagram being created is valid. These were also alluded to in a previous section, but for the code's sake, we must properly specify these conditions.

Let us create a function \mathbf{C} , which simply denotes the number of entries, or 'length', of a given set of values. As an example, the length of a tuple (5, 3, 8, 8) would be four, as there are four total entries. Generally speaking, we can define this function as follows.

$$\mathbf{C}(b_1, b_2, \dots, b_N) = N \tag{7.1}$$

A tuple of length N is typically referred to as an N -tuple. Note as well that the length function only provides a total count of how many values are included, such that duplicate values are all counted separately. The conditions for a valid diagram can then be written as shown in [Table 2](#).

Diagram is only valid if...	Equation Representation
i. All inputs are integers.	$K, L \in \mathbb{Z}$ $i, j, k, \dots \in \mathbb{Z} \quad ; \quad p, q, r, \dots \in \mathbb{Z}$
ii. All exponents are positive (or zero).	$K, L \geq 0$
iii. All indices are positive (and non-zero).	$i, j, k, \dots > 0 \quad ; \quad p, q, r, \dots > 0$
iv. Number of amplitudes fits with the vertex line.	$\mathbf{C}(i, j, k, \dots) \leq L$
v. Sum of connections fits with the vertex line.	$\sum(p, q, r, \dots) \leq L$
vi. Each amplitude has one associated connection.	$\mathbf{C}(i, j, k, \dots) = \mathbf{C}(p, q, r, \dots)$
vii. All amplitude-connection pairs are applicable.	$i \geq p, j \geq q, k \geq r, \dots$

Table 2: Ensuring a diagram is valid.

If the input passes all these checks at initialization, a new diagram object can be successfully created. Addressing the first three can be kept brief, as we expect each input to be a positive integer (aside from the alphabetic coefficient ‘ Q ’). These criteria are stricter for the amplitude and connection values, as any t_0 or zeroth-order connections are undefined. The latter four are more involved criteria, and will likely be better illustrated with counterexamples. The cases below are all specific inputs which would be immediately rejected by the code.

iv. $Q_1^2 a^\dagger a a$ connected with amplitudes $t_1 t_2 t_3 t_4$.

There are too many amplitudes to connect to the limited number of annihilation operators $L = 2$ on the vertex line (i.e., in the given perturbed Hamiltonian term).

v. Attempting a triple-connection with $Q_1^2 a^\dagger aa$.

The attempted connection order exceeds the number of available annihilation operators $L = 2$.

vi. An input $t_1 t_2 t_3 t_4$ with given connections (1, 2, 2).

The amplitudes and connections cannot be paired one-to-one.

vii. Attempting a triple-connection with t_2 .

The amplitude term does not have enough creation operators to support the given connection order.

As such, each object will be subjected to these constraints to ensure our working diagrams are valid. Our challenge, for efficiency's sake, is generating all valid diagrams while never accidentally creating one which is invalid. An invalid output could be filtered out if these rules were applied to every diagram, but the added redundancy in double-checking each structure quickly becomes unreasonable for even low order perturbations and amplitudes. With these constraints being well defined, avoiding false diagrams is a much easier task to accomplish.

The second step at initialization is calculating and storing other attributes surrounding the diagram at hand for fast reference later on. Aspects such as symmetrization or other associated factorial coefficients are more mathematical in nature, and therefore will be calculated at a later time. At this stage, we only wish to carry around information relevant to the diagram's structure.

- The number of creation operators R and annihilation operators S remaining after connections, called the diagram's **signature**. This is crucial when sorting diagrams

and figuring out which collection they will eventually contribute to.

$$R = K + \sum_n (\tau_n - \chi_n) \quad ; \quad S = L - \sum_n (\chi_n) \quad (7.2)$$

- A unique list of amplitude-connection pairs, which we will call the diagrammatic **components**. Let us assume this list is sorted, to ensure that each diagram only has one proper order by which to express its components.

$$\text{components} = ((\tau_1, \chi_1), (\tau_2, \chi_2), (\tau_3, \chi_3), \dots) \quad \text{sorted by } \tau_n \text{ and then } \chi_n \quad (7.3)$$

- Some notion of the diagram's **uniqueness**, which will be addressed later in depth. This is in reference to the list of components above, and will be used to filter out any duplicate diagrams which may arise in the code.

Combined with the three necessary structural requirements (vertex line, amplitudes, and connections), these three extra attributes are all stored for any diagram by default from the moment it's created. We have thusly defined the overall structure of the diagrammatic class, and can provide the code with a few utilities to apply to these diagrams where needed.

7.1 Specifying Inputs

With the base of the diagrammatic class set up, we can discuss where the structural inputs for all generated objects come from. We have the maximum orders of V_M and T_N

introduced in Section 2.1, and all individual diagrams should be derived from these two values alone. Allow us first to give the normal-ordered terms in V a more explicit form for the single oscillator case.

$$V = V_1 + V_2 + V_3 + \dots + V_M \quad ; \quad V_m = \sum_{k=0}^m \frac{1}{k!} \frac{1}{(m-k)!} Q_k^{m-k} a^{\dagger k} a^{m-k} \quad (7.4)$$

Here, the perturbation is truncated at the M th-order. Obtaining the possible value pairs K and L of Table 1 then becomes relatively straightforward, given that the individual orders V_m include all terms with m total operators. In other words, we should be able to quickly generate all terms for which $K + L = m$ as follows.

$$(K, L) = (k, m - k) \quad \text{from all } 0 \leq k \leq m ; 0 \leq m \leq M \quad (7.5)$$

Terms from the perturbed Hamiltonian will act as ‘starter’ diagrammatic objects, as they too have some level of structure despite not being connected to any amplitudes. The other two main inputs for these cases are still well defined, instead denoted by empty tuples (i.e., tuples of length zero). From here, we can build upon the empty starter diagrams by filling in more amplitudes.

Vertex Line	Amplitudes	Connections	Signature	Components
$K, L, 'Q'$	$()$	$()$	K, L	$()$

Table 3: A diagrammatic object from the perturbed Hamiltonian.

For the next step, it should again be noted that the allowed amplitudes are truncated twice. First, the cluster operator itself is directly truncated by the input T_N , in a similar

manner as V_M above. Furthermore, we only need include values based on what V_M is capable of connecting to. Since this allows for M single connections at maximum, the exponent e^T is limited by the M th-order term in its expansion.

$$T = T_1 + T_2 + T_3 + \dots + T_N \quad ; \quad e^T \rightarrow 1 + T + \frac{1}{2!}T^2 + \dots + \frac{1}{M!}T^M \quad (7.6)$$

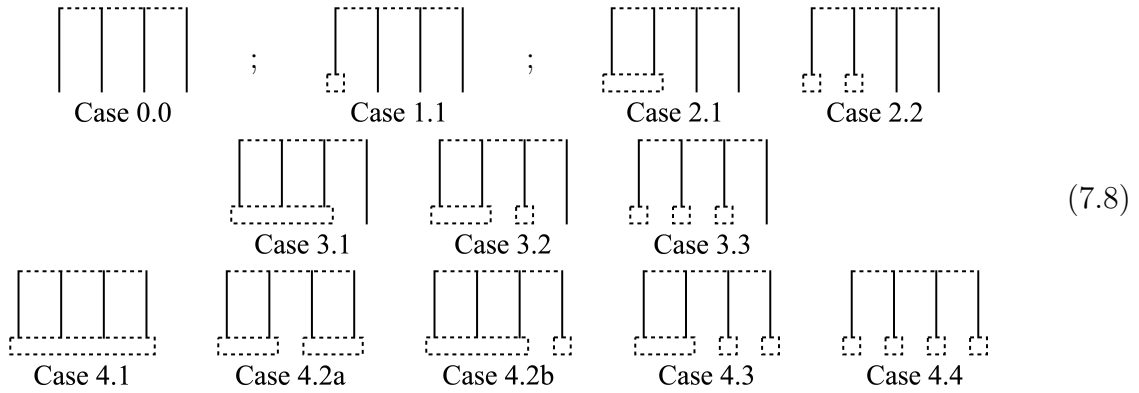
The above truncation at M more specifically occurs as a result of the BCH expansion for a connected Hamiltonian as mentioned before, where the term T^{M+1} has too many operators in V_M to fully connect to as shown in rule (iv). Furthermore, this expansion allows us to streamline the problem as a whole by making use of the fact that all cluster amplitudes commute with each other. Diagrams can then be created progressively for each amplitude order, first using only e^{T_1} terms, then including e^{T_2} , and so on.

$$\begin{aligned} e^{-T}He^T &= (H, e^T)_C = H + [H, T] + \frac{1}{2!} [[H, T], T] + \frac{1}{3!} [[[H, T], T], T] + \dots \\ &\dots \Rightarrow \left(\left((H, e^{T_1})_C, e^{T_2} \right)_C, e^{T_3} \dots \right)_C \end{aligned} \quad (7.7)$$

Generating allowed connections is a discussion of its own, more involved than being directly tied to the maximum V_M or T_N as before. To make connections at a diagrammatic level, we would effectively separate operators into different groups, which then connect together to a specific amplitude term t_i . Grouping elements like this allows the connection input to be framed as a different problem, mirroring the concept of partitioning a mathematical set. This concept arises often in areas of combinatorics and permutations, though we need to adapt it for our own use.

Rather than showing explicit diagrams, allow us to imply n th-order connections by

grouping together operators with dotted boxes. A dotted box could represent any arbitrary (and valid) amplitude in practice, used here for the sake of highlighting the connections themselves. Consider for example the possible connections one could have for a diagram \hat{D}_0^4 (i.e., D_0^4aaaa). This equates to partitioning four elements into different distinct groups.



The goal is then to generate all of the above possibilities, such that they can be input into the diagrammatic class to form proper objects. For reference, Python could store the above partitioned connections as shown in [Table 4](#).

	Connections		Connections		Connections
Diagram 0.0	()	Diagram 3.1	(3)	Diagram 4.2a	(2, 2)
Diagram 1.1	(1)	Diagram 3.2	(2, 1)	Diagram 4.2b	(3, 1)
Diagram 2.1	(2)	Diagram 3.3	(1, 1, 1)	Diagram 4.3	(2, 1, 1)
Diagram 2.2	(1, 1)	Diagram 4.1	(4)	Diagram 4.4	(1, 1, 1, 1)

Table 4: Partitioning a diagram.

The number of ways to partition a general set of n distinct elements into k groups is well known, given by the combinatoric Stirling numbers of the second kind $S(n, k)$.

Our problem is a bit more complex due to the fact that diagrams impose many extra variables and conditions to consider, such as equivalent operators, amplitude-connection pairs, and other caveats which render the general formalism inapplicable. Additionally, we wish to generate the partitions themselves, rather than only knowing how many there are. Generating partitions in Python is typically accomplished using an iterative method, and accounting for these caveats is included as part of the diagram class structure.

7.2 Static Methods

Classes allow us to define static methods, which are functions generally related to a set of objects, while not acting directly on them. These come with a wide range of possibilities, but here we will only need use of two static methods. For one static method, we explore a manner of populating all possible connections between an existing diagram and an amplitude term. Then for the second, we wish to use existing diagrams to create new ones as discussed earlier - slowly building on top of a lower-order e^{T_i} instead of starting from scratch. These static methods are crucial tools in the pursuit of a generalized V_M and T_N code, and need be just as rigorously defined as the definitions in the previous section.

Firstly, we explore the population of connections for given amplitudes. In other words, we wish to find all possible values of χ_n if provided with a given L and amplitudes τ . There are two validity checks directly related to connections, from rules (v) and (vii). We should have enough connections while keeping limits of the associated amplitude and the other connections to be used in mind. Allow us to rewrite these rules in terms of τ

and χ .

$$\text{v. } \sum_n^{\mathbf{C}(\chi)} \chi_n \leq L \quad ; \quad \text{vii. } \chi_n \leq \tau_n \quad (7.9)$$

We write the upper limit above the sum here, as the highest n is given by the number of elements in the associated tuple. For example, a tuple of length 3 should have an index running from 1 to 3. The two above equations are both higher limiting factors to be respected, which means that a general range of allowed connections can now be developed. The most effective way to apply these rules is iterative to some degree, going in order from the first associated connection χ_1 and progressing forward. This way, an expression can be derived from rule (v) for the absolute maximum case. By maximizing a given χ_n , we are in effect minimizing all other connections. The lowest value a connection can have is that of a single order, which means we can write the following for such an assumption.

$$\begin{aligned} \sum_n^{\mathbf{C}(\chi)} \chi_n &= \sum_n^{\mathbf{C}(\tau)} \chi_n \leq L \\ \chi_1 + \chi_2 + \chi_3 + \dots + \chi_n &\leq L \\ \chi_{\max} + 1 + 1 + \dots + 1 &= L \end{aligned} \quad (7.10)$$

Here we have used $\mathbf{C}(\tau) = \mathbf{C}(\chi)$ as required by rule (vi) to write the equation in terms of the input list τ , exercising the fact that both the amplitudes and connections should have the same tuple length. Solving for the maximum connection order becomes straightforward from here, as the number of 1s included can be expressed using the upper limit of the sum. We remove an entry from the total as we've separated χ_{\max} from the

rest, accounting for the -1 in the following equation.

$$\begin{aligned}
 \chi_{\max} &= L - (1 + 1 + \dots + 1) \\
 \chi_{\max} &= L - (\mathbf{C}(\tau) - 1) \\
 \chi_{\max} &= L - \mathbf{C}(\tau) + 1
 \end{aligned}
 \tag{7.11}$$

Thus, we arrive at a definite expression for the maximum number of connections via rule (v). Note that this expression on its own is holistically sufficient, not depending on any specific τ_i nor χ_i . Rule (v) provides us with a limit from the overall diagrammatic structure, while rule (vii) gives an individual limit from the associated amplitude. Taking both rules into account, we can write the following.

$$1 \leq \chi_i \leq \min [\tau_i, (L - \mathbf{C}(\tau) + 1)_i] \tag{7.12}$$

Although derived only in terms of χ_1 , this expression becomes sufficient for partitioning any diagram if handled correctly. The above allows us to generate all possible connections for a single amplitude, without knowing anything about other existing connections overall. This is ideal for an iterative method, so long as we keep in mind that L and $\mathbf{C}(\tau)$ will change as we progressively connect more amplitudes. Our derived right-hand expression must be reevaluated for each step, hence the i subscript.

This also parallels the method for generating partitions of a more simplistic set in code where we lack the extra constraints. Rather than splitting n distinct elements into k groups, we have now derived a method of partitioning L non-distinct operators into $\mathbf{C}(\tau)$ groups - where we have one group paired to each given τ_i . This is sufficient to

generate all possible connections for a given τ , and this process will be shown in further detail later.

It also becomes useful to properly define how we can build on top of an already connected diagram, rather than starting from scratch. Consider the diagrams below, where we begin with some Case 1. This diagram consists of some perturbation term Q_1^3 and has already been singly connected to an amplitude t_2 .

$$\left(\left(\begin{array}{c} \text{Diagram 1} \\ \text{Case 1.} \end{array} \times \frac{1}{2!} \begin{array}{c} \text{Diagram 2} \\ t_3 \quad t_3 \end{array} \right) \right)_C = \begin{array}{c} \text{Diagram 2} \\ \text{Case 2.} \end{array} \quad (7.13)$$

Note that the extra factor of $\frac{1}{2!}$ comes directly from the expansion of e^T in (2.3), and will simply be reintroduced after all other calculations are complete. We wish to use the original diagram in order to create Case 2, a new diagram which has been connected with both t_2 and $t_3 t_3$. Though it may seem trivial visually, expressing this in useful terms for the code is still necessary. Let us ignore the equality and consider these two as separate Pythonic objects for now, shown in Table 5.

	Vertex Line	Amplitudes	Connections	Signature	Components
Diagram 1.	1, 3, 'Q'	(2)	(1)	2, 2	((2, 1))
Diagram 2.	1, 3, 'Q'	(2, 3, 3)	(1, 1, 1)	6, 0	((2, 1), (3, 1), (3, 1))

Table 5: Diagrammatic attributes from (7.13).

If we wish to create these from input alone, it becomes more clear that all we need to do is append the new amplitude-connection pairs (in this case, two singly connected t_3

amplitudes). Any attributes such as remaining terms or eventually factorial coefficients can still be calculated from the adjusted input when needed, either at initialization or in forming the equations later. Generally speaking, if we have an existing diagram with amplitudes and connections τ^A and χ^A which is being compounded with some other amplitudes and connections τ^s and χ^s , we can simply combine both tuples. We should just be slightly careful here, to ensure that the pairs remain in order.

$$\tau^B = (\tau_1^A, \dots, \tau_m^A, \tau_1^s, \dots, \tau_n^s) \quad ; \quad \chi^B = (\chi_1^A, \dots, \chi_m^A, \chi_1^s, \dots, \chi_n^s) \quad (7.14)$$

These two static methods are the only ones needed to generate all diagrammatic equations for any arbitrary order. A slightly more complex example is shown below, to illustrate how these two static methods can be applied to a certain input now that we have defined them mathematically. Depending on the maximum e^T , we expect thousands of diagram objects which will be progressively generated using the following process.

7.3 Allowed Connections

Consider the following example, for a specific perturbation term \hat{Q}_0^4 connected with amplitudes $t_3 t_4 t_5$. This diagram will be partitioned and built progressively as discussed

earlier, so the first step will be calculating the connections that can occur from t_3 alone.

$$L = 4 \quad ; \quad \tau = (3, 4, 5), \quad \tau_1 = 3$$

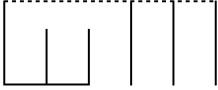
$$\chi_1 \leq \min [\tau_1, L - \mathbf{C}(\tau) + 1] = \min [3, 4 - 3 + 1] = \min [3, 2] = 2 \quad (7.15)$$

$$\chi_1 = 1, 2$$

Despite the fact that this is t_3 , only single and double connections are allowed. A triple connection would take up too many annihilation operators to allow for the given set of amplitudes as a whole, and this way we have avoided such an invalid case. Regardless, we can now evaluate both of these instances separately. Let us move forward by considering t_3 successfully connected and calculating the remaining annihilation operators via (7.2).

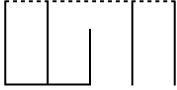
	t_3	t_4	t_5	→	Remaining	
Case 1a.	$\chi_1 = 1$	→	$S = 4 - (1) = 3$	(7.16)
Case 1b.	$\chi_1 = 2$	→	$S = 4 - (2) = 2$	

We will now take a moment in order to visualize the cases above. Note that these are not the resulting diagrams, only a representation of the ‘intermediate’ diagrams we would effectively have from this stage.



Case 1a.

;



Case 1b.

(7.17)

All diagrams from a certain amplitude (e.g., the missing triply connected case here) are still generated in practice, but we have limited our discussion to consider the process

for a larger input such as $t_3t_4t_5$. In other words, these calculations are tailored for cases when we expect higher order amplitudes, where we explicitly wish to avoid creating anything invalid for the sake of efficiency. It should be noted that intermediate diagrams are shown for visualization rather than being used in the code per se, and the diagrams in (7.17) would only appear as a result for their associated input. To generate these diagrams as a final result including their triply connected version, we would use the input $\tau = (3)$ to represent t_3 alone. This way, no other amplitudes are expected and this is reflected in the calculation.

From this stage, the process is repeated to build on top of either diagram. With the first t_3 being taken care of, we can address the next amplitude in the series. This leaves us with the set of amplitudes t_4t_5 , continued on in connecting with the above diagrams via the following calculations. Re-evaluating the limiting expression in (7.12) for both cases then gives us all available connections.


$$\begin{aligned}
\text{Case 1a.} \quad S = 3 \quad ; \quad \tau = (4, 5), \tau_2 = 4 \\
\chi_2 &\leq \min[\tau_2, S - \mathbf{C}(\tau) + 1] = \min[4, 3 - 2 + 1] = \min[4, 2] = 2 \\
\chi_2 &= 1, 2 \\
\text{Case 1b.} \quad S = 2 \quad ; \quad \tau = (4, 5), \tau_2 = 4 \\
\chi_2 &\leq \min[\tau_2, S - \mathbf{C}(\tau) + 1] = \min[4, 2 - 2 + 1] = \min[4, 1] = 1 \\
\chi_2 &= 1
\end{aligned} \tag{7.18}$$

Continuing to fill out the feasible values, we have now derived the allowed cases for t_4 . One thing of note is that as we include more amplitudes, the number of ways to distribute

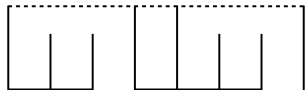
connections increases. Starting from Case 1b., we only get one possible diagram, but Case 1a. branches into two possibilities. The connections thus far and resulting annihilation operators which remain are as follows.

	t_3	t_4	t_5	Remaining	
Case 2a.	$\chi_1 = 1$	$\chi_2 = 1$...	$\rightarrow S = 4 - (1 + 1) = 2$	(7.19)
Case 2b.	$\chi_1 = 1$	$\chi_2 = 2$...	$\rightarrow S = 4 - (1 + 2) = 1$	
Case 2c.	$\chi_1 = 2$	$\chi_2 = 1$...	$\rightarrow S = 4 - (2 + 1) = 1$	

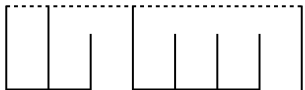
Once again, we've successfully connected a new amplitude and therefore can visualize the new set of intermediate diagrams if we wanted to. It is in this sense that the code 'iterates' through more and more complex diagrams without need to change anything, effectively just applying the same function to different parts of the input (e.g., t_3 , t_4 , and t_5 separately) to build up different results.



Case 2a.



Case 2b.



Case 2c.

(7.20)

Yet again, the above intermediate diagrams are simply for show, but can be generated with an input of only $\tau = (3, 4)$ alongside any other possibilities. Continuing through the process to the final iteration, these are evaluated in a case by case manner where we 'start' with the diagrams above and find the connections allowed for t_5 alone. Repeating

the calculations one last time leaves us with the outcomes below.

$$\text{Case 2a.} \quad S = 2 \quad ; \quad \tau = (5), \tau_3 = 5$$

$$\chi_3 \leq \min [\tau_3, S - \mathbf{C}(\tau) + 1] = \min [5, 2 - 1 + 1] = \min [5, 2] = 2$$

$$\chi_3 = 1, 2$$

$$\text{Case 2b.} \quad S = 1 \quad ; \quad \tau = (5), \tau_3 = 5$$

$$\chi_3 \leq \min [\tau_3, S - \mathbf{C}(\tau) + 1] = \min [5, 1 - 1 + 1] = \min [5, 1] = 1 \quad (7.21)$$

$$\chi_3 = 1$$

$$\text{Case 2c.} \quad S = 1 \quad ; \quad \tau = (5), \tau_3 = 5$$

$$\chi_3 \leq \min [\tau_3, S - \mathbf{C}(\tau) + 1] = \min [5, 1 - 1 + 1] = \min [5, 1] = 1$$

$$\chi_3 = 1$$

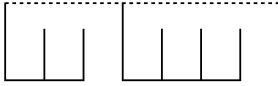
All in all, we have found four different possible connections between some perturbation with L annihilation operators and amplitudes τ . If these are all thought of as separate objects, this would correlate to four different diagrams that could be produced with the same vertex line and amplitudes using this method.

	t_3	t_4	t_5	Remaining	
Case 3a.	$\chi_1 = 1$	$\chi_2 = 1$	$\chi_3 = 1$	$\rightarrow S = 4 - (1 + 1 + 1) = 1$	
Case 3b.	$\chi_1 = 1$	$\chi_2 = 1$	$\chi_3 = 2$	$\rightarrow S = 4 - (1 + 1 + 2) = 0$	(7.22)
Case 3c.	$\chi_1 = 1$	$\chi_2 = 2$	$\chi_3 = 1$	$\rightarrow S = 4 - (1 + 2 + 1) = 0$	
Case 3d.	$\chi_1 = 2$	$\chi_2 = 1$	$\chi_3 = 1$	$\rightarrow S = 4 - (2 + 1 + 1) = 0$	

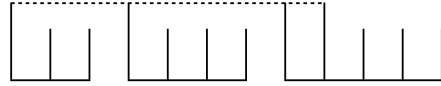
Rather than intermediate diagrams as shown for previous steps, the iterating process

is complete and therefore we can write the full equation here. This equation is an equality, as we have now derived all the ways to connect the given amplitudes.

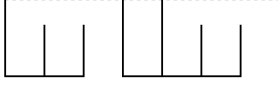
$$\left(\underbrace{\left[\begin{array}{|c|} \hline \text{---} \\ \hline \end{array} \right]}_Q \times \underbrace{\left[\begin{array}{|c|} \hline \text{---} \\ \hline \end{array} \right]}_{t_3} \underbrace{\left[\begin{array}{|c|} \hline \text{---} \\ \hline \end{array} \right]}_{t_4} \underbrace{\left[\begin{array}{|c|} \hline \text{---} \\ \hline \end{array} \right]}_{t_5} \right)_C = \tag{7.23}$$




Case 3a.



Case 3b.



Case 3c.



Case 3d.

All four of these results are then stored as diagrammatic objects in code, each with their own set of attributes. These can later be freely interpreted and sorted into different contributions as necessary, based on the number of remaining operators and component term.

	Vertex Line	Amplitudes	Connections	Signature	Components
Diagram 3a.	0, 4, 'Q'	(3, 4, 5)	(1, 1, 1)	9, 1	((3, 1), (4, 1), (5, 1))
Diagram 3b.	0, 4, 'Q'	(3, 4, 5)	(1, 1, 2)	8, 0	((3, 1), (4, 1), (5, 2))
Diagram 3c.	0, 4, 'Q'	(3, 4, 5)	(1, 2, 1)	8, 0	((3, 1), (4, 2), (5, 1))
Diagram 3d.	0, 4, 'Q'	(3, 4, 5)	(2, 1, 1)	8, 0	((3, 2), (4, 1), (5, 1))

Table 6: Diagrammatic attributes resulting from the connection between \hat{Q}_0^4 and $t_3 t_4 t_5$.

Our iterating process also has a perk of adaptability. Whether we investigate the single oscillator or multiple oscillator case, the presented method and final diagrammatic result stay the same. The code to generate the structures themselves has no need to change, so long as we have a different manner of interpreting the final result.

	$(\hat{Q}^{ijkl} \cdot T_3 T_4 T_5)_C =$	$(\hat{Q}_0^4 \cdot T_3 T_4 T_5)_C =$
Case 3a.	$\frac{1}{9!} \sum_{ij..pq,d} \sum_{abc} (Q^{abcd} t_{aij} t_{bklm} t_{cnopq})_\sigma$	$\frac{1}{9!} Q_0^4 \frac{9!}{2!3!4!} t_3 t_4 t_5$
Case 3b.	$\frac{1}{8!} \frac{1}{2!} \sum_{ij..op} \sum_{abcd} (Q^{abcd} t_{aij} t_{bklm} t_{cdnop})_\sigma$	$\frac{1}{8!} \frac{1}{2!} Q_0^4 \frac{8!}{2!3!3!} t_3 t_4 t_5$
Case 3c.	$\frac{1}{8!} \frac{1}{2!} \sum_{ij..op} \sum_{abcd} (Q^{abcd} t_{aij} t_{bckl} t_{dmnop})_\sigma$	$\frac{1}{8!} \frac{1}{2!} Q_0^4 \frac{8!}{2!2!4!} t_3 t_4 t_5$
Case 3d.	$\frac{1}{8!} \frac{1}{2!} \sum_{ij..op} \sum_{abcd} (Q^{abcd} t_{abi} t_{cjk} t_{dmnop})_\sigma$	$\frac{1}{8!} \frac{1}{2!} Q_0^4 \frac{8!}{1!3!4!} t_3 t_4 t_5$

Table 7: Coefficients for the single and multiple-oscillator interpretation of diagrams for each case.

7.4 Uniqueness

The method presented above can still encounter an occasional issue. Although the result derived in the previous section is completely correct, a few outcomes do exist where a type of structural degeneracy begins to show. There exist multiple ways that a diagram can be considered degenerate, most of which are accounted for with the factorial coefficients and symmetrizing factors. The degeneracy highlighted in this section is a bit more intricate, and has to do with the nature of the step by step approach itself. Since each step is done without consideration of other amplitude-connection pairs, there is a chance to generate diagrammatic components that have already been accounted for.

This only occurs in extremely specific cases depending on the values input, and can be accounted for rather quickly. Consider what happens if we change the above example for $t_3 t_4 t_5$, to $t_3^2 t_5$ instead. It can be shown that the allowed connection values are still identical to the ones found before, following the same method and noting that the results calculated in (7.19) all remain the same. We still find four possible sets of connections

and can write them to directly mirror (7.22).

$$\begin{array}{l}
\begin{array}{cccc}
& t_3 & t_3 & t_5 & \text{Remaining} \\
\text{Case 3a.} & \chi_1 = 1 & \chi_2 = 1 & \chi_3 = 1 & \rightarrow S = 4 - (1 + 1 + 1) = 1 \\
\text{Case 3b.} & \chi_1 = 1 & \chi_2 = 1 & \chi_3 = 2 & \rightarrow S = 4 - (1 + 1 + 2) = 0 \\
\text{Case 3c.} & \chi_1 = 1 & \chi_2 = 2 & \chi_3 = 1 & \rightarrow S = 4 - (1 + 2 + 1) = 0 \\
\text{Case 3d.} & \chi_1 = 2 & \chi_2 = 1 & \chi_3 = 1 & \rightarrow S = 4 - (2 + 1 + 1) = 0
\end{array}
\end{array} \tag{7.24}$$

For these amplitudes, however, structuring things as a diagrammatic object reveals a distinct flaw. Diagrams 3c. and 3d. are now identical, each having a single connection and double connection to the t_3 terms. The component attribute is extremely useful for illustrating this, by keeping only one sorted order for amplitude-connection pairs.

	Vertex Line	Amplitudes	Connections	Signature	Components
Diagram 3a.	0, 4, 'Q'	(3, 3, 5)	(1, 1, 1)	8, 1	((3, 1), (3, 1), (5, 1))
Diagram 3b.	0, 4, 'Q'	(3, 3, 5)	(1, 1, 2)	7, 0	((3, 1), (3, 1), (5, 2))
Diagram 3c.	0, 4, 'Q'	(3, 3, 5)	(1, 2, 1)	7, 0	((3, 1), (3, 2), (5, 1))
Diagram 3d.	0, 4, 'Q'	(3, 3, 5)	(2, 1, 1)	7, 0	((3, 1), (3, 2), (5, 1))

Table 8: Diagrams resulting from the connection between \hat{Q}_0^4 and $t_3^2 t_5$.

Using the definition that all components are sorted in increasing order, first by τ_n and then by χ_n , we can define a simple yet rigorous concept of 'equality' between diagrams. Components already account for the amplitude and connections together, and therefore

the only other requirement is for the vertex line (i.e., the perturbed Hamiltonian term).

$$\text{Diagram A} = \text{Diagram B} \iff \begin{cases} \text{Vertex Line A} = \text{Vertex Line B} \\ \text{Components A} = \text{Components B} \end{cases} \quad (7.25)$$

Although the definition itself is relatively straightforward, applying it in practice becomes more difficult. A massive number of diagrams is expected already, and evaluating each one against another is a vastly unreasonable computational time sink. Realistically, only a small fraction of these diagrams even have the possibility of being degenerate, and we can check for this possibility early on. This is why it becomes necessary to define some level of uniqueness among diagrams before this stage, included as a default attribute at initialization. We only wish to filter through diagrams that *can* be duplicated in the first place, which shaves off a substantial portion of those generated from consideration.

Therefore, let us define three different types of structural uniqueness as follows.

- i. Unique: $\tau_i \neq \tau_j$ for all $i \neq j$

If all involved amplitudes are of unique orders, there is only one way to generate a given component. For these cases, we have no reason to spend time checking for degeneracy. This would be the case for the example discussed at length, with $t_3 t_4 t_5$ in [Table 6](#).

- ii. Semi-Unique: $\tau_i = \tau_j \iff \chi_i = \chi_j$

For cases where some amplitudes are repeated, we should check if they are all treated in an equivalent manner (i.e., connected equally). Cases with duplicate amplitude-connection pairs can only be generated once, for instance the Diagram

3b. in [Table 8](#). In these cases, there is again no need to check for degeneracy.

iii. Degenerate: $\tau_i = \tau_j$ and $\chi_i \neq \chi_j$

This occurs if neither of the above uniqueness checks are true. Degenerate diagrams are the only ones we wish to filter through, instead of wasting our time checking against those which are already unique.

By defining a trait for each diagram at the beginning, we only need consider those that fail the above checks. Unique and semi-unique diagrams are free to move past this step immediately, while degenerate diagrams should be filtered through. The group of ‘degenerate’ diagrams here includes both originals we would wish to keep (such as Diagram 3c.) and duplicates of those originals which should be pruned (such as Diagram 3d.). Specific examples of the uniqueness terms are shown for six amplitude-connection pairs below.

Components	Unique τ	Equivalent χ	Overall Uniqueness
$((1, 1), (2, 2), (4, 3))$	True	\rightarrow	Unique
$((2, 1), (3, 2), (4, 2))$	True	\rightarrow	Unique
$((2, 2), (3, 3), (3, 3))$	False	True	Semi-Unique
$((2, 1), (2, 1), (2, 1))$	False	True	Semi-Unique
$((2, 1), (2, 2), (3, 3))$	False	False	Degenerate
$((3, 1), (3, 1), (3, 2))$	False	False	Degenerate

Table 9: Further examples of degenerate components.

As for how effective the uniqueness definitions are, the amount of degenerate diagrams to sift through only make up about 10% of the total objects, assuming we work with lower-order calculations at a maximum of around T_8 . For those on the order of T_{15} and

higher, the number of degenerate diagrams we need to consider drops from 10% of the total to roughly 5%. This does not reflect the number of degenerate diagrams lessening, but rather the sheer number of unique and semi-unique diagrams growing substantially. Removing these diagrams from the filtering process before it begins leaves us with only a sliver of what we are otherwise faced with, a number much more manageable and efficient for code.

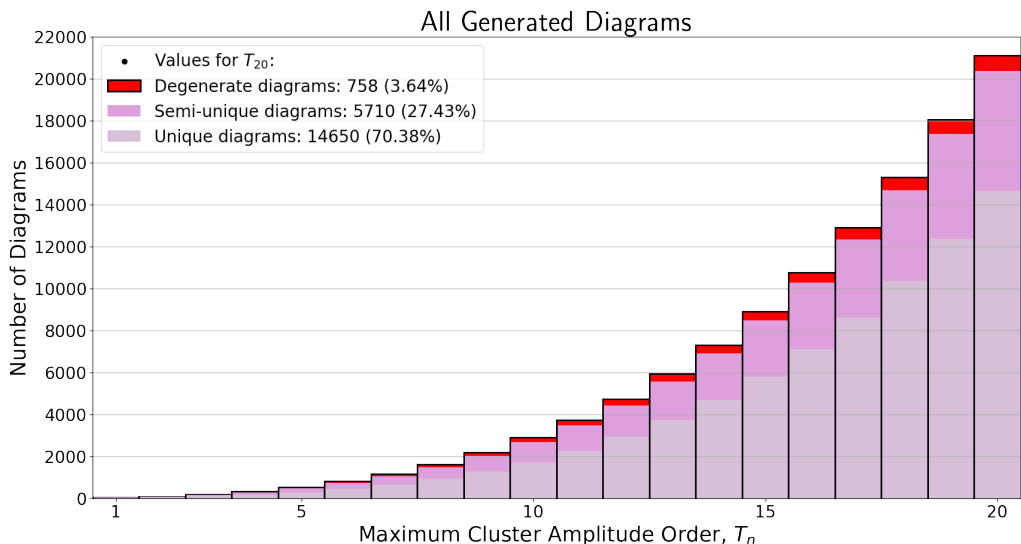


Figure 2: The number of diagrams generated using a maximum order V_4 and a given T_n , sorted into different categories based on their uniqueness. Values in the legend are shown for T_{20} , before filtering for degeneracy.

The precise breakdown in how the diagrams are categorized is presented in [Figure 2](#), for amplitudes up to T_{20} . We note that these are relatively high orders for the cluster amplitudes and are not typically necessary in practice. Still, this acts as an illustration for what the code could easily generate and how it deals with certain types of uniqueness.

The ‘degenerate’ category includes all possible generated diagrams marked as such

before being filtered, including an original copy and any repeated instances. It should then be noted that connecting diagrams iteratively as shown in (7.7) and filtering at each step can help to avoid the creation of certain degeneracies entirely. In doing this, diagrams which need to be filtered out only technically occur at the highest order of T .

Figure 3 then provides insight as to how these degeneracies are handled, as well as how much computation can be saved by avoiding the unique and semi-unique terms.

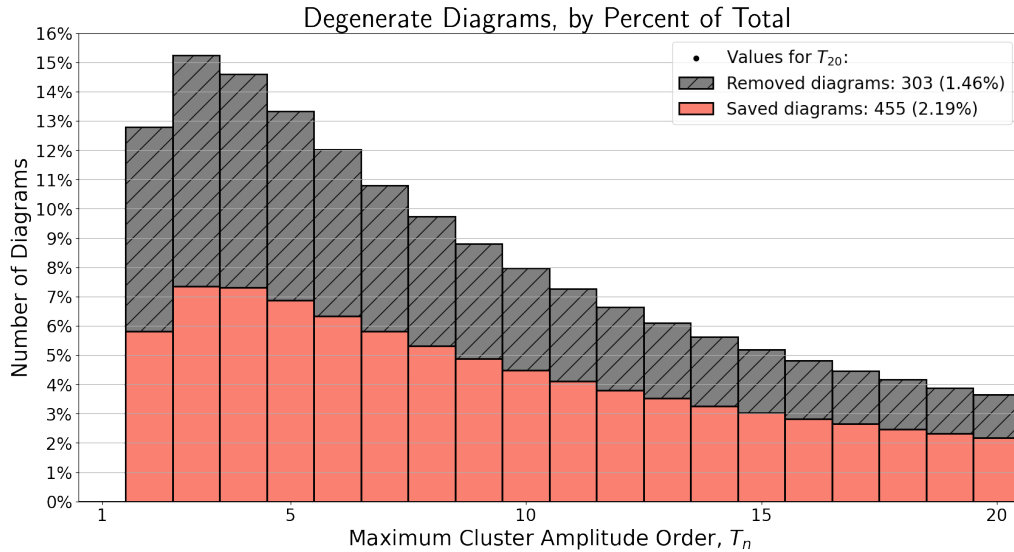


Figure 3: Diagrams marked as degenerate, generated using a maximum order V_4 and a given T_n . One original copy of a degenerate diagram is saved, while any repeated instances are removed. Values in the legend are shown for T_{20} .

For a degenerate set of diagrams, only one object is saved, while any future instances are removed. The saved diagrams can be further split into two categories depending on whether duplicates actually arise or not. Diagrams with a lower order structural degeneracy will still be marked as such, but would not create actual duplicates.

For an example of this in practice, a diagram created with some t_3^2 and filtered for

uniqueness would never create degenerate diagrams on its own later on. Any subsequent terms such as $t_3^2 t_4$, $t_3^2 t_5$, $t_3^2 t_5 t_6$, and so on would already have had their degenerate amplitude ‘pruned’ at its introduction in the BCH expansion. Only when encountering an amplitude term degenerate in a higher order such as $t_3^2 t_5^2$, would filtering be required again.

Max T_n	Diagrams	Max T_n	Diagrams	Max T_n	Diagrams	Max T_n	Diagrams
1	35	6	774	11	3916	16	10564
2	86	7	1120	12	4605	17	12665
3	177	8	1562	13	5772	18	15057
4	315	9	2115	14	7140	19	17765
5	510	10	2795	15	8730	20	20815

Table 10: The number of final diagrams in the generated equations, using maximum orders V_4 and T_n .

At this point, we’ve discussed in depth how diagrams are created and represented in code. Let us also briefly address the manner in which explicit collections for the ground state and excited state energy equations are written. In order to generate these contributions from some given maximum perturbation and amplitude orders V_M and T_N , we split the code into three distinct sections.

Initialization

Based on the input, we can form some initial ‘pool’ of diagrams which come directly from the perturbed Hamiltonian. These would include all of the base unconnected terms, written directly from (1.11).

$$H = H_0 + V = H_0 + \sum_{m=1}^M V_m = H_0 + \sum_{m=1}^M \sum_{k=0}^m (Q_k^{m-k} a^{\dagger k} a^{m-k}) \quad (7.26)$$

Furthermore, we include the two relevant truncations of amplitudes expressed in (7.6). This allows us to generate the limited number of amplitudes to connect in the following section.

Iterative Connections

An explicit flowchart of the steps taken in this section are provided in Figure 4.

- (a.) We wish to perform a loop over all orders of e^{T_i} , running through any connections in an order by order method as outlined in the rewritten BCH expansion.

$$(H, e^T)_C = \left((H, e^{T_1})_C, e^{T_2}_C, \dots, e^{T_N}_C \right)_C \quad (7.27)$$

- (b.) Two further loops are nested within (a), one over eligible diagrams in the pool and one over the amplitude powers in the selected i th order. This allows us to generate all $(H, T_i^n)_C$, one by one.

- (c.) If any amplitudes are included in a term, generate the allowed contractions. This results in some diagrammatic ‘group’ which all have the same vertex line and amplitude attributes, of which the included diagrams are the only ones which could be duplicates of each other.

The diagrams in each group are then run through a filter for degeneracy. Any surviving ones are included in a new result pool, representing all connected terms up to some order T_i .

- (d.) The pool of resulting diagrams can then be connected to the next order of e^{T_i} as the BCH expansion outlines, continuing the loop until the defined maximum truncation

order. Once complete, we have successfully derived all necessary diagrammatic structures.

Interpretation

This section entails returning the diagrams to their operator forms and grouping terms with the same signatures into their respective collections. These collections are all interpreted explicitly, then saved in a file to be called on later for two uses. Firstly, this facilitates calculations such as the amplitude convergence scheme or excited state elements, enabling the collections to be evaluated at any point for any set of amplitude values. Second, this allows us to avoid having to generate the same diagrammatic structures each time we wish to perform a calculation. An example of this generated code is provided in Section C of the Appendix.

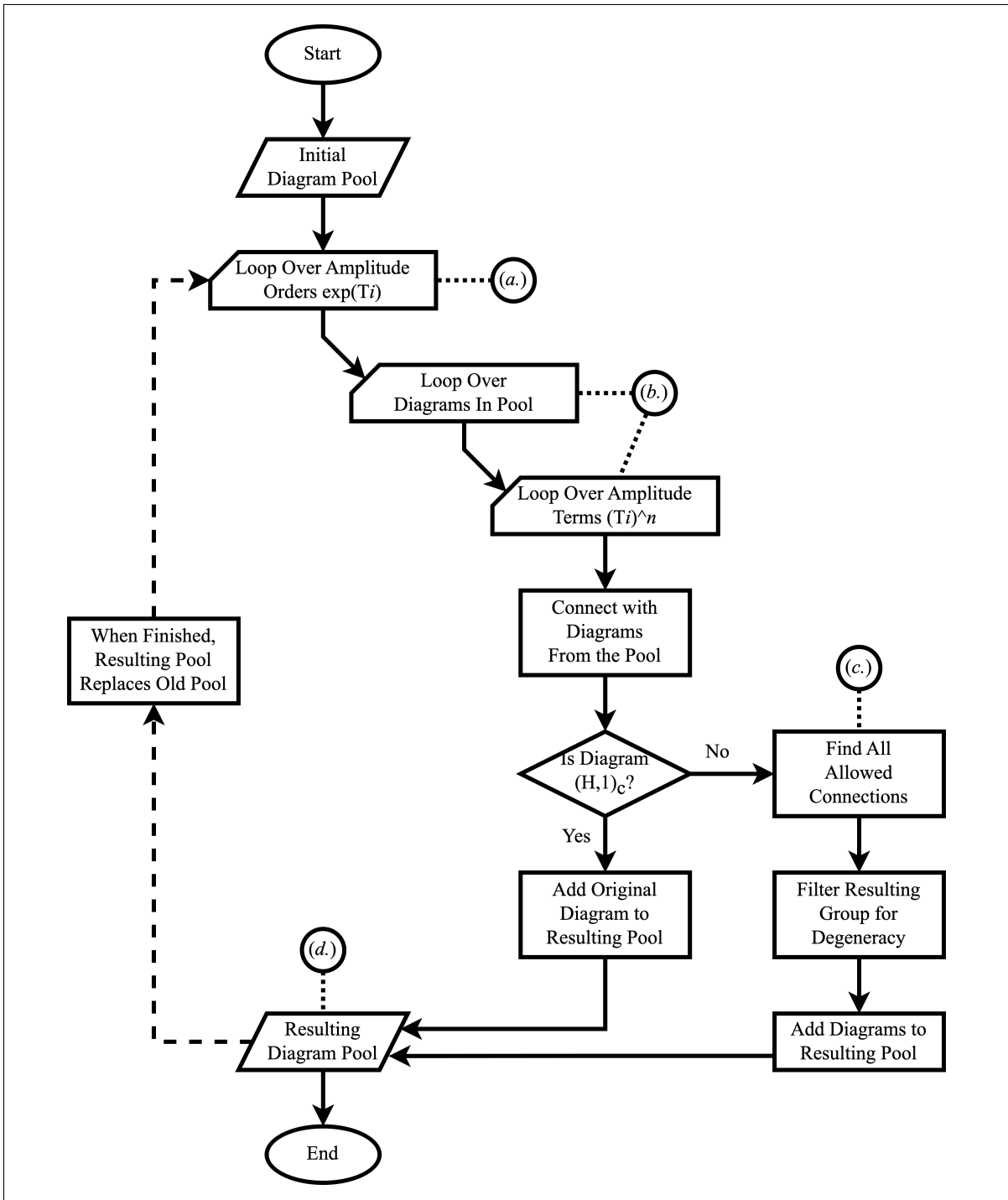


Figure 4: Flowchart for generating iterative connections of all diagrams.

Chapter 8

Generalization for Multiple Oscillators

8.1 Normal Ordering of a Three-Mode System

In order to complete our discussion, allow us to present the adaptation of some three-mode system into our formalism. We begin with a Hamiltonian of three oscillators under an example anharmonic perturbation of cubic order. The three oscillators in the system will be labeled with uppercase letters A , B , and C in the following equation.

$$\begin{aligned} H &= h_A + h_B + h_C + V(q_A, q_B, q_C) \\ h_i &= \frac{1}{2}p_i^2 + \frac{1}{2}\omega_i^2 q_i^2 = \left(a_i^\dagger a_i + \frac{1}{2} \right) \omega_i \\ V &= k_{300}q_A^3 + k_{030}q_B^3 + k_{120}q_A q_B^2 + k_{012}q_B q_C^2 \end{aligned} \tag{8.1}$$

The perturbation above should first be adapted into normal-ordered ladder operators,

in order to fit our diagrammatic scheme. Allow us therefore to rewrite the general cubic term expressed in (1.9).

$$\begin{aligned}
\gamma_{ijk}q_iq_jq_k &= \frac{\gamma_{ijk}}{\sqrt{8\omega_i\omega_j\omega_k}}(a_i^\dagger + a_i)(a_j^\dagger + a_j)(a_k^\dagger + a_k) \\
&= \frac{\gamma_{ijk}}{\sqrt{8\omega_i\omega_j\omega_k}} \left(a_i^\dagger a_j^\dagger a_k^\dagger + a_j^\dagger a_k^\dagger a_i + a_i^\dagger a_k^\dagger a_j + a_i^\dagger a_j^\dagger a_k + \right. \\
&\quad a_k^\dagger a_i a_j + a_j^\dagger a_i a_k + a_i^\dagger a_j a_k + a_i a_j a_k + \\
&\quad \left. \delta_{jk} a_i^\dagger + \delta_{ik} a_j^\dagger + \delta_{ij} a_k^\dagger + \delta_{jk} a_i + \delta_{ik} a_j + \delta_{ij} a_k \right)
\end{aligned} \tag{8.2}$$

Applying this expansion to each of the position terms in V , we find the associated normal-ordered operators. The k_{300} and k_{030} terms are thereby written as follows, where each operator product acts purely on oscillator A or B .

$$\begin{aligned}
k_{300}q_A^3 &= \frac{k_{300}}{\sqrt{8\omega_A^3}} \left(a_A^\dagger a_A^\dagger a_A^\dagger + 3a_A^\dagger a_A^\dagger a_A + 3a_A^\dagger a_A a_A + a_A a_A a_A + 3a_A^\dagger + 3a_A \right) \\
k_{030}q_B^3 &= \frac{k_{030}}{\sqrt{8\omega_B^3}} \left(a_B^\dagger a_B^\dagger a_B^\dagger + 3a_B^\dagger a_B^\dagger a_B + 3a_B^\dagger a_B a_B + a_B a_B a_B + 3a_B^\dagger + 3a_B \right)
\end{aligned} \tag{8.3}$$

In terms where the oscillators are mixed, the normal-ordered result changes as shown below for k_{120} and k_{012} . Note that all cubic perturbations will result in some combination of V_3 and V_1 terms as a result of Wick's Theorem.

$$\begin{aligned}
k_{120}q_Aq_B^2 &= \frac{k_{120}}{\sqrt{8\omega_A\omega_B^2}} \left(a_A^\dagger a_B^\dagger a_B^\dagger + a_B^\dagger a_B^\dagger a_A + 2a_A^\dagger a_B^\dagger a_B + \right. \\
&\quad \left. 2a_B^\dagger a_A a_B + a_A^\dagger a_B a_B + a_A a_B a_B + a_A^\dagger + a_A \right) \\
k_{012}q_Bq_C^2 &= \frac{k_{012}}{\sqrt{8\omega_B\omega_C^2}} \left(a_B^\dagger a_C^\dagger a_C^\dagger + a_C^\dagger a_C^\dagger a_B + 2a_B^\dagger a_C^\dagger a_C + \right. \\
&\quad \left. 2a_C^\dagger a_B a_C + a_B^\dagger a_C a_C + a_B a_C a_C + a_B^\dagger + a_B \right)
\end{aligned} \tag{8.4}$$

Allow us now to collect terms, calling the coefficients of each operator product some η . This will be done straightforwardly, without regard for normalization or other factorials.

$$\begin{aligned} \eta_{AAA} = \eta^{AAA} &= \frac{k_{300}}{\sqrt{8\omega_A^3}} & ; & & \eta_{BBB} = \eta^{BBB} &= \frac{k_{030}}{\sqrt{8\omega_B^3}} \\ \eta_{ABB} = \eta^{ABB} &= \frac{k_{120}}{\sqrt{8\omega_A\omega_B^2}} & ; & & \eta_{BCC} = \eta^{BCC} &= \frac{k_{012}}{\sqrt{8\omega_B\omega_C^2}} \end{aligned} \quad (8.5)$$

Since there only exists one way to obtain a product of three purely creation or annihilation operators from (8.2), the above $\eta_3^0 = \eta_0^3$ terms have no multiplicative integers. The $\eta_2^1 = \eta_1^2$ terms may include some, depending on how their indices are distributed.

$$\begin{aligned} \eta_{AA}^A = \eta_A^{AA} &= \frac{3k_{300}}{\sqrt{8\omega_A^3}} & ; & & \eta_{BB}^B = \eta_B^{BB} &= \frac{3k_{030}}{\sqrt{8\omega_B^3}} \\ \eta_{BB}^A = \eta_A^{BB} &= \frac{k_{120}}{\sqrt{8\omega_A\omega_B^2}} & ; & & \eta_{AB}^B = \eta_B^{AB} &= \frac{2k_{120}}{\sqrt{8\omega_A\omega_B^2}} \\ \eta_{CC}^B = \eta_B^{CC} &= \frac{k_{012}}{\sqrt{8\omega_B\omega_C^2}} & ; & & \eta_{BC}^C = \eta_C^{BC} &= \frac{2k_{012}}{\sqrt{8\omega_B\omega_C^2}} \end{aligned} \quad (8.6)$$

Unlike the previous cases with terms of three operators only coming from one unique expansion, terms of only one operator can be sourced from multiple different normal-ordered results. These are shown below for the final coefficients, where $\eta_1^0 = \eta_0^1$.

$$\eta_A = \eta^A = \frac{3k_{300}}{\sqrt{8\omega_A^3}} + \frac{k_{120}}{\sqrt{8\omega_A\omega_B^2}} & ; & \eta_B = \eta^B = \frac{3k_{030}}{\sqrt{8\omega_B^3}} + \frac{k_{012}}{\sqrt{8\omega_B\omega_C^2}} \quad (8.7)$$

With the above expansions, we can begin to mirror the form of the ordered perturbation in (1.11). A bit of caution must be exercised in doing so, as now we must include

factors which account for multiple permutations of indices.

$$\begin{aligned}
V_1 &= \sum_i \left(Q_i a_i^\dagger + Q^i a_i \right) \\
V_3 &= \sum_{ijk} \left(\frac{1}{3!} Q_{ijk} a_i^\dagger a_j^\dagger a_k^\dagger + \frac{1}{2!} Q_{ij}^k a_i^\dagger a_j^\dagger a_k + \frac{1}{2!} Q_i^{jk} a_i^\dagger a_j a_k + \frac{1}{3!} Q^{ijk} a_i a_j a_k \right)
\end{aligned} \tag{8.8}$$

We now write expressions relating the η terms from the problem and the Q terms above. Since the original perturbation V in (8.1) is Hermitian, we have that all $Q_{ijk} = Q^{ijk}$, $Q_{ij}^k = Q_k^{ij}$, and $Q_i = Q^i$. We will therefore only provide the relations between half of the η 's and Q 's, as the other half are effectively identical.

$$\eta_{AAA} = \frac{1}{3!} Q_{AAA} \quad ; \quad \eta_{BBB} = \frac{1}{3!} Q_{BBB} \tag{8.9}$$

For cases where permutations apply, we must include each possible coefficient to ensure that the summations in (8.8) give rise to the correct value. The Q coefficients must be symmetrical under exchange of indices such that $Q_{ijk} = Q_{jik} = Q_{kji} = \dots$, which allows for the following expressions.

$$\begin{aligned}
\eta_{ABB} &= \frac{1}{3!} (Q_{ABB} + Q_{BAB} + Q_{BBA}) = \frac{1}{2!} Q_{ABB} \\
\eta_{BCC} &= \frac{1}{3!} (Q_{BCC} + Q_{CBC} + Q_{CBB}) = \frac{1}{2!} Q_{BCC}
\end{aligned} \tag{8.10}$$

A similar approach is taken for the remaining terms as shown below. Note that as no permutations nor factorials can be applied to the single operator terms, the two

coefficients are equal.

$$\begin{aligned}
\eta_{AA}^A &= \frac{1}{2!} Q_{AA}^A & ; & & \eta_{BB}^B &= \frac{1}{2!} Q_{BB}^B \\
\eta_{BB}^A &= \frac{1}{2!} Q_{BB}^A & ; & & \eta_{AB}^B &= \frac{1}{2!} (Q_{AB}^A + Q_{BA}^A) = Q_{AB}^A \\
\eta_{CC}^B &= \frac{1}{2!} Q_{CC}^B & ; & & \eta_{BC}^C &= \frac{1}{2!} (Q_{BC}^C + Q_{CB}^C) = Q_{BC}^C \\
\eta_A &= Q_A & ; & & \eta_B &= Q_B
\end{aligned} \tag{8.11}$$

Inverting all of the above expressions, we can write the normal-ordered perturbation coefficients in terms of the original three-mode k parameters.

$$\begin{aligned}
Q_{AAA} &= \frac{3!k_{300}}{\sqrt{8\omega_A^3}} & ; & & Q_{BBB} &= \frac{3!k_{030}}{\sqrt{8\omega_B^3}} \\
Q_{ABB} &= \frac{2!k_{120}}{\sqrt{8\omega_A\omega_B^2}} & ; & & Q_{BCC} &= \frac{2!k_{012}}{\sqrt{8\omega_B\omega_C^2}} \\
Q_{AA}^A &= \frac{2! \cdot 3k_{300}}{\sqrt{8\omega_A^3}} & ; & & Q_{BB}^B &= \frac{2! \cdot 3k_{030}}{\sqrt{8\omega_B^3}} & ; & & Q_{BB}^A &= \frac{2!k_{120}}{\sqrt{8\omega_A\omega_B^2}} \\
Q_{AB}^B &= \frac{2k_{120}}{\sqrt{8\omega_A\omega_B^2}} & ; & & Q_{CC}^C &= \frac{2!k_{012}}{\sqrt{8\omega_B\omega_C^2}} & ; & & Q_{BC}^C &= \frac{2k_{012}}{\sqrt{8\omega_B\omega_C^2}} \\
Q_A &= \frac{3k_{300}}{\sqrt{8\omega_A^3}} + \frac{k_{120}}{\sqrt{8\omega_A\omega_B^2}} & ; & & Q_B &= \frac{3k_{030}}{\sqrt{8\omega_B^3}} + \frac{k_{012}}{\sqrt{8\omega_B\omega_C^2}}
\end{aligned} \tag{8.12}$$

With these as the coefficients Q in (8.8), we now know their specific values when interpreting the diagrams. The diagrammatic representations in this problem still proceed

as expected, shown below for H_{open} alongside the energy term.

$$\begin{aligned}
 H_{open} = & \text{---} \times \left| \begin{array}{c} i \\ j \end{array} \right. + \left. \begin{array}{c} \text{---} \\ \text{---} \end{array} \right| i + \left. \begin{array}{c} \text{---} \\ \text{---} \end{array} \right| i + \\
 & i \left[\begin{array}{c} j \\ k \end{array} \right] + \begin{array}{c} i \\ k \end{array} \left[\begin{array}{c} j \\ \text{---} \end{array} \right] + \begin{array}{c} i \\ j \end{array} \left[\begin{array}{c} \text{---} \\ k \end{array} \right] + i \left[\begin{array}{c} \text{---} \\ j \\ k \end{array} \right]
 \end{aligned} \tag{8.13}$$

From here, the ground state energy is derived from the diagrammatic connections. The process of truncating the cluster amplitudes at some maximum T and collecting any closed diagrams in $(He^T)_C$ remains the same as shown in the examples for other perturbations. Rather than showing this again explicitly, let us briefly direct our attention to the excited state energy calculations.

8.2 Changes in the Effective Hamiltonian

Until this point, the excited states for different perturbations have been discussed almost exclusively in the single oscillator case. Excited state energies are still derived from the effective Hamiltonian matrix $\bar{\mathbf{H}}$ for multiple oscillators, but a handful of concepts surrounding their calculation must be generalized.

Let us begin this process by discussing the states of the system themselves. The ground state of the three-mode system is defined as that for which each oscillator (A , B , and C) is in its respective ground state.

$$|\phi\rangle = |n_A, n_B, n_C\rangle \quad ; \quad |0\rangle = |0, 0, 0\rangle \tag{8.14}$$

While the ground state of the system is still unique, excitations can now be applied in multiple ways. Consider, for example, the first excited states. In the three-mode system, there are three ways for one quanta of energy to excite an oscillator, shown below.

$$|1\rangle \rightarrow |1,0,0\rangle, |0,1,0\rangle, |0,0,1\rangle \quad (8.15)$$

These three states are all different, and must be accounted for separately in the $\overline{\mathbf{H}}$ matrix. Furthermore, the number of states grows quickly even for relatively low excitations. Taking the second excited states as another example, we must account for states with the two excitations applied to the same oscillator, as well as those with the excitations applied to different oscillators.

$$|2\rangle \rightarrow |2,0,0\rangle, |0,2,0\rangle, |0,0,2\rangle, |1,1,0\rangle, |1,0,1\rangle, |0,1,1\rangle \quad (8.16)$$

The continued expansion of multiple oscillator states displayed here poses a large complication when calculating and manipulating elements in $\overline{\mathbf{H}}$. Let us also show the expansion of $|3\rangle$ and $|4\rangle$, for reference.

$$\begin{aligned} |3\rangle \rightarrow & |3,0,0\rangle, |0,3,0\rangle, |0,0,3\rangle, |2,1,0\rangle, |2,0,1\rangle, \\ & |1,2,0\rangle, |0,2,1\rangle, |1,0,2\rangle, |0,1,2\rangle, |1,1,1\rangle \\ |4\rangle \rightarrow & |4,0,0\rangle, |0,4,0\rangle, |0,0,4\rangle, |3,1,0\rangle, |3,0,1\rangle, \\ & |1,3,0\rangle, |0,3,1\rangle, |1,0,3\rangle, |0,1,3\rangle, |2,2,0\rangle, \\ & |2,0,2\rangle, |0,2,2\rangle, |2,1,1\rangle, |1,2,1\rangle, |1,1,2\rangle \end{aligned} \quad (8.17)$$

For a single oscillator, calculating the first four excited state energies (and corrections to the ground state energy) would simply require a 5×5 matrix. In the three-mode case, however, we see that the size needed for the same calculation increases to 35×35 . The required size of $\overline{\mathbf{H}}$ therefore depends both on the number of oscillators N , as well as the desired maximum excitation Z .

To further specify this effect, we will derive the necessary size for the $\overline{\mathbf{H}}$ matrix, given some general N and Z . This entails finding the number of ways to distribute anywhere from 0 to Z quanta of energy, among N ordered oscillators. We accomplish this by first defining the total excitation value of a particular state as some z .

$$|\phi\rangle = |n_A, n_B, n_C, \dots\rangle \quad ; \quad z = \sum_i^N n_i = n_A + n_B + n_C + \dots \quad (8.18)$$

As an example, (8.17) shows that there are 10 unique states with $z = 3$, and 15 unique states with $z = 4$. Rather than continuing with states and oscillators, let us represent each individual state as its respective sum.

$$\begin{aligned} 3 &= 3+0+0 ; 0+3+0 ; 0+0+3 ; 2+1+0 ; 2+0+1 ; \\ &1+2+0 ; 0+2+1 ; 1+0+2 ; 0+1+2 ; 1+1+1 \\ 4 &= 4+0+0 ; 0+4+0 ; 0+0+4 ; 3+1+0 ; 3+0+1 ; \\ &1+3+0 ; 0+3+1 ; 1+0+3 ; 0+1+3 ; 2+2+0 ; \\ &2+0+2 ; 0+2+2 ; 2+1+1 ; 1+2+1 ; 1+1+2 \end{aligned} \quad (8.19)$$

Using this representation, each excited state corresponds to a so-called ‘weak com-

position' of z . These are defined as the ways to write some integer z as the sum of N non-negative integers (i.e., including zeroes). The number of weak compositions are well known and have a closed form, expressed below.

$$f_N(z) = \binom{z + N - 1}{z} = \binom{z + N - 1}{N - 1} = \frac{(z + N - 1)!}{z!(N - 1)!} \quad (8.20)$$

Note that unique permutations of the same sum are considered separate when counting weak compositions, which is required for our excited state application. The value above can also be directly expressed by the multiset coefficient $\left(\left(\begin{matrix} N \\ z \end{matrix}\right)\right)$, but we will avoid using such notation for the sake of simplicity.

Knowing the number of states corresponding to a particular excitation z , we can write the size of the matrix for a maximum excitation Z as follows.

$$D_N(Z) = \sum_{z=0}^Z f_N(z) = \sum_{z=0}^Z \binom{z + N - 1}{z} \quad (8.21)$$

We then take advantage of the fact that $D_N(Z)$ is written as a sum of binomial coefficients of a specific form. The summation can be further simplified using a version of the Christmas stocking identity (or, hockey-stick identity), stated below.

$$\sum_{j=0}^{m-r} \binom{j+r}{j} = \binom{m+1}{m-r} \quad (8.22)$$

Substituting $j = z$, $r = N - 1$, and $m = N - 1 + Z$, the size of the matrix can be

expressed with a singular binomial coefficient.

$$D_N(Z) = \sum_{z=0}^Z \binom{z+N-1}{z} = \binom{N+Z}{Z} = \binom{N+Z}{N} \quad (8.23)$$

We have therefore derived the new number of z th excited states $f_N(z)$, as well as the size of the truncated $\overline{\mathbf{H}}$ matrix $D_N(Z)$. Both values are shown below for comparison.

$$f_N(z) = \binom{z+N-1}{N-1} \quad ; \quad D_N(Z) = \binom{Z+N}{N} \quad (8.24)$$

The $\overline{\mathbf{H}}$ matrix is thus shown to expand from a size of $Z+1$ in the single oscillator case, to a size of $\binom{Z+N}{N}$ in the multiple oscillator case. Constructing the $\overline{\mathbf{H}}$ matrix in practice requires some nuance as well, due to the number of possible z th excited states. In order to save space during the coming discussion, we introduce the following shorthand for the matrix elements.

$$\langle 0, 2, 1 | \overline{\mathbf{H}} | 1, 1, 1 \rangle = \overline{\mathbf{H}}_{021,111} \quad (8.25)$$

In the single oscillator case, the matrix elements are calculated between two states as some $\langle m | \overline{\mathbf{H}} | n \rangle$. As there are now multiple ways to excite the system m or n times, it becomes convenient to define some block matrix \mathbf{A}_{mn} , which accounts for all possible m th and n th matrix elements.

$$\langle 1 | \overline{\mathbf{H}} | 1 \rangle \quad \rightarrow \quad \mathbf{A}_{11} = \begin{pmatrix} \overline{\mathbf{H}}_{100,100} & \overline{\mathbf{H}}_{100,010} & \overline{\mathbf{H}}_{100,001} \\ \overline{\mathbf{H}}_{010,100} & \overline{\mathbf{H}}_{010,010} & \overline{\mathbf{H}}_{010,001} \\ \overline{\mathbf{H}}_{001,100} & \overline{\mathbf{H}}_{001,010} & \overline{\mathbf{H}}_{001,001} \end{pmatrix} \quad (8.26)$$

These block matrices are then used to express the effective Hamiltonian $\bar{\mathbf{H}}$. For instance, the matrix truncated at the second excited states can be written as follows.

$$\bar{\mathbf{H}} = \begin{pmatrix} \langle 0|\bar{\mathbf{H}}|0\rangle & \langle 0|\bar{\mathbf{H}}|1\rangle & \langle 0|\bar{\mathbf{H}}|2\rangle \\ \langle 1|\bar{\mathbf{H}}|0\rangle & \langle 1|\bar{\mathbf{H}}|1\rangle & \langle 1|\bar{\mathbf{H}}|2\rangle \\ \langle 2|\bar{\mathbf{H}}|0\rangle & \langle 2|\bar{\mathbf{H}}|1\rangle & \langle 2|\bar{\mathbf{H}}|2\rangle \end{pmatrix} \rightarrow \bar{\mathbf{H}} = \begin{pmatrix} \mathbf{A}_{00} & \mathbf{A}_{01} & \mathbf{A}_{02} \\ \mathbf{A}_{10} & \mathbf{A}_{11} & \mathbf{A}_{12} \\ \mathbf{A}_{20} & \mathbf{A}_{21} & \mathbf{A}_{22} \end{pmatrix} \quad (8.27)$$

The blocks \mathbf{A}_{mn} will be of increasing size, given by the corresponding number of states $f_N(z)$ for their rows and columns. We also note that block matrices \mathbf{A}_{mm} along the diagonal must be square matrices, while other non-diagonal blocks will not be. For example, the size of block \mathbf{A}_{21} in the three-mode system is given by $f_3(2) \times f_3(1) = 6 \times 3$.

$$\mathbf{A}_{21} = \begin{pmatrix} \bar{\mathbf{H}}_{200,100} & \bar{\mathbf{H}}_{200,010} & \bar{\mathbf{H}}_{200,001} \\ \bar{\mathbf{H}}_{020,100} & \bar{\mathbf{H}}_{020,010} & \bar{\mathbf{H}}_{020,001} \\ \bar{\mathbf{H}}_{002,100} & \bar{\mathbf{H}}_{002,010} & \bar{\mathbf{H}}_{002,001} \\ \bar{\mathbf{H}}_{110,100} & \bar{\mathbf{H}}_{110,010} & \bar{\mathbf{H}}_{110,001} \\ \bar{\mathbf{H}}_{101,100} & \bar{\mathbf{H}}_{101,010} & \bar{\mathbf{H}}_{101,001} \\ \bar{\mathbf{H}}_{011,100} & \bar{\mathbf{H}}_{011,010} & \bar{\mathbf{H}}_{011,001} \end{pmatrix} \quad (8.28)$$

Given the manner in which the block matrices are defined, \mathbf{A}_{mn} and \mathbf{A}_{nm} will necessarily have the same size as each other's transpose. However, the effective Hamiltonian

$\bar{\mathbf{H}}$ is not Hermitian, and the two \mathbf{A} matrices have no direct relation (i.e., $\mathbf{A}_{mn}^\dagger \neq \mathbf{A}_{nm}$).

$$\mathbf{A}_{12} = \begin{pmatrix} \bar{\mathbf{H}}_{100,200} & \bar{\mathbf{H}}_{100,020} & \bar{\mathbf{H}}_{100,002} & \bar{\mathbf{H}}_{100,110} & \bar{\mathbf{H}}_{100,100} & \bar{\mathbf{H}}_{100,011} \\ \bar{\mathbf{H}}_{010,200} & \bar{\mathbf{H}}_{010,020} & \bar{\mathbf{H}}_{010,002} & \bar{\mathbf{H}}_{010,110} & \bar{\mathbf{H}}_{010,101} & \bar{\mathbf{H}}_{010,011} \\ \bar{\mathbf{H}}_{001,200} & \bar{\mathbf{H}}_{001,020} & \bar{\mathbf{H}}_{001,002} & \bar{\mathbf{H}}_{001,110} & \bar{\mathbf{H}}_{001,101} & \bar{\mathbf{H}}_{001,011} \end{pmatrix} \quad (8.29)$$

Just like the case for single oscillators, the matrix elements of $\bar{\mathbf{H}}$ must all be calculated individually. Along with the newly increased size of the matrix, this is a major source of computational strain for multiple oscillator calculations which drastically increases for higher excited states. As an example, the truncated matrix only covering the first two excited states shown in (8.27) will be of size $D_3(2) = 10$, requiring 100 unique matrix elements to be evaluated.

$$\bar{\mathbf{H}} = \begin{pmatrix} \bar{\mathbf{H}}_{000,000} & \bar{\mathbf{H}}_{000,100} & \bar{\mathbf{H}}_{000,010} & \bar{\mathbf{H}}_{000,001} & \bar{\mathbf{H}}_{000,200} & \cdots & \bar{\mathbf{H}}_{000,011} \\ \bar{\mathbf{H}}_{100,000} & \bar{\mathbf{H}}_{100,100} & \bar{\mathbf{H}}_{100,010} & \bar{\mathbf{H}}_{100,001} & \bar{\mathbf{H}}_{100,200} & \cdots & \bar{\mathbf{H}}_{100,011} \\ \bar{\mathbf{H}}_{010,000} & \bar{\mathbf{H}}_{010,100} & \bar{\mathbf{H}}_{010,010} & \bar{\mathbf{H}}_{010,001} & \bar{\mathbf{H}}_{010,200} & \cdots & \bar{\mathbf{H}}_{010,011} \\ \bar{\mathbf{H}}_{001,000} & \bar{\mathbf{H}}_{001,100} & \bar{\mathbf{H}}_{001,010} & \bar{\mathbf{H}}_{001,001} & \bar{\mathbf{H}}_{001,200} & \cdots & \bar{\mathbf{H}}_{001,011} \\ \bar{\mathbf{H}}_{200,000} & \bar{\mathbf{H}}_{200,100} & \bar{\mathbf{H}}_{200,010} & \bar{\mathbf{H}}_{200,001} & \bar{\mathbf{H}}_{200,200} & \cdots & \bar{\mathbf{H}}_{200,011} \\ \vdots & \vdots & \vdots & \vdots & \vdots & \ddots & \vdots \\ \bar{\mathbf{H}}_{011,000} & \bar{\mathbf{H}}_{011,100} & \bar{\mathbf{H}}_{011,010} & \bar{\mathbf{H}}_{011,001} & \bar{\mathbf{H}}_{011,200} & \cdots & \bar{\mathbf{H}}_{011,011} \end{pmatrix} \quad (8.30)$$

A 10×10 matrix for the single oscillator would be sufficient to calculate energy eigenvalues up to the $|9\rangle$ excited state. Attempting to perform excited state calculations with $Z = 9$ in the three-mode case would in turn require a matrix of size $D_3(9) = 220$.

Such a matrix contains 48400 elements which, again, would necessarily be evaluated one-by-one.

With the structure of the effective Hamiltonian matrix as the last major addition to the multiple oscillator formalism, let us take a step back to consider the requirements a code must meet to achieve a numerical value for the ground states and excited states. Due in part to the complications listed above, no code has yet been developed to handle such calculations. Therefore, this will all be considered future work.

8.3 Future Work

Let us round out the multiple oscillator discussion by explicitly outlining the steps needed to calculate numerical values for energies of an N oscillator system. This entails performing the same steps outlined by the EoM-CC process, while making the generalizations needed for multiple oscillators.

Beginning with the manipulation of diagrams, a handful of difficulties immediately arise for their evaluation. Consider the following result from a connection between \hat{Q}_i^{jklm} and cluster amplitudes $\frac{1}{2!}T_3^2$, which was shown in (3.28).

$$\begin{array}{c}
 \begin{array}{|c|c|c|} \hline & & i \\ \hline j & k & a \\ \hline \end{array}
 \begin{array}{|c|} \hline \dots \\ \hline \end{array}
 \begin{array}{|c|c|c|} \hline & & \\ \hline m & b & c \\ \hline & & l \\ \hline \end{array}
 = \frac{1}{4!} \frac{1}{1!} \frac{1}{2!} \frac{1}{2!} \overset{\diamond}{\sum}_{ijkl,m} \sum_{abc} (Q_i^{abcm} t_{ajk} t_{bcl})_{\sigma} a_i^{\dagger} a_j^{\dagger} a_k^{\dagger} a_l^{\dagger} a_m
 \end{array} \tag{8.31}$$

The operators themselves need not be dealt with directly in practice, but are included here for the sake of completeness. Apart from the factorials, the critical parts of the

term are the summations over operator indices and connected indices, as well as the symmetrized coefficients marked by the σ subscript. Let us therefore explicitly expand the coefficients in this example.

$$\begin{aligned}
V_n &= \frac{4!}{1!2!1!} = 12 \\
(Q_i^{abcm} t_{ajk} t_{bcl})_\sigma &= Q_i^{abcm} t_{ajk} t_{bcl} + Q_i^{abcm} t_{alk} t_{bcj} + Q_i^{abcm} t_{ajl} t_{bck} + \\
&Q_j^{abcm} t_{aik} t_{bcl} + Q_j^{abcm} t_{alk} t_{bci} + Q_j^{abcm} t_{ail} t_{bck} + \\
&Q_k^{abcm} t_{aji} t_{bcl} + Q_k^{abcm} t_{ali} t_{bcj} + Q_k^{abcm} t_{ajl} t_{bci} + \\
&Q_l^{abcm} t_{ajk} t_{bci} + Q_l^{abcm} t_{aik} t_{bcj} + Q_l^{abcm} t_{aji} t_{bck}
\end{aligned} \tag{8.32}$$

- The formalism for *generating* diagrammatic structures applies for both single and multiple oscillators, which means that there is no need to change this particular part of the code. However, a method of *interpreting* the diagrams for the multiple oscillator case must still be developed.
- The first part of this would be developing a manner of summing over any indices i, j, k, \dots and a, b, \dots in a given diagram. The second part, which is arguably more difficult, entails reliably expressing and evaluating the full sum of permuted symmetrized coefficients $(Q_{ij\dots}^{ab\dots} t_{kl\dots})_\sigma$.

Completing these steps would allow for multiple oscillator diagrams to be sorted into collections $\hat{W}_{ij\dots}^{rs\dots}$ and numerically evaluated given some amplitudes $t_{ij\dots}$. The next step in the EoM-CC formalism is solving the cluster equations for these amplitudes, using the convergence schemes as outlined earlier. What was once a limited system of coupled equations for t_1, t_2, t_3 , and so on also becomes more complicated, as there is now a

different $t_{ij\dots}$ value associated with different combinations of oscillator excitations.

$$\hat{W}_{ij\dots} = 0 \quad \rightarrow \quad t_{ij\dots} \quad (8.33)$$

- An iterative scheme covering the convergence of all cluster amplitudes must be developed. While the general equation for a given order of cluster amplitudes (e.g., $t_{ijk}^{(n)}$) can be straightforwardly expressed as shown before, the equation in practice refers to the multiple cluster amplitudes within that order (e.g., $t_{ABC}^{(n)}$, $t_{ABB}^{(n)}$, $t_{AAC}^{(n)}$, etc.). Each of these amplitudes must therefore be evaluated individually, before moving onto the next step in the iteration.
- To ease computations here, one would ideally take advantage of the fact that the cluster amplitudes are symmetric. For example, $t_{AB} = t_{BA}$, $t_{ABC} = t_{BAC} = t_{CAB} = \dots$, and so on. While this does not *completely* remove the necessity of converging multiple cluster operators (e.g., $t_{ABB} \neq t_{AAB}$), removing the aforementioned redundancy does make the process far more efficient.

With knowledge of the converged cluster amplitudes and the ability to evaluate any given diagrams, one can now calculate the ground state energy.

$$\tilde{E}_0 = H_{closed} + (He^T)_{C,closed} = \frac{1}{2} \sum_i \omega_i + V_0 + W_0^0 \quad (8.34)$$

The excited state formalisms were elaborated on in the previous section, but we will now discuss their adaptation into code. The elements of $\bar{\mathbf{H}} = (He^T)_{C,open}$ are given by the contributions of all relevant collections of diagrams $\hat{W}_{ij\dots}^{rs\dots}$, as outlined in (3.45).

Obtaining numerical values for these is an extension of the diagrammatic interpretation and evaluation.

For the task of constructing the $\overline{\mathbf{H}}$ matrix, the first problem one might encounter is how to reliably reference states based on their position in the matrix. In the single oscillator case, mapping rows and columns with their corresponding states is trivial. The first row and column correspond to $|0\rangle$, the second row and column to $|1\rangle$, the third to $|2\rangle$, and so on. As the block matrices \mathbf{A}_{mn} have variable size, referencing states as such is not so simple.

- An efficient way to map the row or column in $\overline{\mathbf{H}}$ to its corresponding state therefore becomes necessary for any N and Z . As an example, the code should know that the 5th column in (8.30) is associated with the $|2, 0, 0\rangle$ state.
- As mentioned before, calculating elements by the contributions of $\hat{W}_{ij\dots}^{rs\dots}$ is the last step to constructing the matrix. A more general form of (3.45) should therefore be employed for multiple oscillators, either explicitly written or implicitly coded.
- Once the matrix element calculations can be approached regularly, note that the size of the matrix means that there are significantly more elements to calculate. This will likely be the biggest limiting computational factor for finding higher excited state energies.

This concludes the work required to derive the ground state and excited state energies for an N oscillator system. Still, a number of peripheral areas also exist in which progress can be made. A few of these areas are listed as follows.

- In order to reduce error in the energy calculations, one may attempt to perform a Bogoliubov transformation to generate a new Hamiltonian. Thus far, however, the formalism for Bogoliubov transformations tailored to the problem have only been derived in the single oscillator case. The multiple oscillator transformation entails writing the Hamiltonian in terms of a new set of operators b_i^\dagger and b_i , defined roughly as follows.

$$b_i^\dagger = \sum_j \left(F_{ij} a_j^\dagger + G_{ij} a_j + D_{ij} \delta_{ij} \right) \quad ; \quad b_i = \sum_j \left(F_{ij}^* a_j + G_{ij}^* a_j^\dagger + D_{ij}^* \delta_{ij} \right) \quad (8.35)$$

- There is also plenty of room for further numerical study in the singular oscillator case. As one example, we have shown that a Bogoliubov transformation (and therefore a new Hamiltonian) can be created with *any* amplitudes s_1 and s_2 . We customarily choose the converged values of $s_1 = t_1$ and $s_1 = t_2$, but using different starting values would result in different transformed Hamiltonians with their own ground state and excited state energies. Although running multiple transformations to convergence would result in the true values regardless, studying the numerical effects of a singular transformation with different s_1 and s_2 values may be of interest.
- Other areas to further investigate may include the convergence schemes of cluster amplitudes t_m , the behavior of relatively large perturbations, or any unforeseen phenomena in the multiple oscillator case.

In the single oscillator case, numerical integration suffices as a reliable way to benchmark the code and compare numerical results. However, numerical integration only works over one coordinate, and cannot be applied for multiple oscillators. One may still

consider a handful of different sources for comparing results as follows.

- Consider a ‘decoupled’ Hamiltonian, where the perturbation does not include any cross-terms (i.e., $Q_{ij\dots}^{rs} \neq 0$ iff $i = j = r = s = \dots$). In such a case, the eigenvalues found could be straightforwardly expressed as the sum of eigenvalues from each individual perturbed oscillator.

$$\begin{aligned}
 H &= \sum_i (h_i + V_i(q_i)) \\
 h_i &= \frac{1}{2}p_i^2 + \frac{1}{2}\omega_i^2q_i^2 = \left(a_i^\dagger a_i + \frac{1}{2} \right) \omega_i
 \end{aligned}
 \tag{8.36}$$

- Though general systems of N oscillators at high excitations Z may be difficult to compare, studies of specific systems and their energies using other methods do exist. As one example mentioned earlier, the three-mode system itself has multiple different approaches and results for comparison in the literature.
- In an earlier section, isotopes of a diatomic molecule were briefly explored as a physical analogue to the quadratic perturbation of one oscillator. As larger molecules can be described by systems of multiple oscillators, one may also eventually compare molecular spectra with the transitions between states (i.e., difference in energy eigenvalues) from the code.

8.4 Conclusion

In this paper, we have presented a practical methodology by which to describe a system of coupled anharmonic oscillators. This methodology combines coupled cluster theory and iterative Bogoliubov transformations, which was later adapted into a Python

code capable of generating explicit equations for any perturbation order V_M and cluster amplitudes T_N . This was accomplished independently using a handful of steps which we make individual conclusions for below.

The first major note to highlight is the adaptation of Wick's Theorem into a general diagrammatic scheme applicable to any system of oscillators. As shown in the earlier sections, this is a practical scheme complete with its own rigorous set of rules which can be readily used alongside the equation-of-motion coupled cluster method. This also greatly streamlines the process of contracting operators associated with the BCH expansion by hand, instead allowing us to represent terms by connected diagrammatic structures.

For the lowest-order quadratic case, we proved by hand that the perturbed Hamiltonian reduces to a new 'unperturbed' system with equally spaced eigenvalues after a suitable Bogoliubov transformation. While the code is written for the general case and therefore does not explicitly apply certain parity-specific simplifications, it still becomes extremely useful to highlight the symmetries in a given system. This provides us with a better understanding of the system itself, and eases any smaller calculations we may choose to execute by hand.

While the diagrams themselves can assist in calculations visually and by hand, manually evaluating energies with higher cluster amplitudes or higher excited states quickly becomes unreasonable to accomplish as shown for the quartic case. The same rules and methodology surrounding the scheme have therefore been adapted into Python code. This allows us to efficiently perform calculations given any arbitrary V_M and T_N , as outlined by the coupled cluster theory.

Building upon the code for diagrammatic generation, we have also proven that the

methodology is valid in the single oscillator case by the independent development of other Python codes. We have essentially developed a virtual laboratory within which we may freely study the anharmonic oscillator problem. This also works for an arbitrarily high order of cluster amplitudes, and can feasibly be generalized to the multiple oscillator case.

Lastly, we discussed the future of the project in both theoretical and physical areas. The required developments to generalize the single oscillator code to multiple oscillators were all listed in a step by step manner. Once accomplished, this would allow us to accurately study the system of anharmonic oscillators under a power series perturbation, using whichever cluster amplitudes are desired. As the molecule provides an analogue to the multiple oscillator system, this code could also be used to simulate molecular spectra from the transitions between states.

Appendix

A Details of Symmetrization

In this section, we will derive and discuss the values $U_n(L, M)$ and $V_n(K, M)$ given in equations (3.19) and (3.20). Let us begin with U_n , the number of possible unique n th contractions which could be represented by a given diagram. Forming an n th contraction is best described as a process in three separate steps.

1. First, n annihilation operators are selected from the L amount offered by the perturbed Hamiltonian term \hat{Q}_K^L .
2. Then, n creation operators are selected from the M amount offered by the amplitude term T_M .
3. Lastly, the n creation and annihilation operators are connected.

We will refer to the number of ways each step can be accomplished individually as u_1 , u_2 , and u_3 . The total number of ways an n th contraction can be formed is then the

product of the three individual values.

$$U_n = u_1 u_2 u_3 \tag{A.1}$$

Note here that the annihilation operators chosen in Step 1 commute, and the creation operators chosen in Step 2 commute. The order in which these operators are chosen does not matter, and therefore we expect to be dealing with combinations (as opposed to permutations). Anticipating this, the three steps can be rewritten using more general language.

1. First, n unordered elements are selected from a set of L elements.
2. Then, n unordered elements are selected from a set of M elements.
3. Lastly, the two subsets of n items each are paired together.

The first two steps conveniently entail the use of binomial coefficients, most commonly found in combinatoric problems such as this. The coefficient $\binom{A}{B}$ describes the number of different ways an unordered subset of B elements can be chosen from a larger set of A elements, expressed below for u_1 and u_2 .

$$u_1 = \binom{L}{n} = \frac{L!}{n!(L-n)!} \quad ; \quad u_2 = \binom{M}{n} = \frac{M!}{n!(M-n)!} \tag{A.2}$$

The value u_3 can be achieved by pairing the two subsets, one element at a time. An element in the first subset has n total choices to connect to in the second subset. Once this connection is made, $(n-1)$ choices remain for the next element. This incremental decrease

in options continues until the last element has only 1 remaining option. Multiplying the options for each element together, the total number of possible connections that can be made is given by the factorial $n!$.

$$u_3 = n \times (n - 1) \times (n - 2) \times \dots \times 1 = n! \quad (\text{A.3})$$

With all three values known, the full product U_n is written as follows.

$$\begin{aligned} U_n = u_1 u_2 u_3 &= \binom{L}{n} \binom{M}{n} n! \\ &= \frac{L!}{n!(L-n)!} \frac{M!}{n!(M-n)!} n! \\ &= \frac{L!M!}{(L-n)!(M-n)!} \frac{1}{n!} \end{aligned} \quad (\text{A.4})$$

Let us now move on to V_n , the number of unique permuted terms a coefficient must be separated into for symmetry. Recall the number of operators R and S after connection, provided in (3.13). As there are R total creation operators in the diagram, the total number of ways to permute their indices is simply given by $R!$. Some of these permutations will be redundant, due to the fact that creation operators on the same vertex line are already symmetrized by definition (i.e., \hat{Q}_K^L is symmetric, and t_M is symmetric).

The K creation operators provided by \hat{Q}_K^L are unaffected by connections, and therefore $K!$ of these permutations will be redundant. Similarly, $(M - n)$ creation operators associated with t_M are left unconnected, which means that $(M - n)!$ further permutations

are redundant. By dividing these two factors out, we find the symmetrizing value V_n .

$$V_n = \frac{R!}{K!(M-n)!} = \frac{(K+M-n)!}{K!(M-n)!} = \binom{R}{K} \quad (\text{A.5})$$

We note that this value can be written using the binomial coefficient, though it is typically unnecessary. The symmetrizing value can also be generalized to the product of multiple operators (i.e., \hat{Q}_K^L connected to multiple T_M terms), following similar logic. The general form is written below without the use of variables, to illustrate how the diagrammatic structure is taken into account.

$$V_n = \frac{(\text{total remaining creation operators})!}{\prod (\text{remaining creation operators on each vertex})!} \quad (\text{A.6})$$

A few examples of symmetrizing coefficients with multiple amplitudes are provided below. Note that the inclusion of annihilation operators in \hat{Q}_K^L has no effect on the symmetrizing coefficient, as they will all be on the same vertex line.

$$\begin{array}{l}
 \begin{array}{c} i \quad \boxed{a} \quad b \quad \boxed{c} \quad d \quad \boxed{j} \\ \hline \end{array} \quad \rightarrow \quad V_n = \frac{2!}{1!1!} \\
 \\
 \begin{array}{c} \quad \quad \quad i \quad j \\ \quad \quad \quad \boxed{a} \quad \boxed{b} \quad \boxed{l} \\ \quad \quad \quad \hline k \end{array} \quad \rightarrow \quad V_n = \frac{4!}{2!1!1!} \\
 \\
 \begin{array}{c} i \quad j \\ \hline a \quad b \quad \boxed{c} \quad k \quad l \quad m \\ \bullet \end{array} \quad \rightarrow \quad V_n = \frac{5!}{2!3!}
 \end{array} \quad (\text{A.7})$$

B Isotopes and Elasticity

Since the physical parallel in the singular oscillator case is a diatomic molecule, we may wish to explore what occurs in the isotopic case. In other words, we will discuss the behavior of the system if the oscillator mass m is perturbed to some m' , representing a change in the atomic nuclei. We begin with the original Hamiltonian in (1.1), written in terms of position q and momentum p .

$$H_0 = \frac{1}{2m}p^2 + \frac{1}{2}kq^2 \quad ; \quad p = -i\frac{d}{dq} \quad (\text{B.1})$$

The coefficient $k = m\omega^2$ is the force constant of the oscillator, related to how stiff or elastic the molecular bond is. At first glance, a mass perturbation is not straightforwardly expressed using additive ladder operators as in $H = H_0 + V$. We will instead approach the problem by comparing the Hamiltonian before and after the mass perturbation is applied, using some δH to represent the change in the system.

$$H = H_0 + \delta H \quad \rightarrow \quad \delta H = H - H_0 \quad (\text{B.2})$$

This representation is extremely helpful for dealing with ‘indirect’ perturbations such as isotopes. The difference between the two Hamiltonians is expressed below, using the m subscript as we discuss the change in mass.

$$\delta H_m = \left(\frac{1}{2m'}p^2 + \frac{1}{2}kq^2 \right) - \left(\frac{1}{2m}p^2 + \frac{1}{2}kq^2 \right) = \frac{1}{2} \left(\frac{1}{m'} - \frac{1}{m} \right) p^2 \quad (\text{B.3})$$

In order to return to the more familiar ladder operator representation, we simply use the inverted definitions in (1.6) for the single oscillator.

$$\begin{aligned}\delta H_m &= \frac{1}{2} \left(\frac{1}{m'} - \frac{1}{m} \right) p^2 = -\frac{1}{2} \left(\frac{1}{m'} - \frac{1}{m} \right) \frac{m\omega}{2} (a^\dagger - a)^2 \\ &= \frac{\omega}{4} \left(1 - \frac{m}{m'} \right) (a^\dagger - a)^2\end{aligned}\tag{B.4}$$

Noting that δH_m only consists of products of two ladder operators, we have proven that the mass perturbation is quadratic. A similar derivation applies to an elasticity perturbation, where the force constant k changes to some new k' .

$$\delta H_k = \left(\frac{1}{2m} p^2 + \frac{1}{2} k' q^2 \right) - \left(\frac{1}{2m} p^2 + \frac{1}{2} k q^2 \right) = \frac{1}{2} (k' - k) q^2\tag{B.5}$$

Returning to the operator representation as before, we quickly find that such a perturbation is also quadratic.

$$\begin{aligned}\delta H_k &= \frac{1}{2} (k' - k) q^2 = \frac{1}{2} (k' - k) \frac{1}{2m\omega} (a^\dagger + a)^2 \\ &= \frac{\omega}{4} \left(\frac{k'}{k} - 1 \right) (a^\dagger + a)^2\end{aligned}\tag{B.6}$$

Allow us to simplify the above expressions by collecting the coefficients into some strength parameters ϵ_m and ϵ_k . We will keep the ω term separate, such that the strength parameters are dimensionless.

$$\epsilon_m = 1 - \frac{m}{m'} \quad ; \quad \epsilon_k = \frac{k'}{k} - 1\tag{B.7}$$

Our mass and elasticity perturbations can then be expressed as follows after normal

ordering the squared combinations of operators.

$$\begin{aligned}\delta H_m &= \frac{\omega}{4}\epsilon_m (a^\dagger a^\dagger - 2a^\dagger a + aa - 1) \\ \delta H_k &= \frac{\omega}{4}\epsilon_k (a^\dagger a^\dagger + 2a^\dagger a + aa + 1)\end{aligned}\tag{B.8}$$

In order to define a molecular perturbation applicable to mass or elasticity, we will combine both δH_m and δH_k into some general V . Anticipating this step, we first define two coefficients B_+ and B_- as combinations of the strength parameters.

$$B_+ = \frac{\omega}{2}(\epsilon_k + \epsilon_m) \quad ; \quad B_- = \frac{\omega}{2}(\epsilon_k - \epsilon_m)\tag{B.9}$$

The form of the perturbation can then be written directly as the more familiar V_2 and some constant V_0 , collecting terms and replacing them with the new coefficients.

$$\begin{aligned}V &= \delta H_m + \delta H_k \\ &= \frac{\omega}{4}\epsilon_m (a^\dagger a^\dagger - 2a^\dagger a + aa - 1) + \frac{\omega}{4}\epsilon_k (a^\dagger a^\dagger + 2a^\dagger a + aa + 1) \\ &= \frac{\omega}{4} [(\epsilon_k + \epsilon_m) a^\dagger a^\dagger + 2(\epsilon_k - \epsilon_m) a^\dagger a + (\epsilon_k + \epsilon_m) aa + (\epsilon_k - \epsilon_m)] \\ &= \left(\frac{1}{2}B_+ a^\dagger a^\dagger + B_- a^\dagger a + \frac{1}{2}B_+ aa \right) + \frac{1}{2}B_-\end{aligned}\tag{B.10}$$

As expected of a physical perturbation, we note that V here is Hermitian. Any change of mass or elasticity in a diatomic molecule can thus be expressed in the quadratic order with the following coefficients.

$$Q_2^0 = Q_0^2 = B_+ \quad ; \quad Q_1^1 = B_- \quad ; \quad V_0 = \frac{1}{2}B_-\tag{B.11}$$

This fact also works in reverse, such that any Hermitian quadratic perturbation can be said to directly represent a physical change in mass or elasticity. To prove this, allow us to invert the coefficients in (B.9).

$$\epsilon_m = \frac{1}{\omega} (B_+ - B_-) \quad ; \quad \epsilon_k = \frac{1}{\omega} (B_+ + B_-) \quad (\text{B.12})$$

Expanding the strength parameters as in (B.7), solving each equation for m' and k' , and then returning to the standard coefficients Q reveals the following equalities.

$$\frac{1}{m'} = \frac{1}{m} \left(1 - \frac{Q_2^0 - Q_1^1}{\omega} \right) \quad ; \quad k' = k \left(1 + \frac{Q_2^0 + Q_1^1}{\omega} \right) \quad (\text{B.13})$$

As long as the relations in (B.11) hold true, the above equations can be used to directly express a quadratic perturbation as its equivalent perturbations in mass and elasticity. This effectively creates some new harmonic oscillator with angular frequency $\tilde{\omega}$, as shown from discussions in Chapter 5.

$$\omega = \sqrt{\frac{k}{m}} \quad \rightarrow \quad \tilde{\omega} = \sqrt{\frac{k'}{m'}} \quad (\text{B.14})$$

C Generated Code

The file presented in this section is generated by Python, given orders M and N by which to truncate V_M and T_N . We have chosen to present the V_4 and T_4 output to mirror the collections in (6.5) through (6.8), but note that these truncations are entirely arbitrary. The purpose of this file is to define a function `get_diagrams`, which takes an input of relevant parameters in the Hamiltonian and coupled cluster process. These include the generalized unperturbed coefficients Δ , Λ , and Γ outlined in (3.52), the normal ordered perturbation coefficients Q_K^L , any amplitudes t_n , and the angular frequency ω of the oscillator. Also included is some `mode` parameter, which helps to load certain collections only at whichever point they are utilized (i.e., in the ground state energy calculation, amplitude convergence, or excited states).

The output of `get_diagrams` is then a dictionary of all collections \hat{W}_R^S , paired with their numerical evaluation given the input parameters. This allows us the freedom to evaluate diagrammatic contributions at any point, including the critical steps below.

- During the amplitude convergence scheme at each iteration as shown in (3.39).
- When calculating the ground state \tilde{E}_0 using closed diagrams in (3.44).
- While constructing the effective Hamiltonian $\bar{\mathbf{H}}$ element by element, with contributions given by (3.45).
- Repeating any of the above calculations with a new Hamiltonian after a number of Bogoliubov transformations.

Let us therefore make a handful of notes regarding the collections before providing

the generated code itself. Due to their identical structure, we first note that the $\hat{\omega}$ and \hat{Q}_1^1 terms appear on the same line of code, and are therefore counted as one diagrammatic entry rather than two. This explains the ‘missing’ entry when comparing the number of terms in the passage before (6.5). The diagrammatic contributions are also written in anticipation of Bogoliubov transformations, such that a few choice terms are interpreted using the coefficients in (3.58).

Additionally, we note that the explicit form of the operator products in (3.27) have been slightly reduced, as follows.

$$\begin{aligned}\hat{\Pi}_R^S &= \frac{1}{R!} \frac{1}{S!} Q_K^L \frac{1}{n!} \frac{(K+M-n)!}{K!(M-n)!} t_M(a^\dagger)^R (a)^S \\ &= \frac{1}{S!} Q_K^L \frac{1}{n!} \frac{1}{K!(M-n)!} t_M(a^\dagger)^R (a)^S\end{aligned}\tag{C.1}$$

The factorials associated with $R = K + M - n$ are thus cancelled out. This is done to avoid the inclusion of very large factorials $R!$ which may result when dealing with higher-order diagrams. Such factorials could lead to numerical errors relating to the treatment of large numbers in code (i.e., rounding or truncation), and therefore removing them is ideal. The ‘reduced’ symmetrizing coefficient $\frac{1}{K!(M-n)!}$ is provided explicitly in each line of code, while other factorials $S!$ and $n!$ are conserved for readability where applicable.

For further readability, the collections themselves have been sorted and ordered based on where they appear in the effective Hamiltonian. Any collections \hat{W}_R^S which are not already grouped as part of the ground state or amplitude calculations are commented with a particular ‘offset’, corresponding to a diagonal line in $\overline{\mathbf{H}}$. Specifically, contributions

labeled by ‘Offset: k ’ will appear along the diagonal with elements $\langle m + k | \overline{\mathbf{H}} | m \rangle$. For example, the ‘Offset: -1 ’ group includes collections \hat{W}_0^1 , \hat{W}_1^2 , and \hat{W}_2^3 , all contributing to $\langle m - 1 | \overline{\mathbf{H}} | m \rangle$.

With these notes in mind, the generated file which contains all diagrammatic equations associated with V_4 and T_4 is shown below.

loadeqns_sho_V4_T4.py

```

1 from scipy.special import factorial as fac
2
3 invf2 = 1/fac(2)
4 invf3 = 1/fac(3)
5 invf4 = 1/fac(4)
6
7 def get_diagrams(unpert, normal_ordered_coefficients, amplitudes,
8                 angu_freq, mode):
9
10    contrib = dict({})
11
12    hamil_delta, hamil_lambda, hamil_gamma = unpert
13    R = 2*hamil_lambda
14    Q_0_0, Q_0_1, Q_0_2, Q_0_3, Q_0_4 = normal_ordered_coefficients[0]
15    Q_1_0, Q_1_1, Q_1_2, Q_1_3, _ = normal_ordered_coefficients[1]
16    Q_2_0, Q_2_1, Q_2_2, _ , _ = normal_ordered_coefficients[2]
17    Q_3_0, Q_3_1, _ , _ , _ = normal_ordered_coefficients[3]
18    Q_4_0, _ , _ , _ , _ = normal_ordered_coefficients[4]
19
20    t1, t2, t3, t4 = amplitudes
21
22    if mode in ["all", "closed"]:
23
24        #Ground State | 12 entries.
25        contrib["0,0"] = (Q_0_0 + (1/2)*angu_freq + hamil_gamma) + \
26            Q_0_1*t1 + \
27            (Q_0_2 + R)*invf2*t2 + \
28            (Q_0_2 + R)*invf2*t1*t1 + \
29            Q_0_3*invf3*t3 + \
30            Q_0_3*invf2*t1*t2 + \
31            Q_0_3*invf3*t1*t1*t1 + \
32            Q_0_4*invf4*t4 + \
33            Q_0_4*invf3*t1*t3 + \
34            Q_0_4*invf2*invf2*invf2*t2*t2 + \
35            Q_0_4*invf2*invf2*t1*t1*t2 + \
36            Q_0_4*invf4*t1*t1*t1*t1
37
38    if mode in ["all", "open", "amplitude"]:
39

```

```

40 #Amplitude t1 | 20 entries.
41 contrib["1,0"] = Q_0_1*1*t2 + \
42   Q_1_0 + \
43   (Q_0_2 + R)*invf2*1*t3 + \
44   (Q_0_2 + R)*1*t1*t2 + \
45   (Q_1_1 + hamil_delta)*1*t1 + \
46   Q_0_3*invf3*1*t4 + \
47   Q_0_3*invf2*1*t1*t3 + \
48   Q_0_3*invf2*invf2*1*t2*t2 + \
49   Q_0_3*invf2*1*t1*t1*t2 + \
50   Q_1_2*invf2*1*t2 + \
51   Q_1_2*invf2*1*t1*t1 + \
52   Q_0_4*invf3*1*t1*t4 + \
53   Q_0_4*invf3*1*t2*t3 + \
54   Q_0_4*invf2*invf2*1*t2*t3 + \
55   Q_0_4*invf2*invf2*1*t1*t1*t3 + \
56   Q_0_4*invf2*invf2*1*t1*t2*t2 + \
57   Q_0_4*invf3*1*t1*t1*t1*t2 + \
58   Q_1_3*invf3*1*t3 + \
59   Q_1_3*invf2*1*t1*t2 + \
60   Q_1_3*invf3*1*t1*t1*t1
61
62
63 #Amplitude t2 | 30 entries.
64 contrib["2,0"] = Q_0_1*0.5*t3 + \
65   (Q_0_2 + R)*invf2*0.5*t4 + \
66   (Q_0_2 + R)*0.5*t1*t3 + \
67   (Q_0_2 + R)*invf2*1*t2*t2 + \
68   (Q_1_1 + hamil_delta)*1*t2 + \
69   invf2*(Q_2_0 + R) + \
70   Q_0_3*invf2*0.5*t1*t4 + \
71   Q_0_3*invf2*1*t2*t3 + \
72   Q_0_3*invf2*0.5*t2*t3 + \
73   Q_0_3*invf2*0.5*t1*t1*t3 + \
74   Q_0_3*invf2*1*t1*t2*t2 + \
75   Q_1_2*invf2*1*t3 + \
76   Q_1_2*1*t1*t2 + \
77   Q_2_1*0.5*t1 + \
78   Q_0_4*invf3*1*t2*t4 + \
79   Q_0_4*invf2*invf2*0.5*t2*t4 + \
80   Q_0_4*invf2*invf2*invf2*1*t3*t3 + \
81   Q_0_4*invf3*invf2*0.5*t3*t3 + \
82   Q_0_4*invf2*invf2*0.5*t1*t1*t4 + \
83   Q_0_4*invf2*1*t1*t2*t3 + \
84   Q_0_4*invf2*0.5*t1*t2*t3 + \
85   Q_0_4*invf2*invf3*1*t2*t2*t2 + \
86   Q_0_4*invf3*0.5*t1*t1*t1*t3 + \
87   Q_0_4*invf2*invf2*1*t1*t1*t2*t2 + \
88   Q_1_3*invf3*1*t4 + \
89   Q_1_3*invf2*1*t1*t3 + \
90   Q_1_3*invf2*invf2*1*t2*t2 + \
91   Q_1_3*invf2*1*t1*t1*t2 + \
92   Q_2_2*invf2*0.5*t2 + \
93   Q_2_2*invf2*0.5*t1*t1

```

```

94
95
96 #Amplitude t3 | 34 entries.
97 contrib["3,0"] = Q_0_1*0.1666666666666666*t4 + \
98 (Q_0_2 + R)*0.1666666666666666*t1*t4 + \
99 (Q_0_2 + R)*0.5*t2*t3 + \
100 (Q_1_1 + hamil_delta)*0.5*t3 + \
101 Q_0_3*invf2*0.5*t2*t4 + \
102 Q_0_3*invf2*0.1666666666666666*t2*t4 + \
103 Q_0_3*invf2*invf2*0.5*t3*t3 + \
104 Q_0_3*invf2*0.1666666666666666*t1*t1*t4 + \
105 Q_0_3*0.5*t1*t2*t3 + \
106 Q_0_3*invf3*1*t2*t2*t2 + \
107 Q_1_2*invf2*0.5*t4 + \
108 Q_1_2*0.5*t1*t3 + \
109 Q_1_2*invf2*1*t2*t2 + \
110 Q_2_1*0.5*t2 + \
111 invf3*Q_3_0 + \
112 Q_0_4*invf3*0.5*t3*t4 + \
113 Q_0_4*invf2*invf2*0.5*t3*t4 + \
114 Q_0_4*invf3*0.1666666666666666*t3*t4 + \
115 Q_0_4*invf2*0.5*t1*t2*t4 + \
116 Q_0_4*invf2*0.1666666666666666*t1*t2*t4 + \
117 Q_0_4*invf2*invf2*0.5*t1*t3*t3 + \
118 Q_0_4*invf2*invf2*1*t2*t2*t3 + \
119 Q_0_4*invf2*invf2*0.5*t2*t2*t3 + \
120 Q_0_4*invf3*0.1666666666666666*t1*t1*t1*t4 + \
121 Q_0_4*invf2*0.5*t1*t1*t2*t3 + \
122 Q_0_4*invf3*1*t1*t2*t2*t2 + \
123 Q_1_3*invf2*0.5*t1*t4 + \
124 Q_1_3*invf2*1*t2*t3 + \
125 Q_1_3*invf2*0.5*t2*t3 + \
126 Q_1_3*invf2*0.5*t1*t1*t3 + \
127 Q_1_3*invf2*1*t1*t2*t2 + \
128 Q_2_2*invf2*0.5*t3 + \
129 Q_2_2*0.5*t1*t2 + \
130 Q_3_1*0.1666666666666666*t1
131
132
133 #Amplitude t4 | 34 entries.
134 contrib["4,0"] = (Q_0_2 + R)*0.1666666666666666*t2*t4 + \
135 (Q_0_2 + R)*invf2*0.25*t3*t3 + \
136 (Q_1_1 + hamil_delta)*0.1666666666666666*t4 + \
137 Q_0_3*invf2*0.25*t3*t4 + \
138 Q_0_3*invf2*0.1666666666666666*t3*t4 + \
139 Q_0_3*0.1666666666666666*t1*t2*t4 + \
140 Q_0_3*invf2*0.25*t1*t3*t3 + \
141 Q_0_3*invf2*0.5*t2*t2*t3 + \
142 Q_1_2*0.1666666666666666*t1*t4 + \
143 Q_1_2*0.5*t2*t3 + \
144 Q_2_1*0.25*t3 + \
145 Q_0_4*invf2*invf2*invf2*0.25*t4*t4 + \
146 Q_0_4*invf3*invf2*0.1666666666666666*t4*t4 + \
147 Q_0_4*invf2*0.25*t1*t3*t4 + \

```

```

148 Q_0_4*invf2*0.1666666666666666*t1*t3*t4 + \
149 Q_0_4*invf2*invf2*0.5*t2*t2*t4 + \
150 Q_0_4*invf2*invf2*0.1666666666666666*t2*t2*t4 + \
151 Q_0_4*invf2*invf2*0.5*t2*t3*t3 + \
152 Q_0_4*invf2*invf2*0.25*t2*t3*t3 + \
153 Q_0_4*invf2*0.1666666666666666*t1*t1*t2*t4 + \
154 Q_0_4*invf2*invf2*0.25*t1*t1*t3*t3 + \
155 Q_0_4*invf2*0.5*t1*t2*t2*t3 + \
156 Q_0_4*invf4*1*t2*t2*t2*t2 + \
157 Q_1_3*invf2*0.5*t2*t4 + \
158 Q_1_3*invf2*0.1666666666666666*t2*t4 + \
159 Q_1_3*invf2*invf2*0.5*t3*t3 + \
160 Q_1_3*invf2*0.1666666666666666*t1*t1*t4 + \
161 Q_1_3*0.5*t1*t2*t3 + \
162 Q_1_3*invf3*1*t2*t2*t2 + \
163 Q_2_2*invf2*0.25*t4 + \
164 Q_2_2*0.25*t1*t3 + \
165 Q_2_2*invf2*0.5*t2*t2 + \
166 Q_3_1*0.1666666666666666*t2 + \
167 invf4*Q_4_0
168
169
170 if mode in ["all", "open", "other"]:
171
172     #==
173
174     #Offset: -4 | 1 entries.
175     contrib["0,4"] = invf4*Q_0_4
176
177     #==
178
179     #Offset: -3 | 2 entries.
180     contrib["0,3"] = invf3*Q_0_3 + \
181         invf3*Q_0_4*1*t1
182
183     #==
184
185     #Offset: -2 | 4 entries.
186     contrib["0,2"] = invf2*(Q_0_2 + R) + \
187         invf2*Q_0_3*1*t1 + \
188         invf2*Q_0_4*invf2*1*t2 + \
189         invf2*Q_0_4*invf2*1*t1*t1
190
191     #Offset: -2 | 2 entries.
192     contrib["1,3"] = invf3*Q_0_4*1*t2 + \
193         invf3*Q_1_3
194
195     #==
196
197     #Offset: -1 | 7 entries.
198     contrib["0,1"] = Q_0_1 + \
199         (Q_0_2 + R)*1*t1 + \
200         Q_0_3*invf2*1*t2 + \
201         Q_0_3*invf2*1*t1*t1 + \

```

```

202     Q_0_4*invf3*1*t3 + \
203     Q_0_4*invf2*1*t1*t2 + \
204     Q_0_4*invf3*1*t1*t1*t1
205
206     #Offset: -1 | 5 entries.
207     contrib["1,2"] = invf2*Q_0_3*1*t2 + \
208         invf2*Q_1_2 + \
209         invf2*Q_0_4*invf2*1*t3 + \
210         invf2*Q_0_4*1*t1*t2 + \
211         invf2*Q_1_3*1*t1
212
213     #Offset: -1 | 1 entries.
214     contrib["2,3"] = invf3*Q_0_4*0.5*t3
215
216     #==
217
218     #Offset: 0 | 11 entries.
219     contrib["1,1"] = (Q_0_2 + R)*1*t2 + \
220         (Q_1_1 + hamil_delta) + \
221         Q_0_3*invf2*1*t3 + \
222         Q_0_3*1*t1*t2 + \
223         Q_1_2*1*t1 + \
224         Q_0_4*invf3*1*t4 + \
225         Q_0_4*invf2*1*t1*t3 + \
226         Q_0_4*invf2*invf2*1*t2*t2 + \
227         Q_0_4*invf2*1*t1*t1*t2 + \
228         Q_1_3*invf2*1*t2 + \
229         Q_1_3*invf2*1*t1*t1
230
231     #Offset: 0 | 6 entries.
232     contrib["2,2"] = invf2*Q_0_3*0.5*t3 + \
233         invf2*Q_0_4*invf2*0.5*t4 + \
234         invf2*Q_0_4*0.5*t1*t3 + \
235         invf2*Q_0_4*invf2*1*t2*t2 + \
236         invf2*Q_1_3*1*t2 + \
237         invf2*invf2*Q_2_2
238
239     #Offset: 0 | 1 entries.
240     contrib["3,3"] = invf3*Q_0_4*0.16666666666666666*t4
241
242     #==
243
244     #Offset: 1 | 14 entries.
245     contrib["2,1"] = (Q_0_2 + R)*0.5*t3 + \
246         Q_0_3*invf2*0.5*t4 + \
247         Q_0_3*0.5*t1*t3 + \
248         Q_0_3*invf2*1*t2*t2 + \
249         Q_1_2*1*t2 + \
250         invf2*Q_2_1 + \
251         Q_0_4*invf2*0.5*t1*t4 + \
252         Q_0_4*invf2*1*t2*t3 + \
253         Q_0_4*invf2*0.5*t2*t3 + \
254         Q_0_4*invf2*0.5*t1*t1*t3 + \
255         Q_0_4*invf2*1*t1*t2*t2 + \

```

```

256     Q_1_3*invf2*1*t3 + \
257     Q_1_3*1*t1*t2 + \
258     Q_2_2*0.5*t1
259
260     #Offset: 1 | 4 entries.
261     contrib["3,2"] = invf2*Q_0_3*0.1666666666666666*t4 + \
262     invf2*Q_0_4*0.1666666666666666*t1*t4 + \
263     invf2*Q_0_4*0.5*t2*t3 + \
264     invf2*Q_1_3*0.5*t3
265
266     #==
267
268     #Offset: 2 | 15 entries.
269     contrib["3,1"] = (Q_0_2 + R)*0.1666666666666666*t4 + \
270     Q_0_3*0.1666666666666666*t1*t4 + \
271     Q_0_3*0.5*t2*t3 + \
272     Q_1_2*0.5*t3 + \
273     Q_0_4*invf2*0.5*t2*t4 + \
274     Q_0_4*invf2*0.1666666666666666*t2*t4 + \
275     Q_0_4*invf2*invf2*0.5*t3*t3 + \
276     Q_0_4*invf2*0.1666666666666666*t1*t1*t4 + \
277     Q_0_4*0.5*t1*t2*t3 + \
278     Q_0_4*invf3*1*t2*t2*t2 + \
279     Q_1_3*invf2*0.5*t4 + \
280     Q_1_3*0.5*t1*t3 + \
281     Q_1_3*invf2*1*t2*t2 + \
282     Q_2_2*0.5*t2 + \
283     invf3*Q_3_1
284
285     #Offset: 2 | 3 entries.
286     contrib["4,2"] = invf2*Q_0_4*0.1666666666666666*t2*t4 + \
287     invf2*Q_0_4*invf2*0.25*t3*t3 + \
288     invf2*Q_1_3*0.1666666666666666*t4
289
290     #==
291
292     #Offset: 3 | 11 entries.
293     contrib["4,1"] = Q_0_3*0.1666666666666666*t2*t4 + \
294     Q_0_3*invf2*0.25*t3*t3 + \
295     Q_1_2*0.1666666666666666*t4 + \
296     Q_0_4*invf2*0.25*t3*t4 + \
297     Q_0_4*invf2*0.1666666666666666*t3*t4 + \
298     Q_0_4*0.1666666666666666*t1*t2*t4 + \
299     Q_0_4*invf2*0.25*t1*t3*t3 + \
300     Q_0_4*invf2*0.5*t2*t2*t3 + \
301     Q_1_3*0.1666666666666666*t1*t4 + \
302     Q_1_3*0.5*t2*t3 + \
303     Q_2_2*0.25*t3
304
305     #Offset: 3 | 1 entries.
306     contrib["5,2"] = invf2*Q_0_4*0.0833333333333333*t3*t4
307
308     #==
309

```



```

364 Q_0_3*0.0833333333333333*t2*t3*t4 + \
365 Q_0_3*invf3*0.125*t3*t3*t3 + \
366 Q_1_2*0.0833333333333333*t3*t4 + \
367 Q_0_4*invf2*invf2*0.0833333333333333*t2*t4*t4 + \
368 Q_0_4*invf2*invf2*0.02777777777777776*t2*t4*t4 + \
369 Q_0_4*invf2*invf2*0.125*t3*t3*t4 + \
370 Q_0_4*invf2*invf2*0.0833333333333333*t3*t3*t4 + \
371 Q_0_4*invf2*invf2*0.02777777777777776*t1*t1*t4*t4 + \
372 Q_0_4*0.0833333333333333*t1*t2*t3*t4 + \
373 Q_0_4*invf3*0.125*t1*t3*t3*t3 + \
374 Q_0_4*invf3*0.1666666666666666*t2*t2*t2*t4 + \
375 Q_0_4*invf2*invf2*0.25*t2*t2*t3*t3 + \
376 Q_1_3*invf2*invf2*0.0833333333333333*t4*t4 + \
377 Q_1_3*0.0833333333333333*t1*t3*t4 + \
378 Q_1_3*invf2*0.1666666666666666*t2*t2*t4 + \
379 Q_1_3*invf2*0.25*t2*t3*t3 + \
380 Q_2_2*0.0833333333333333*t2*t4 + \
381 Q_2_2*invf2*0.125*t3*t3 + \
382 Q_3_1*0.02777777777777776*t4
383
384 #Offset: 6 | 3 entries.
385 contrib["7,1"] = Q_0_4*invf2*0.02777777777777776*t2*t4*t4 + \
386 Q_0_4*invf2*0.04166666666666664*t3*t3*t4 + \
387 Q_1_3*invf2*0.02777777777777776*t4*t4
388
389 #==
390
391 #Offset: 7 | 13 entries.
392 contrib["7,0"] = Q_0_3*invf2*0.02777777777777776*t2*t4*t4 + \
393 Q_0_3*invf2*0.04166666666666664*t3*t3*t4 + \
394 Q_1_2*invf2*0.02777777777777776*t4*t4 + \
395 Q_0_4*invf2*invf2*0.04166666666666664*t3*t4*t4 + \
396 Q_0_4*invf2*invf2*0.02777777777777776*t3*t4*t4 + \
397 Q_0_4*invf2*0.02777777777777776*t1*t2*t4*t4 + \
398 Q_0_4*invf2*0.04166666666666664*t1*t3*t3*t4 + \
399 Q_0_4*invf2*0.0833333333333333*t2*t2*t3*t4 + \
400 Q_0_4*invf3*0.125*t2*t3*t3*t3 + \
401 Q_1_3*invf2*0.02777777777777776*t1*t4*t4 + \
402 Q_1_3*0.0833333333333333*t2*t3*t4 + \
403 Q_1_3*invf3*0.125*t3*t3*t3 + \
404 Q_2_2*0.04166666666666664*t3*t4
405
406 #Offset: 7 | 1 entries.
407 contrib["8,1"] = Q_0_4*invf2*0.01388888888888888*t3*t4*t4
408
409 #==
410
411 #Offset: 8 | 9 entries.
412 contrib["8,0"] = Q_0_3*invf2*0.01388888888888888*t3*t4*t4 + \
413 Q_0_4*invf2*invf3*0.01388888888888888*t4*t4*t4 + \
414 Q_0_4*invf2*0.01388888888888888*t1*t3*t4*t4 + \
415 Q_0_4*invf2*invf2*0.02777777777777776*t2*t2*t4*t4 + \
416 Q_0_4*invf2*0.04166666666666664*t2*t3*t3*t4 + \
417 Q_0_4*invf4*0.0625*t3*t3*t3*t3 + \

```

```

418 Q_1_3*invf2*0.027777777777777776*t2*t4*t4 + \
419 Q_1_3*invf2*0.041666666666666664*t3*t3*t4 + \
420 Q_2_2*invf2*0.013888888888888888*t4*t4
421
422 #Offset: 8 | 1 entries.
423 contrib["9,1"] = Q_0_4*invf3*0.004629629629629629*t4*t4*t4
424
425 #==
426
427 #Offset: 9 | 5 entries.
428 contrib["9,0"] = Q_0_3*invf3*0.004629629629629629*t4*t4*t4 + \
429 Q_0_4*invf3*0.004629629629629629*t1*t4*t4*t4 + \
430 Q_0_4*invf2*0.013888888888888888*t2*t3*t4*t4 + \
431 Q_0_4*invf3*0.020833333333333332*t3*t3*t3*t4 + \
432 Q_1_3*invf2*0.013888888888888888*t3*t4*t4
433
434 #==
435
436 #Offset: 10 | 3 entries.
437 contrib["10,0"] = Q_0_4*invf3*0.004629629629629629*t2*t4*t4*t4 + \
438 Q_0_4*invf2*invf2*0.006944444444444444*t3*t3*t4*t4 + \
439 Q_1_3*invf3*0.004629629629629629*t4*t4*t4
440
441 #==
442
443 #Offset: 11 | 1 entries.
444 contrib["11,0"] = Q_0_4*invf3*0.0023148148148148147*t3*t4*t4*t4
445
446 #==
447
448 #Offset: 12 | 1 entries.
449 contrib["12,0"] = Q_0_4*invf4*0.0007716049382716049*t4*t4*t4*t4
450
451 return contrib

```

Bibliography

- Banik, S., Pal, S., & Prasad, M. D. 2008, *The Journal of Chemical Physics*, 129, 134111
- Bartlett, R. J. & Musiał, M. 2007, *Rev. Mod. Phys.*, 79, 291
- Bishop, R. 1991, *Theoretica Chimica Acta*, 80, 95
- Bishop, R. F. & Flynn, M. F. 1988, *Phys. Rev. A*, 38, 2211
- Bogoljubov, N. N. 1958, *Il Nuovo Cimento (1955-1965)*, 7, 794
- Christiansen, O. 2004a, *The Journal of Chemical Physics*, 120, 2140
- . 2004b, *The Journal of Chemical Physics*, 120, 2149
- Coester, F. 1958, *Nuclear Physics*, 7, 421
- Coester, F. & Kümmel, H. 1960, *Nuclear Physics*, 17, 477
- Geertsen, J., Rittby, M., & Bartlett, R. J. 1989, *Chemical Physics Letters*, 164, 57
- Hsue, C.-S. & Chern, J. L. 1984, *Phys. Rev. D*, 29, 643
- Hsue, C.-S., Kümmel, H., & Ueberholz, P. 1985, *Phys. Rev. D*, 32, 1435
- Huey-You, C. 2020, Master's thesis, Texas Christian University
- Huey-You, C. & Rittby, C. M. L. 2024, (submitted, under review)
- Kaulfuss, U. B. & Altenbokum, M. 1986, *Phys. Rev. D*, 33, 3658
- Paldus, J. & Čížek, J. 1975, in *Advances in Quantum Chemistry*, Vol. 9, *Advances in Quantum Chemistry*, ed. P.-O. Löwdin (Academic Press), 105–197
- Sekino, H. & Bartlett, R. J. 1984, *International Journal of Quantum Chemistry*, 26, 255
- Szabo, A. & Ostlund, N. 1996, *Modern Quantum Chemistry* (Dover)
- Čížek, J. 1966, *The Journal of Chemical Physics*, 45, 4256

VITA

Name Carson Huey-You

Education Texas Christian University - Fort Worth, TX, USA
Doctor of Philosophy, Physics, 2024
Master of Science, Physics, 2019
Bachelor of Science, Physics, 2017
(Mathematics & Chinese Language Double-Minor)
Accommodated Learning Academy - Grapevine, TX, USA
High School Diploma, 2013

Research Experience

- Determining the Eigenvalues and Associated Isotopic Spectra of Systems using Coupled Cluster Techniques, with Dr. Magnus Rittby: 2017 - Present
- Quantum Mechanics in the Complex Plane, with Dr. Magnus Rittby: 2015 - 2017
- Mathematics of Signal Processing, with Dr. Ken Richardson: 2016
- Tumor Growth Modeling, with Dr. Hana Dobrovolny: 2015

Work Experience

- Internship at the Discovery Science Channel (Mythbusters Jr.): 2018

Posters & Presentations

- “Exploring a System of Coupled Quartic Oscillators with Coupled Cluster Methods”
C. Huey-You, M. Rittby, 2019,
TCU Student Research Symposium
- “In Search of Elusive Complex Eigenvalues to the Schrödinger Equation using Numerical Techniques”
C. Huey-You, M. Rittby, 2017,
TCU Student Research Symposium
- “Tumor growth model choice in the presence of limited data”
C. Huey-You, D. Barth, H. Jaafari, H. Murphy, M. Ellis, H.M. Dobrovolny, 2015,
Fall 2015 Joint Meeting of the Texas Section of the AAPT, Texas Section of the APS
and Zone 13 of the Society of Physics Students, Waco, TX.
- “Searching for an Optimal ODE Model to Describe and Differentiate Cancers”
D. Barth, C. Huey-You, H. Jaafari, H. Murphy, M. Ellis, H.M. Dobrovolny, 2015,
Fall 2015 Joint Meeting of the Texas Section of the AAPT, Texas Section of the APS
and Zone 13 of the Society of Physics Students, Waco, TX.

ABSTRACT

DIAGRAM DRIVEN COMPUTER GENERATION OF EQUATION-OF-MOTION COUPLED CLUSTER EQUATIONS FOR PERTURBED QUANTUM OSCILLATORS

by Carson Huey-You, Ph.D., 2024
Department of Physics and Astronomy
Texas Christian University

Major Professor: Dr. Magnus Rittby

We consider a set of quantum harmonic oscillators subjected to perturbations expressible as a power series in position and momentum. A diagrammatic scheme is developed, by which to generate equation-of-motion coupled cluster (EoM-CC) equations for the calculation of the perturbed energy spectrum of the system. The diagrammatic scheme is then adapted into a Python code, capable of generating the necessary equations and computer code associated with any arbitrary order of the perturbation and coupled cluster excitation levels. The generated equations are made readily accessible for numerical evaluation, alongside convergence schemes and the application of iterative Bogoliubov transformations.